

Diplomarbeit

Diploma Thesis

**SIMULATION EINES
U-BAHN-UNTERWERKS MIT PSCAD/EMTDC**

**METRO-SUBSTATION SIMULATION
WITH PSCAD/EMTDC**

erstellt bei

SIEMENS AG Transportation Systems

Erlangen, Germany

Vorgelegt von:

Yin YING
m0335315

Betreuer:

AsP. Dipl.-Ing. Dr. mont. Franz Aschenbrenner
O.Univ.Prof. Dipl.-Ing. Dr. techn. Helmut Weiss

Leoben, September, 2007

EIDESSTATTLICHE ERKLÄRUNG

Ich erkläre an Eides statt, dass ich die vorliegende Diplomarbeit selbständig und ohne fremde Hilfe verfasst, andere als die angegebenen Quellen und Hilfsmittel nicht benutzt und die den benutzten Quellen wörtlich und inhaltlich entnommenen Stellen als solche erkenntlich gemacht habe.

Kurzfassung

SIMULATION EINES U-BAHN-UNTERWERKS MIT PSCAD/EMTDC

Grundlegende Anforderungen an die Energiebereitstellung für elektrische Lokomotiven sind Regelung der Spannung, niedrige Amplituden von Oberschwingungen und beste Zuverlässigkeit der Versorgung. Einsparung von Verlustenergie ist ein wesentlicher Beitrag zum Klimaschutz. Die europäischen Richtlinien hierfür sind strenger als diejenigen in den USA. Konzepte für neue elektrische Lokomotiven, welche das Rückarbeiten von Bremsenergie („Rekuperation“) nützen, werden durch viele Firmen und in vielen Staaten erforscht.

Diese Arbeit beginnt mit grundlegender Beschreibung der ungesteuerten Dreiphasen-Diodenbrücke (B6U). Fortgesetzt wird mit 6-pulsigen, 12-pulsigen und 24-pulsigen Gleichrichterschaltungen und schließlich wird die Diode durch gesteuerte Thyristoren ersetzt (Schaltung B6C), um die Regelung der Spannung zu ermöglichen.

Anschließend werden Unterwerke mit Umkehrstromrichter in Thyristortechnik bearbeitet, bestehend aus einem Gleichrichter und antiparallel geschaltetem Wechselrichter zur Spannungsregelung. Durch diese Schaltungstopologie wird die beim Bremsen entstehende Energie zurück in das Versorgungsnetz gespeist. Auch wird eine Realisierung mittels Pulswechselrichter beschrieben.

Alle Untersuchungen erfolgen mittels Simulation mit dem Programm PSCAD/EMTDC. Die Simulationsergebnisse werden mit Messungen an zwei unterschiedlichen Projekten verglichen; es gibt eine gute Übereinstimmung. Hierdurch erweist sich das Programm PSCAD/EMTDC als zuverlässiges und wirkungsvolles Werkzeug für die Computerunterstützte Entwicklung von Energieversorgungsanlagen.

Abstract

METRO-SUBSTATION SIMULATION WITH PSCAD/EMTDC

Basic requirements for supplying energy to electrical locomotives are voltage control, low amplitudes of harmonics and optimum reliability of supply. Saving loss energy is an essential contribution for climate protection. European rules for this are much more severe than those from the USA. Research on concepts for electrical locomotives that utilize recuperation of deceleration energy is done by many companies and in many countries.

This thesis starts with a basic description of the uncontrolled three-phase diode bridge circuit (B6U). It continues with 6-pulse, 12-pulse, and 24-pulse rectifier circuits. Finally, the diode is replaced by a controlled thyristor in order to accomplish closed loop control of the voltage.

In next part we describe sub-stations with a two-way rectifier/inverter at thyristor technology being composed of a rectifier bridge and an inverter in anti-parallel connection for voltage control. Through this circuit topology, the energy produced by deceleration can be fed back into the grid. Realization by a pulse-width-modulation inverter is described, too.

All investigations are done by simulation using the program PSCAD/EMTDC. Simulation results are compared to measurements obtained at two different projects; we observe good coincidence. Therefore, the program PSCAD/EMTDC proves to be reliable and efficient tool for computer-aided development of energy supply plants.

Acknowledgements

From February 2004 to November 2007, I make my Diploma study in Montanuniversität Leoben. Many people helped me in one way or another to complete my Diploma work during that time.

In the institute of Electrical Engineering at Montanuniversität Leoben I would like to thank everyone in the institute, especially my advisor O.Univ.Professor.Dipl.-Ing.Dr.techn.Helmut Weiss, for his guidance, his care and his help during these three years and AsP.Dipl.-Ing.Dr. Franz Aschenbrenner in the Electrical Engineering Institute.

In SIEMENS AG Transportation Systems, where I make practice from March to September 2007, first I thank Mr. Tomas Greif, Mr. Roland Schuster and everyone in this company, you all give me a nice place to let me compose my paper.

Mr. Tomas Greif, without your help during the practice of this work in SIEMENS, I think I can not learn so much knowledge, my thanks sincere to you.

Thanks also to my teachers, who are o.Univ.Prof.Dipl.-Ing.Dr.mont.Werner L. Kepplinger, Ao.Univ.Prof.Dr. Josef Draxler in the Process Technology and Industrial Environmental Protection Institute.

Colleagues who give me important help. They are Mr. Andreas Schmid, Mr. Günther Kaserer, Mr. Alois Lang, Mrs. Johanna Rabel and other members in the Electrical Engineering institute.

Thanks the colleagues at SIEMENS AG: Mrs. Barbara Seidling, Mrs. Barbara Först, Mrs. Karin Thiel, Mrs. Katja Elschner, Mr. Reiner Papp, Mr. Hans Ullmann,

Mr. Georg Kuderewski, Mr. Wolfgang Braun, Mr. Stephan Zenglein, Mr. Andreas Fischer, Mr. Jörg Lehmpfuhl, Mr. Bernd Altmann, Mr. Carsten Burlein, Mr. Jochen Steinbauer, Mr. Imre Pomeisl, Mr. Martin Altmann and others for their knowledge shared during these month.

The friendship in Montanuniversität Leoben has made my stay more pleasant and enjoyable. Special thanks are given to all Chinese colleagues in our university and to all Austria colleagues who had taken the classes with me, made group practices with me.

Most of all I would like to thank all my family, especially my parents and grandparents for their unconditional support. And thanks God for allowing me to reach this goal.

TO MYPARENTS
QIANGYUN YING
GUOYING WANG

AND MY GRANDMOTHER
CHUYING WANG

Table of Contents

| | | |
|----------|--|-----------|
| 1 | Introduction | 4 |
| 1.1 | Background..... | 4 |
| 1.2 | Description of the tool PSCAD | 7 |
| 1.2.1 | Diode | 7 |
| 1.2.2 | Thyristor | 7 |
| 1.2.3 | FFT | 8 |
| 1.3 | History, Today and Future | 9 |
| 2 | Characters in Substation | 11 |
| 2.1 | Power factor..... | 11 |
| 2.2 | Voltage regulation..... | 12 |
| 2.3 | Energy Losses..... | 12 |
| 2.4 | Short-circuit current | 13 |
| 2.5 | Ripple factor | 13 |
| 2.6 | THD | 15 |
| 2.7 | Commutation ratio..... | 16 |
| 2.8 | Harmonics on AC and DC side | 16 |
| 3 | AC/DC Rectification | 18 |
| 3.1 | Basics from B6U | 18 |
| 3.2 | Z-transformer to 24-pulse..... | 18 |
| 3.2.1 | Shifting Angle..... | 19 |
| 3.2.2 | Test by PSCAD..... | 23 |
| 3.2.3 | 24-Pulse Rectifier | 24 |
| 3.2.4 | 24-Pulse Profile | 26 |
| 3.3 | Characteristics | 28 |
| 3.3.1 | Basic Characteristics | 28 |
| 3.3.2 | Harmonics on AC and DC Side..... | 30 |
| 3.3.3 | THD and Voltage Profile | 31 |
| 3.3.4 | Inductive Direct Voltage Drop (d_x)..... | 32 |

| | | |
|-------|---|----|
| 3.4 | Summary..... | 34 |
| 3.5 | 36-Pulse Rectification and Improvement..... | 35 |
| 3.5.1 | Normal 36-Pulse rectification | 35 |
| 3.5.2 | Principle of Advancing Rectification | 35 |
| 3.5.3 | Assessment | 38 |
| 4 | Faults and Harms | 39 |
| 4.1 | Short-circuit on Diode | 39 |
| 4.2 | Interruption on a Diode | 42 |
| 4.3 | Harmonics from Net..... | 44 |
| 5 | Harmonic Analysis for SNCF | 45 |
| 5.1 | SNCF Requirements on rectifier | 45 |
| 5.2 | Software Familiarization and Preparation before Simulation..... | 46 |
| 5.3 | Assessment | 48 |
| 6 | Metro Test in Phoenix | 52 |
| 6.1 | Introduction | 52 |
| 6.2 | No-load Operation..... | 54 |
| 6.3 | Operation with Auxiliary system..... | 60 |
| 6.3.1 | Low Level Auxiliary Operation | 61 |
| 6.3.2 | High Level Auxiliary Operation..... | 62 |
| 6.4 | Characteristic in Crossing Feeder | 64 |
| 6.5 | Unbalancment of the Output | 69 |
| 6.6 | Assessment | 71 |
| 7 | DC/AC Inversion | 72 |
| 7.1 | Rectifier-Inverter Operation | 72 |
| 7.1.1 | Prerequisites | 72 |
| 7.1.2 | Dynamic control | 74 |
| 7.1.3 | Results and Assessment..... | 75 |
| 7.2 | Inverter with PWM..... | 76 |
| 8 | Conclusion and Future | 80 |
| 8.1 | Conclusion..... | 80 |

| | |
|--|-----|
| 8.2 Further work | 81 |
| References | 82 |
| List of Nomenclature | 85 |
| List of Illustrations | 87 |
| List of Tables | 90 |
| APPENDIX A Rectifier Diode | I |
| APPENDIX B IEC 60146-1 | III |
| APPENDIX C Harmonic Disturbances | V |
| APPENDIX D SNCF Data | VII |
| APPENDIX E TPSS in Phoenix | IX |
| APPENDIX F 12pDGR6pWR | XIV |
| Curriculum Vitae | XVI |

1 Introduction

1.1 Background

The high speed of development of modern science and technology causes the change in every aspect of life, from getting news on the internet to going to the countryside by electrical train to enjoy sunshine, all not to be done without energy, particularly electrical energy.

The development on transportation with electrical train is also an important area in which various countries heavily research and develop. For example in China, especial after entering the 21st century, the government raises the speed of transportation in railroad through all national scopes in several times.

In the beginning half year of 2007, there are nearly 6 003 kilometers of completed railroad line for speed of minimum 200 kilometer per hour. Railroad line for speed of 250 kilometers per hour amounts to 846 kilometers (on these line a brand new locomotive type is running, “HeXie”, which meaning harmonious relation between living and nature in Chinese) (Figure 1-1).



Figure 1-1 2007 The HeXie train running*

To the end of 2010, the entire in operation railroad in China will achieve 85 000 kilometers. The railroad in electrification will be 35 000 kilometers, consisting of the redeveloped railway in electrification with almost 15 000 kilometers and the newly built railway nearly 20 000 kilometers. (In Figure 1-2 we see the railway building plan of “eight vertical eight horizontal” in China: the solid line means having developed the railroad on the old line before 2010, the dashed line is the new built line, and the red line is direction from north to south, the blue line means direction from east to west).

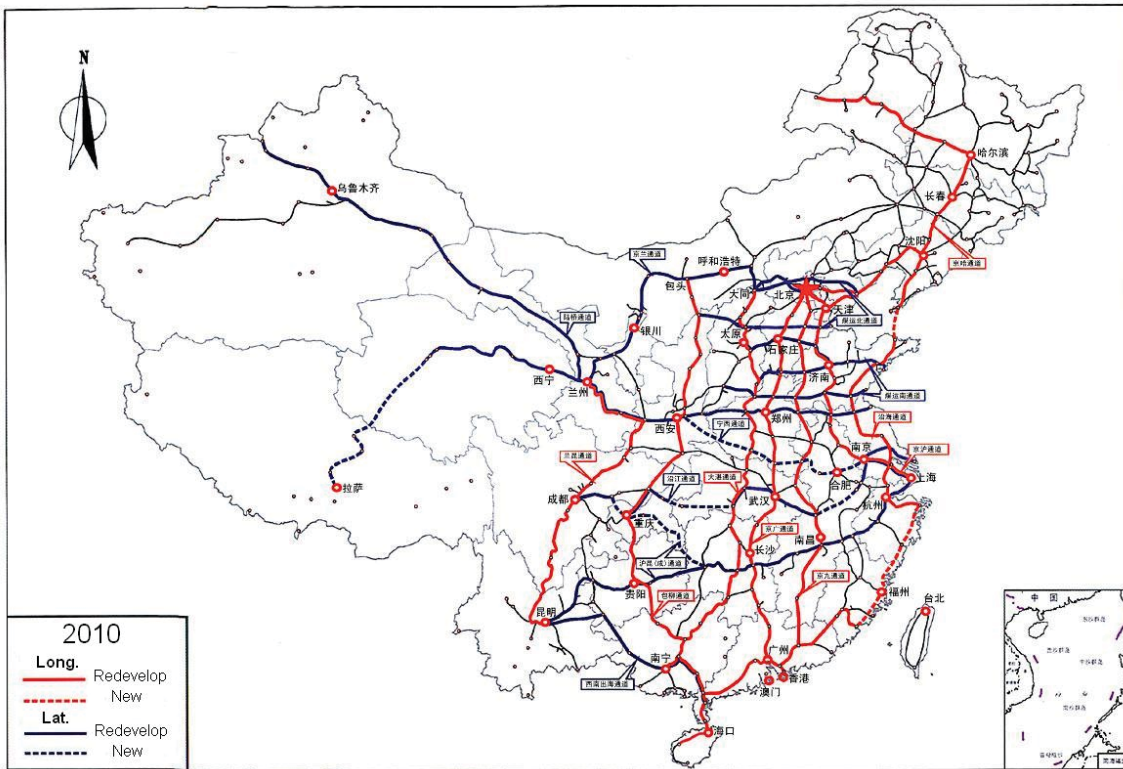


Figure 1-2 Railway Plan “8 vertical 8 horizontal” in China
 (Source from www.china-mor.gov.cn)

At the same time, every large or middle city builds or plans to build electrical transportation (underground or others) in their city, too. The demand increases day by day, but, regarding to the voltage stability on the net, the robustness, the higher harmonic waves elimination and other demands.

The introduction of electric traction in the late 19th century in Europe and the USA was to replace the use of steam traction on heavy duty rapid transit suburban railways, underground railways and, subsequently main line railways. The original idea of railway electrification evolved from implementations on electric trams that were fed with direct current (DC) or alternating current (AC) from overhead wires through a trolley pole.

The substations, as a result for the need of special voltage of electric locomotive trains, are built between the transmission net (high voltage grid) and the inner net (overhead contact line). The substations play the role to limit abnormal currents (short circuit current, lightning over current...) at the same time. There are basic function loops in the substation: rectification loop, voltage adjustment, changing frequency and inversion loop.

In these processes we extremely pay attention to the higher harmonic waves. The harmonic waves not only cause electromagnetic compatibility (EMC) problems, but also result in additional consumption of electrical energy.

Direct current (DC) overhead contact net or alternating current (AC) overhead contact net (Figure 1-4, 1-5) has the rectification-invert loops, therefore controlling the higher harmonics under the given standards (EN, IEC or IEEE) is always a demanding topic for the engineers. Especially in the project of redeveloping the old substations and overhead contact

nets, matching the old apartments to the new elements is a hard work. Many complex design calculations are necessary for the aim of eliminating or reducing harmonics.

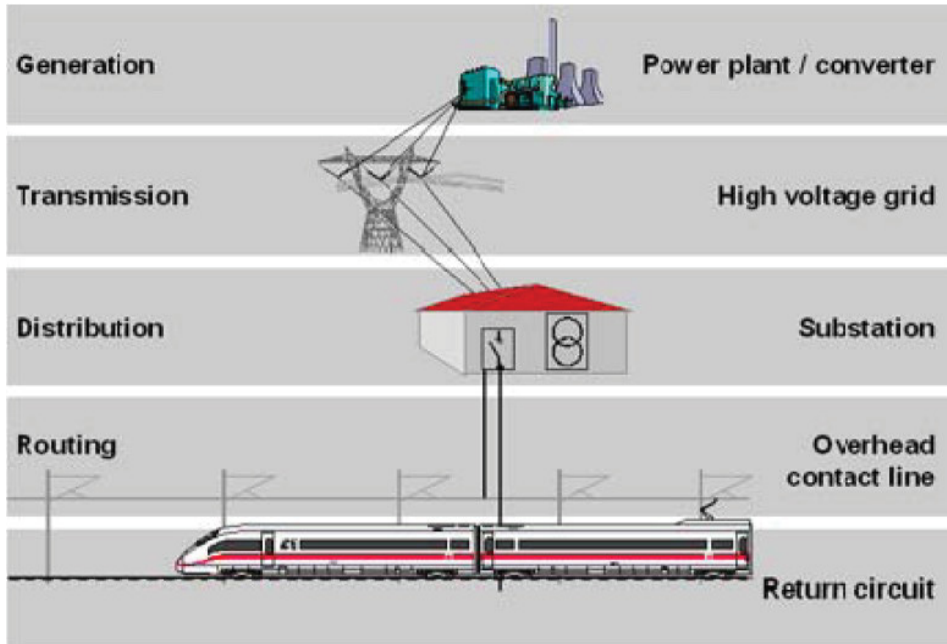


Figure 1-3 AC power supply*

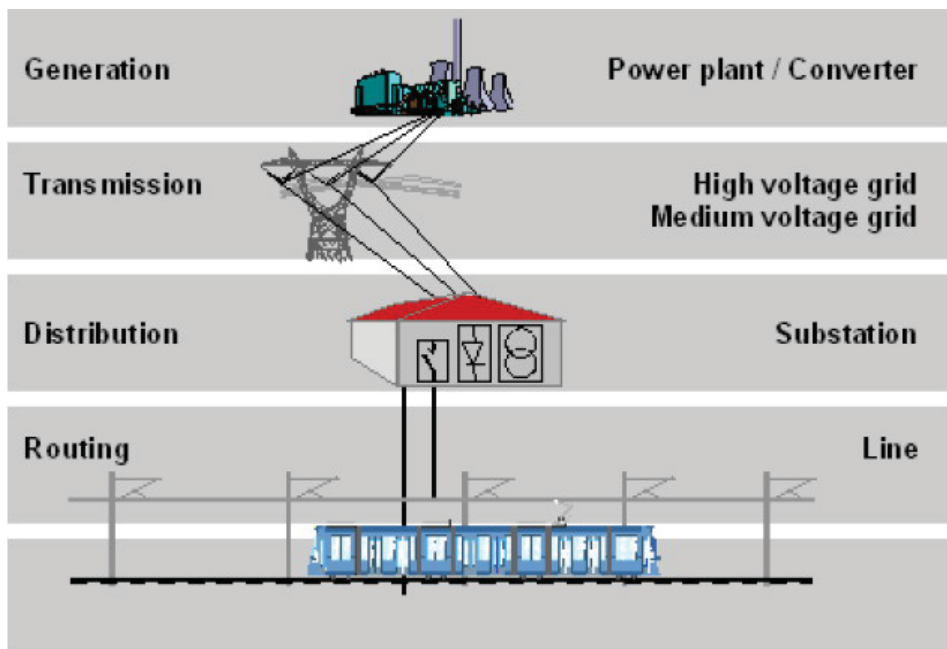


Figure 1-4 DC power supply*

In order to enhance the working efficiency, today we use real-time simulation with the aid of computer assistance software CAD. This concept is widely used in all kinds of technical engineering. In order to analyze the electrical current in real-time, PSCAD/EMTDC (software is developed by a Canadian company) provides the necessary functions now in version 4.2.

This thesis is based on the described software condition and hardware condition.

1.2 Description of the tool PSCAD

PSCAD (Power Systems CAD) is a powerful and flexible graphical user interface to the world-renowned EMTDC solution engine. PSCAD enables the user to construct a circuit schematically, run a simulation, analyze the results, and manage the data in a completely integrated, graphical environment. Online plotting functions, controls and meters are also included, so that the user can alter system parameters during a simulation run, and view the results directly. PSCAD can easily analyze the operation.

The following chapter describes some important model elements. This information is included in the PSCAD/EMTDC Online Help System, too.

1.2.1 Diode

The diode ON and OFF states are controlled by the voltage and current conditions across the device itself.

The diode assumes a fixed small ON and a large OFF resistance. Conduction commences when the device is forward biased and the forward voltage exceeds the forward voltage drop input parameter. The diode turns OFF at a current zero and remains OFF as long as it is reverse biased.

The U-I characteristic for the GTO/IGBT model is shown below:

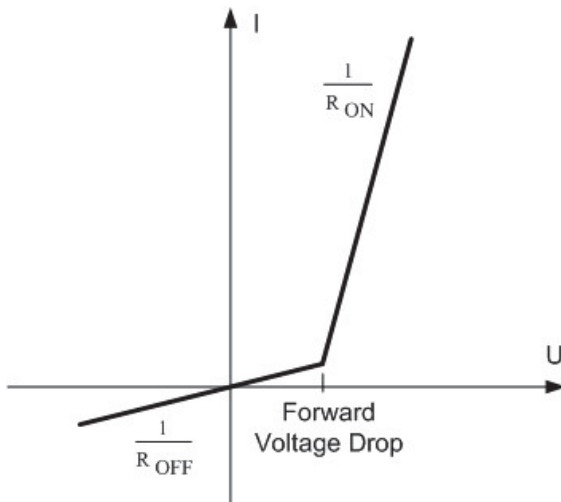


Figure 1-5 U-I Line for GTO/IGBT

Both ON and OFF events use the interpolation algorithm to calculate the instant of switching. Thus, turn ON occurs exactly when forward voltage reaches the Forward Voltage Drop and turn OFF occurs exactly when current reaches zero.

1.2.2 Thyristor

The thyristor is usually latched ON by a firing pulse supplied to the gate terminal, but is turned OFF according to voltage and current conditions across the device itself. An external control signal is required to generate the gate firing pulses.

The thyristor assumes a fixed small ON and a large OFF resistance. The thyristor state will change under the following conditions:

1. The forward bias voltage across the device is greater than or equal to the Forward Voltage Drop parameter input AND the gate signal goes from 0 to 1 (i.e. firing pulse is issued).
2. The forward bias voltage across the device is greater than or equal to the Forward Voltage Drop parameter input AND the gate signal is preset to 1 (i.e. firing angle = 0°). A turn ON under this situation is NOT interpolated (for an interpolated turn ON with firing angle = 0°, use the Diode).
3. The forward bias voltage across the device is greater than or equal to Forward Break-Over Voltage parameter input.
4. Turning OFF occurs with the device current is reaching zero.

The U-I characteristic for the thyristor model is shown below:

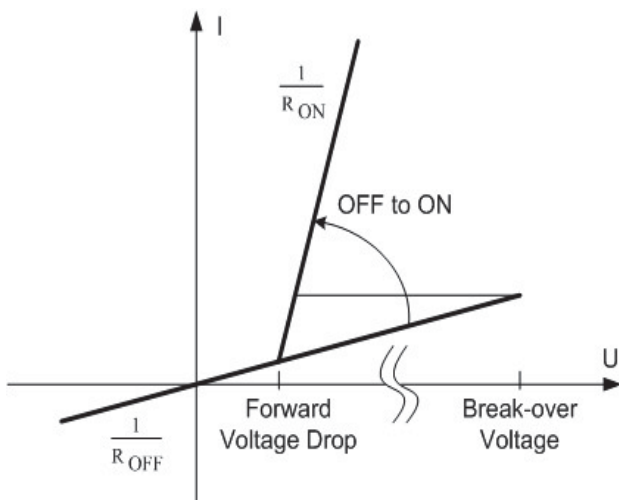


Figure 1-6 U-I Line for GTO/IGBT

The interpolation algorithm is automatically invoked during all naturally commutated turn ON and turn OFF events (including Forward Break-Over), to calculate the exact instant of switching. However, the user can provide a choice to interpolate the incoming gate signal.

The circuit commutated recover time is also represented. Therefore, the thyristor will re-fire following a turn OFF if the minimum extinction time parameter input has not elapsed before the forward voltage rises above the forward voltage drop parameter input. This will occur even in the absence of a turn ON signal.

1.2.3 FFT

This online Fast Fourier Transform (FFT) can determine the harmonic magnitude

amplitude and phase of the input signal as a function of time. The input signals are sampled before they are decomposed into harmonic components.

$$X(t) = \frac{1}{\sqrt{2\pi}} \int_{-\infty}^{\infty} X(\omega) \cdot e^{j\omega t} d\omega \quad (1.1)$$

Options are provided to use one, two or three inputs. In the case of three inputs, the component can provide output in the form of sequence components.

The user may select one of the following three FFT block types:

- **1-phase:** This is a standard 1-phase FFT. The input is processed to provide the magnitudes **Mag** and phase angle **Ph** of the fundamental frequency and its harmonics (including the DC component **dc**).
- **2-phase:** These are two 1-phase FFTs in a single block, in order to keep the schematic compact and organized.
- **3-phase:** As above, is merely three 1-phase FFTs combined in one block.
- **+/-/0 seq:** This takes a 3-phase input **X_A**, **X_B**, **X_C** and calculates the FFT preliminary output through a sequencer, which outputs positive sequence(+), negative sequence(-), and zero-sequence magnitude and phase components of the fundamental wave and each harmonic. The DC components of each phase are also output signals.

The sequence components are computed based on the standard transformation equation:

$$\begin{bmatrix} V_0 \\ V_+ \\ V_- \end{bmatrix} = \begin{bmatrix} 0 & 2 & 1+1\angle 60^\circ \\ 0 & 1\angle -60^\circ & -1-1\angle 60^\circ \\ 0 & 1\angle 60^\circ & 0 \end{bmatrix} \cdot \begin{bmatrix} V_a \\ V_b \\ V_c \end{bmatrix} \quad (1.2)$$

The Polymer can directly show the frequency-analysis results. A polymer is a special Runtime object used specifically for monitoring multiple-trace curves (for example, a harmonic spectrum). The Polymer dynamically displays the magnitude of each individual trace in bar type format (called gauges) which results in an appearance similar to a spectrum analyzer. The power of this device lies in its ability to compress a large amount of data into a small viewing area. This is particularly helpful when viewing harmonic spectrums such as data output from the On-Line Frequency Scanner (FFT) component.

1.3 History, Today and Future

Electric traction was found to offer higher energy efficiency, ability to meet increased capacity demands, provision of frequent rail services, and environmental friendliness

compared to steam traction, along with higher scheduled speeds and conservation of fossil. From the financial point of view, operating costs for electric traction are lower for steam traction at the same amount of traffic. The use of overhead wires conducting electricity, invented by Granville T. Woods in 1888, amongst several other improvements, led to the development of electrified railways, the first of which in the United States was operated at Coney Island from 1892.

After the 1950's, many countries, especially in Europe and North America, try to use electrified trains in large number. The DB (German Federal Railways) used the train sets of Class 401 (ICE 1) which had been put into service in 1989. From 1997, the successor ICE 2 pulled by Class 402 power heads was put into service. To overcome the restrictions imposed on the ICE 1 and ICE 2, their successor, the ICE 3, in service since May 2006, was built to a smaller loading gauge to permit usability throughout Europe.



Figure 1-7 New Train developments by SIEMENS*

And now SIEMENS AG pushes the newest train, which is more comfortable, more safety and faster. (Figure 1-7)

In future 20 years every large city in Asia (including China) is building or planning to build the electrical transportation (underground or others). Also SIEMENS AG will help many other countries to develop their own railways in those areas. People want to use new types and designs of locomotives which are considered being solutions to protect environment.

2 Characters in Substation

2.1 Power factor

Power is defined as the flow rate of energy past a given point. In alternating current circuits, energy storage elements such as inductors and capacitors may cause periodic reversals in the direction of instantaneous energy flow. The portion of power flow averaged over a complete cycle of the AC waveform that results in net transfer of energy into one direction is known as active power. On the other hand, the portion of power flow due to stored energy, which returns to the source in each cycle, is known as reactive power.

Engineers use three types of power to describe energy flow in a system:

Active power (P) [W]

Reactive power (Q) [Var]

Apparent power (S) [VA] A complex power S can be defined using P and Q:

$$\underline{S} = P + jQ$$

$$S = |\underline{S}|$$

Displacement factor $\cos(\varphi)$ is defined as: active power P divided by apparent power S.

For purely fundamental wave signals (without harmonics) the power factor (POF) is equal to displacement factor $\cos(\varphi)$. (IEV 551-06-04)

With measurement of power (Figure 2-1 and Figure 2-2), we can take all values in Table 3-2 and the value of $\cos(\varphi)$ is under full load operation.

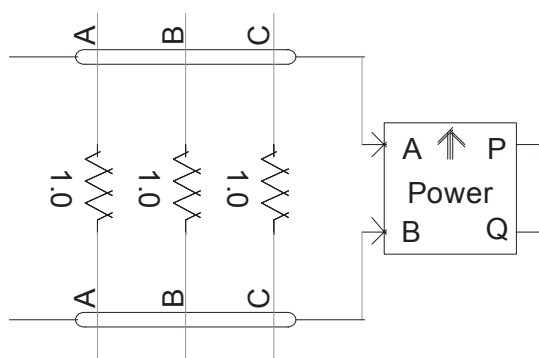


Figure 2-1 Measurement of Power

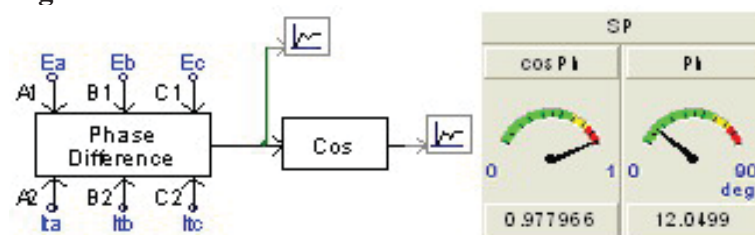


Figure 2-2 Power factor measurement in PSCAD**

2.2 Voltage regulation

In electrical engineering, particularly power engineering, voltage regulation is the ability of a system to provide nearly constant voltage over a wide range of load conditions. It is a dimensionless quantity defined as: (IEC 60146-1):

$$VR = \frac{U_{d0} - U_{dN}}{U_{dN}} \cdot 100\% \quad (2.1)$$

,where U_{d0} is no-load voltage and U_{dN} is rated direct voltage. (Figure 2-3) A smaller value of VR is usually considered being better.

Sometimes the term voltage regulation is used to describe processes by which the quantity VR is reduced, especially concerning special circuits and devices for this purpose: voltage regulators. Voltage regulators are an important part of power systems and power supplies.

At the transition current value, the voltage/current characteristic bends. Transition current can be obtained, for example in the case of back electromotive force (e.m.f.) load because the inductance of the d.c. circuit cannot maintain direct current over the entire period or in case of interphase transformer connection, because the direct current decreases below the critical value where the interphase transformer becomes ineffective.

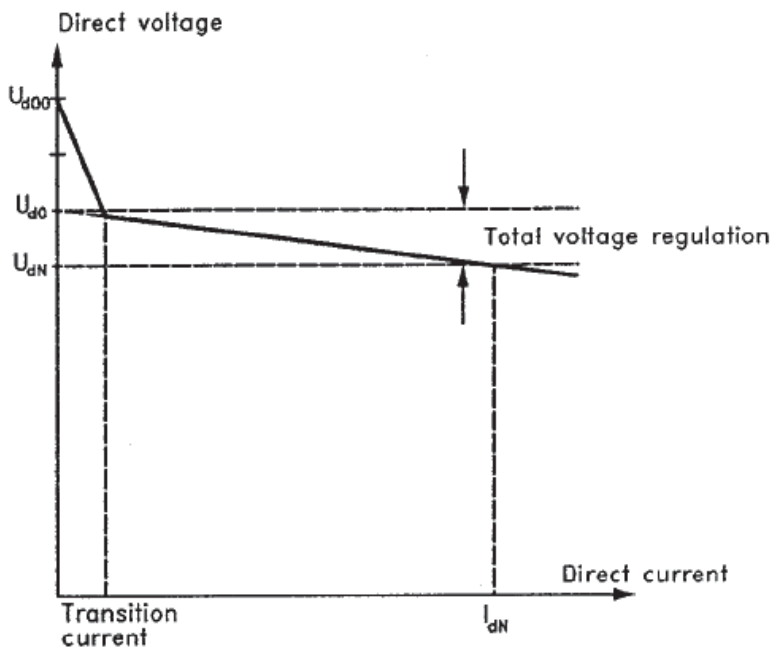


Figure 2-3 Voltage Regulation [4]

2.3 Energy Losses

Since in the no-load operation the power input of the transformer is very small the

copper losses caused in the coil at this operation can be neglected.

The power measured in the no-load operation is generally equal to the iron core losses:

$$P_0 = P_{Fe} \quad (2.2)$$

On the other hand, the voltage applied with the short-circuit test is so small that the core losses become negligible. The short-circuit power amounts to:

$$P_K = P_{Cu} \quad (2.3)$$

Thus the efficiency results from the output P in the case of full load to:

$$\eta = \frac{P_N}{P_N + P_0 + P_K} \cdot 100\% \quad (2.4)$$

For small transformers we get about 90%, for large ones over 96% efficiency. (Refer to [27])

From the values of iron core losses, copper losses and rated power we can easily calculate the efficiency. (Table 3-4)

2.4 Short-circuit current

When there is short circuit fault in the DC side extremely large current will flow through the commutation diodes. With the standard IEC 60146 [4] there is a maximum current value (40 kA) flowing at the rectifiers on DC side. The active values are different for the four connections considered. (Table 3-5)

2.5 Ripple factor

Its ripple factor and total harmonic distortion (THD) are directly depending on the pulsation cycle (Pulse).

$$\text{ripple factor (\%)} = ((U_{\max} - U_{\min}) / (U_{\max} + U_{\min})) * 100 (\%) \quad (2.5)$$

where U_{\max} and U_{\min} are the maximum and minimum values of the periodic function. (IEC 61287-1:2005)

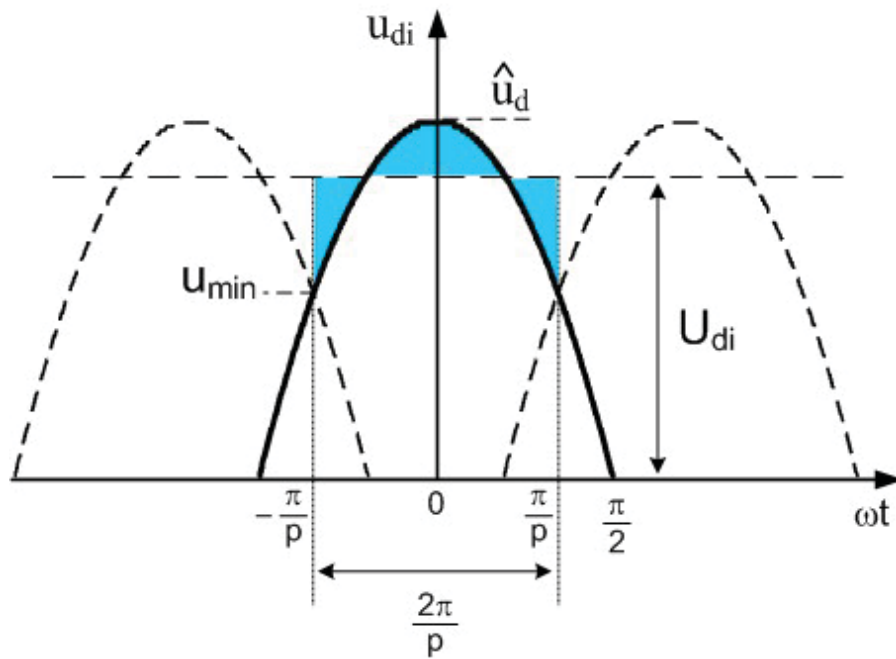


Figure 2-4 DC voltage values with arbitrary pulse [16]

Figure 2-4 shows the maximum value $U_{d\ peak} (\hat{u}_d)$ and the minimum value being $U_{d\ peak} * \cos(\pi/p)$, so: (only for No-load operation)

$$\text{ripple factor (\%)} = (1 - \cos(\pi/p)) / (1 + \cos(\pi/p)) * 100\%$$

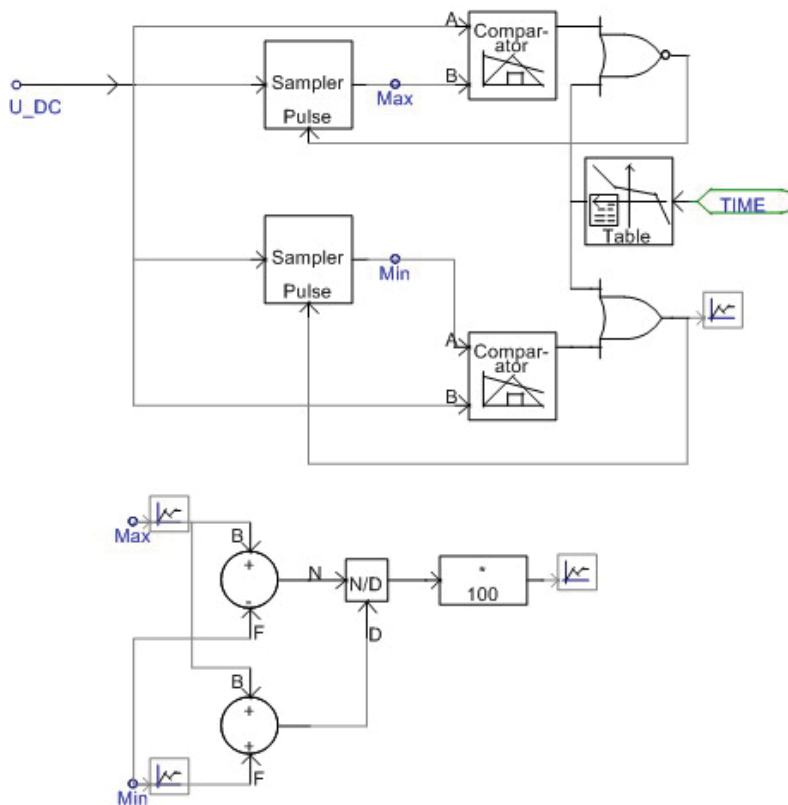


Figure 2-5 Ripple factor measurement in PSCAD

2.6 THD

The total harmonic distortion or THD of a signal is an indicator for the harmonic distortion present and is defined as the ratio of the squared sum of the voltages of all harmonic components to the power of the fundamental.

$$THD = \frac{\sqrt{\sum_{h=1}^{\infty} U_h^2}}{U_{di}} = \sqrt{\left(\frac{U_{dieff}}{U_{di}}\right)^2 - 1} \quad (2.6)$$

From Figure 2-4 we get

$$U_{dieff} = \hat{u}_{dieff} \sqrt{\frac{p}{2\pi} \int_{-\pi/p}^{\pi/p} \cos^2(\omega \cdot t) d(\omega \cdot t)} = \hat{u}_{di} \sqrt{\frac{1}{2} + \frac{p}{4\pi} \sin \frac{2\pi}{p}} \quad (2.7)$$

$$U_{di} = \hat{u}_{di} \cdot \frac{p}{2\pi} \cdot \int_{-\pi/p}^{\pi/p} \cos(\omega \cdot t) d(\omega \cdot t) = \hat{u}_{di} \frac{p}{\pi} \cdot \sin \frac{\pi}{p} \quad (2.8)$$

This only valid for no-load operation

$$THD = \sqrt{\left(\frac{\pi}{p \cdot \sin\left(\frac{\pi}{p}\right)}\right)^2 \cdot \left(\frac{1}{2} + \frac{p}{4\pi} \cdot \sin\left(\frac{2\pi}{p}\right)\right) - 1} \quad (2.9)$$

This formula calculates the THD for any pulse number. We get data with 24-pulse rectification. These data are displayed in Table 3-6

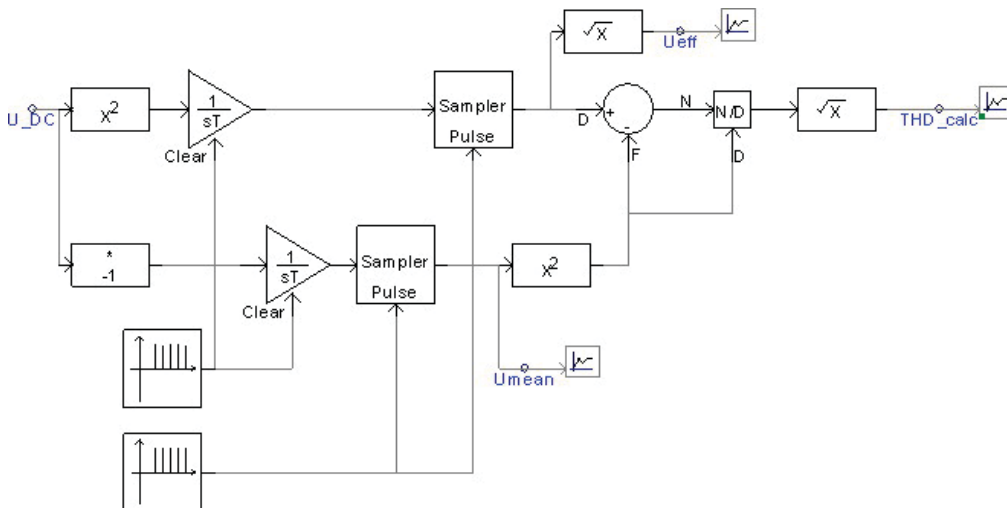


Figure 2-6 THD measure in PSCAD

From the formula 2.6, we can build the measurement in PSCAD as in Figure 2-6. The triangle with $\frac{1}{ST}$ and the square with Sample Pulse are made as the integration loop.

2.7 Commutation ratio

The ratio is the DC voltage (U_{di}) divide by AC voltage (U_{V0}) at the secondary side (root mean square value, r.m.s.). The voltage (U_{V0}) is measured just on the valve (diodes) side of the transformer. It also depends on the pulse number. (Refer to Figure 2-7 and formula 2.10 [16]).

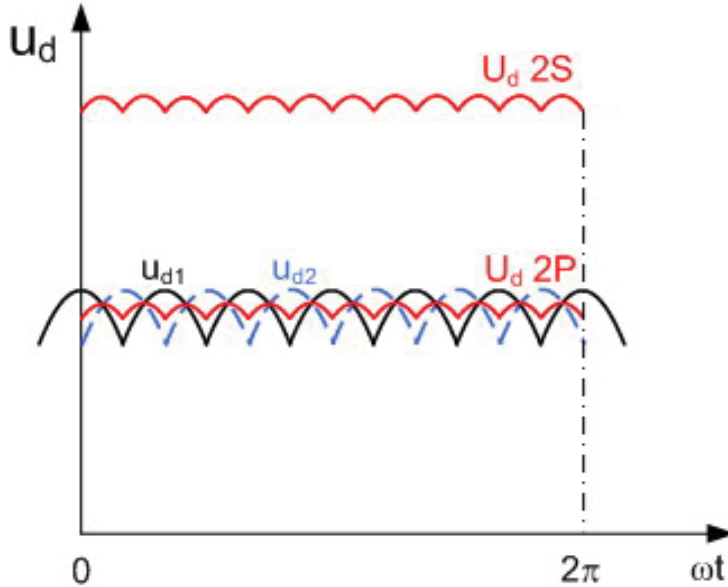


Figure 2-7 DC output Voltage profile [16]

$$U_{di} = \frac{qs}{\pi} \cdot \frac{\sqrt{2}}{\sqrt{3}} \cdot U_{V0} \cdot \sin\left(\frac{\pi}{q}\right) \quad (2.10)$$

The calculation results are in Table 3-8.

2.8 Harmonics on AC and DC side

On the DC side the DC voltage U_d (arithmetic average value) is superposed (no-sinusoidal) by an alternating voltage (Refer to [9]). The overlaid alternating voltage consists of sinusoidal components of different frequencies $h \cdot f$. The order of the characteristic harmonics (h) depends on the pulse number (p):

$$h = k \cdot p \quad \text{also} \quad k = 1, 2, 3, \dots, n$$

The idealistic alternating voltage component of the order (h) has the r.m.s. with full conduction :

$$U_h = \frac{\sqrt{2}}{h^2 - 1} \cdot U_{di} \quad (2.11)$$

The alternating current contains the frequency f of harmonic current, which is near the frequency $h \cdot f$. The harmonics on the AC side affect the current on the commutation side through the transformer. These harmonics are caused due to the inductive, capacitive and

ohmic resistances existing in the net. The harmonic currents also depend on the pulse number (p) and have delay angle with frequencies $h \cdot f$:

$$h = k \cdot p - 1 \quad \text{also} \quad k = 1, 2, 3 \dots n$$

The harmonic current of order (h) in r.m.s. is given for ideal conditions and is independent on the degree of saturation :

$$I_h = \frac{1}{h} \cdot I_{1i} \quad (2.12)$$

We calculate up to the 50th harmonic. This adequate for analyzing and the results are in Table 3-9 and Table 3-10.

3 AC/DC Rectification

3.1 Basics from B6U

In the DC track transportation system, the AC/DC rectification unit is inevitable. The usual rectification is the basic 6-pulse rectification which is realized through the bridge type rectifier. Today B6 is the basic circuit to build the 12-pulse or even 24-pulse rectification bridges which are developed now.

From beginning it is important to know how the B6 works in line commutated rectifier operation with two commutation groups. There is a component in TPSS (Traction Power Supply Substation). Normally there are two different type semiconductor elements to provide a B6 group. B6U is made by Diodes (Figure 3-1) and B6C made by Thyristors. B6C controls the output voltage by changing the firing angle.

Here we analyze from 6-pulse, 12-pulse and 24-pulse rectifiers realized by B6 Commutation Bridge. The basic B6 topology is shown in Figure 3-1. The 24-pulse rectification is more modern than the other topologies mentioned.

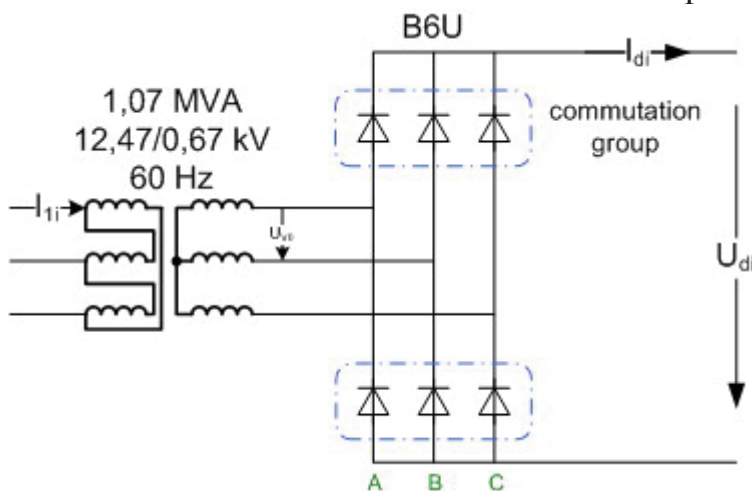


Figure 3-1 6-pulse rectifier by B6U**

3.2 Z-transformer to 24-pulse

The traditional star/delta transformer can only obtain the output side voltage with limited for phase shifting (leading or lagging), for example, the Yd-11 transformer is shifting the output voltage phase into 30 degree leading. But from Table 3-1 we know that if we want to rectify AC to DC using 12-pulse, 24-pulse, and even 36-pulse rectifiers we have to adjust the transformer output voltage phase with a specified shift angle.

This leads us thinking about the utilization of Zigzag transformers, and about changing the coil numbers of the two windings which are used with the same iron core at the

transformer's secondary side. In Figure 3-2, the #2 and the #3 coils' numbers of windings are connected as shown.

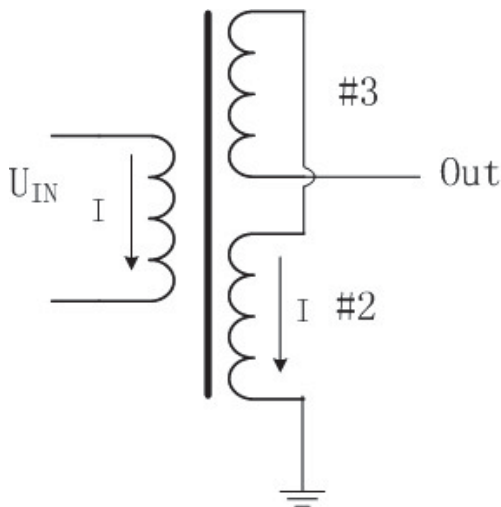


Figure 3-2 Zigzag Transformer**

Table 3-1 Phase shifting in Transformer**

| Pulse | 6 | 12 | 24 | 36 |
|-----------------------|----|-------------|------------------------------|-----------------------------------|
| Phase leading/lagging | 0° | 15° -15° | 7,5°; -7,5° 22,5°; -22,5° | 5°; -5° 15°; -15° 25°; -25° |

3.2.1 Shifting Angle

By changing the numbers of winding turns at secondary side we can change the voltage into the desired phase angle (the voltage considered as a vector value).

First we consider the three-phase zigzag transformer winding connection (Figure 3-3), one end of #2 coils in each phase connected directly to the earth and the other end connected to the next phase's #3 coil.

At the same time, another end of #3 coil as the voltage output's end. We should pay attention to the current flowing direction in the two coils with the same iron core and the currents now must flow into the same direction. When the winding ratios between #2 and #3 coils are one, the output voltage on secondary side has the same phase as the primary side (The primary side is Delta connection). This voltage vector direction is called as 0 position, and the phase shifting angle is zero degree.

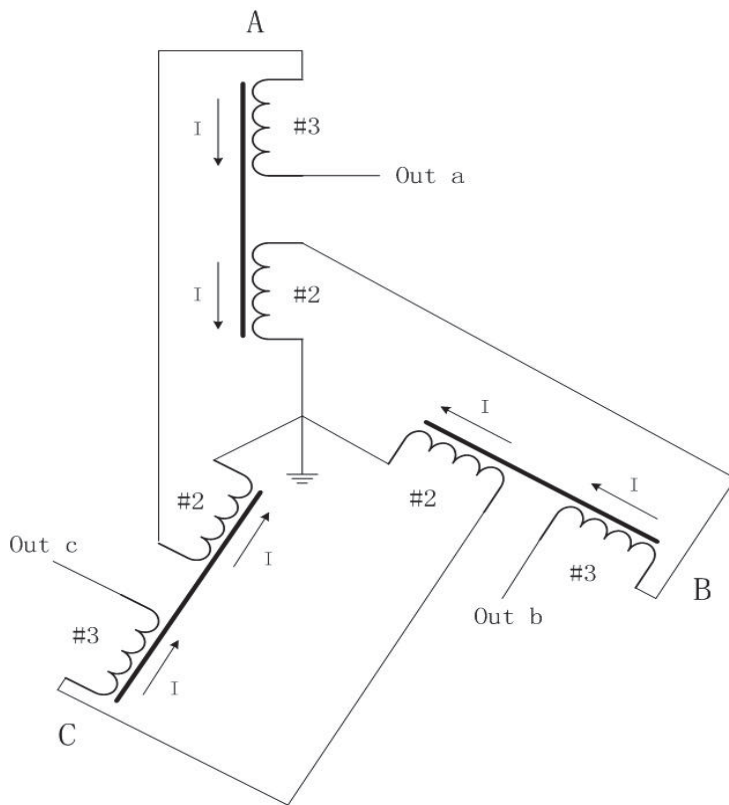


Figure 3-3 Z-Transformer (1)**

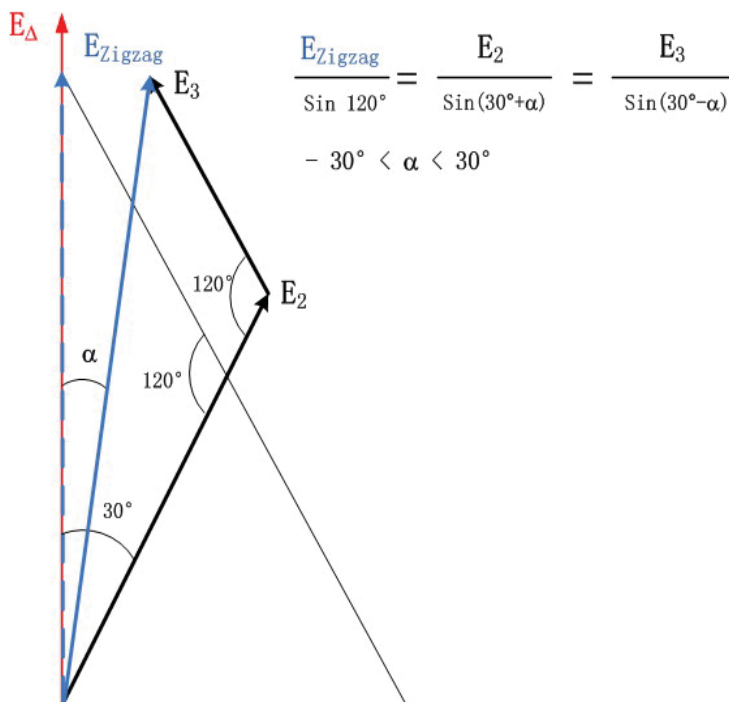


Figure 3-4 Voltage Vector Analysis (1)**

Next we change the numbers of winding turns, actually to change the parameter of voltage in #2 and #3 coils. The vector direction of voltage in these coils is obtained. From Figure 3-4 we know that the output voltage E_{ZigZag} is vector added by the vectors (E_2, E_3). It is important that one must keep the length of output voltage in this process. In this time the shift angle (α) is defined as shown on Figure 3-4.

Normally, we just need leading/lagging angles in the interval negative 30 degree to positive 30 degree. In case we want the angle moving out of this interval. We should refer to the new winding connection method proposed to achieve the goal.

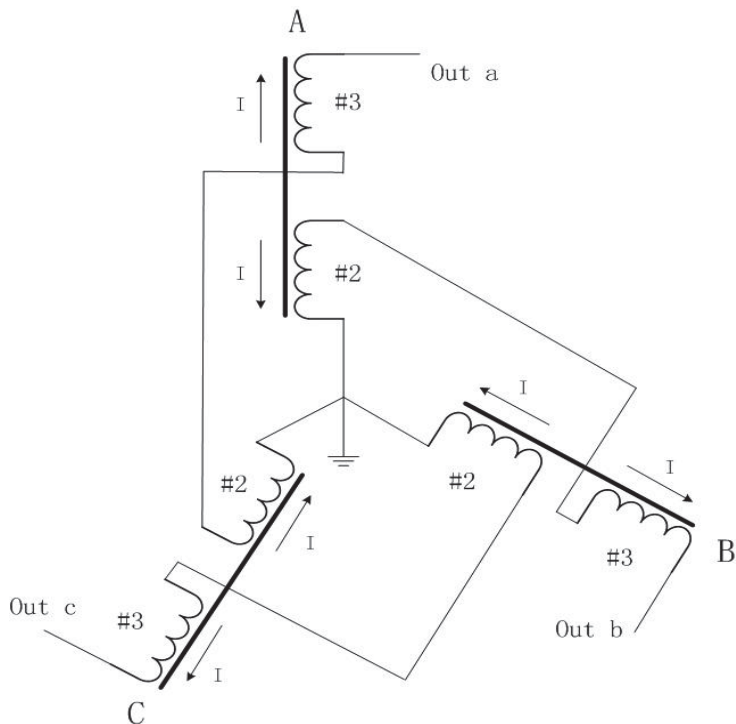


Figure 3-5 Z-Transformer (2)**

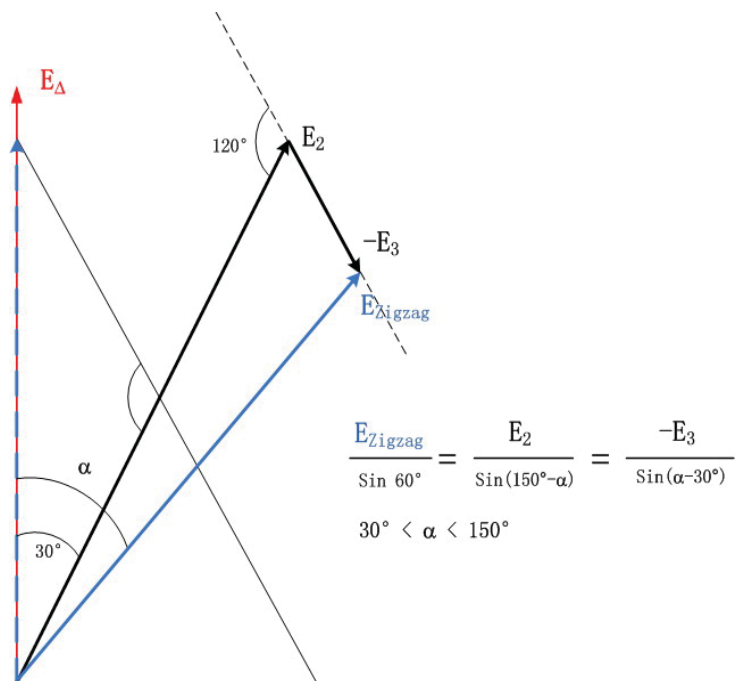


Figure 3-6 Voltage Vector Analysis (2)**

Figure 3-5 and 3-6 show how to obtain angles larger than 30 degree. The minus signal on the voltages value (E_3) only represents that the current flows in the opposite direction to the current flowing in #2 coils. These two coils use the same iron core.

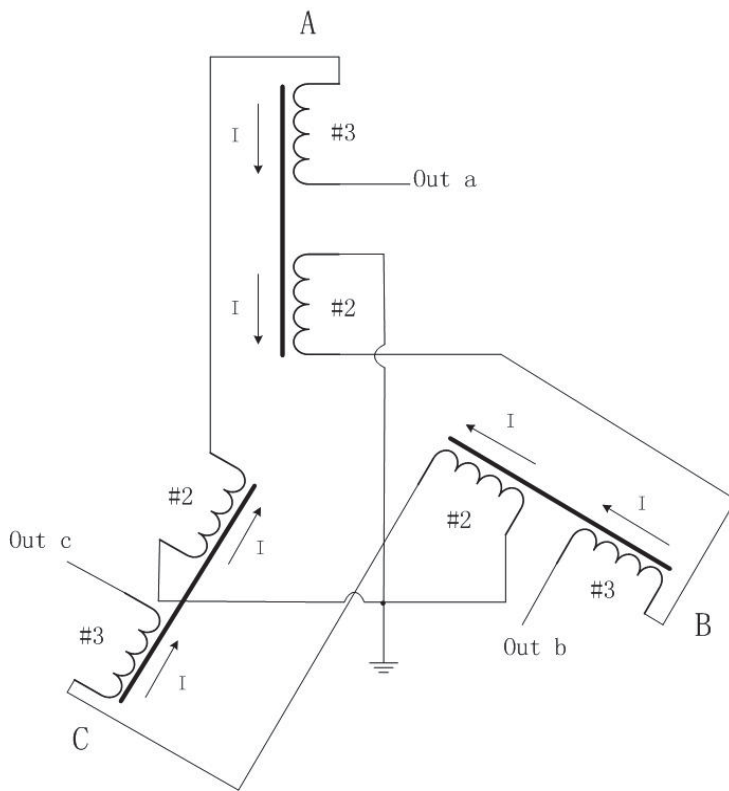


Figure 3-7 Z-Transformer (3)**

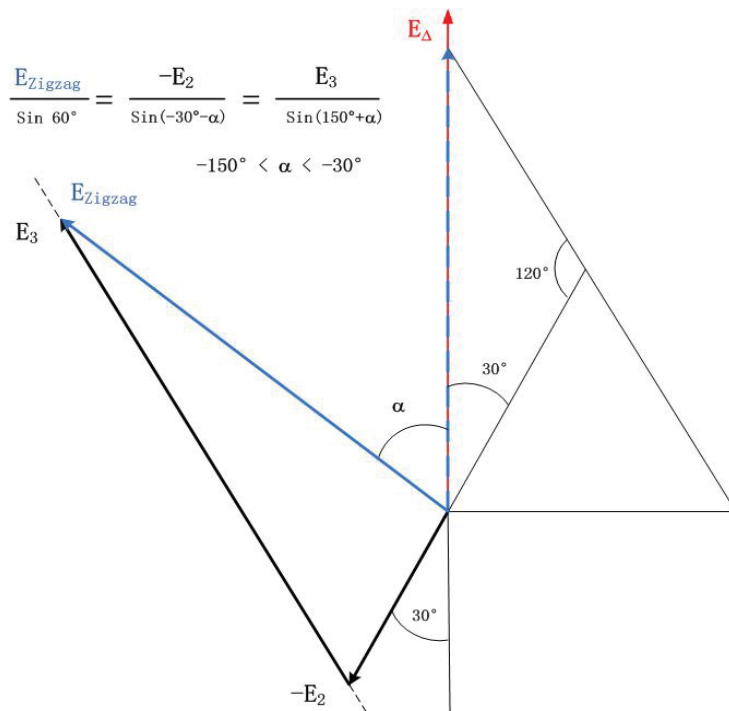


Figure 3-8 Voltage Vector Analysis (3)**

Similar conditions occur when we have to surpass negative 30 degree. Figure 3-7 and 3-8 provide just one possible way.

3.2.2 Test by PSCAD

The parameters E_{ZigZag} (E_1) is given by 20 kV, leading/lagging angle 7,5 degree and using MathCAD to calculate the numbers of winding (Figure 3-9), and get the voltages (the value is also the winding ratios) in #2 coil and #3 coil (E_2, E_3) respectively are 14,0587 kV and 8,8377 kV. We introduce the transformer standard parameter when we set (Figure 3-13).

$$\begin{aligned}
 & \circ := \text{Grad} & i^2 &= -1 \\
 & u_1(E_1, \beta^\circ) := E_1 \cdot e^{i \cdot \beta^\circ} & u_2(E_2, \theta^\circ) &:= E_2 \cdot e^{i \cdot \theta^\circ} & u_3(E_3, \gamma^\circ) &:= E_3 \cdot e^{i \cdot \gamma^\circ} \\
 & \alpha^\circ := 7.5^\circ & \theta^\circ(\alpha^\circ) &:= 30^\circ - \alpha^\circ & \gamma^\circ &:= 120^\circ \\
 & \beta^\circ(\theta^\circ) := 60^\circ - \theta^\circ & \theta^\circ(\alpha^\circ) + \beta^\circ(\theta^\circ(\alpha^\circ)) + \gamma^\circ &= 180\text{Grad} \\
 \\
 & E_2(E_1) := \frac{\sin(60^\circ - \theta^\circ(\alpha^\circ)) \cdot E_1}{\sin(120^\circ)} \\
 & E_3(E_1) := E_1 \frac{\sin(\theta^\circ(\alpha^\circ))}{\sin(120^\circ)} \\
 & E_1 := 20 & E_2(E_1) &= 14.0587 & E_3(E_1) &= 8.8377 \\
 \\
 & Q := 5\% \\
 & E_{2N} := E_2[E_1(1 + Q)] & E_{3N} &:= \frac{E_3(E_1) \cdot E_{2N}}{E_2(E_1)} \\
 & E_{2N} = 14.7617 & E_{3N} &= 9.2796 \\
 \\
 & A := 30\text{Grad} - \arccos\left[\frac{(E_1^2 + E_{2N}^2 - E_3(E_1)^2)}{2 \cdot E_1 \cdot E_{2N}}\right] \\
 & A = 6.092\text{Grad}
 \end{aligned}$$

Figure 3-9 Calculate Shift Angle with MathCAD Software**

At the same time simulate all those winding connections in PSCAD we also use a three phase voltage comparator watcher included in program. This can display the phase difference between the output voltage and the input voltage. (Figure 3-10)

After computing, the read out of the phase difference is 7,50001 degree being perfectly getting 7,5 degree which is wanted. It proves that the method of changing the numbers of winding turn to obtain different angle in Zigzag transformer is very effective.

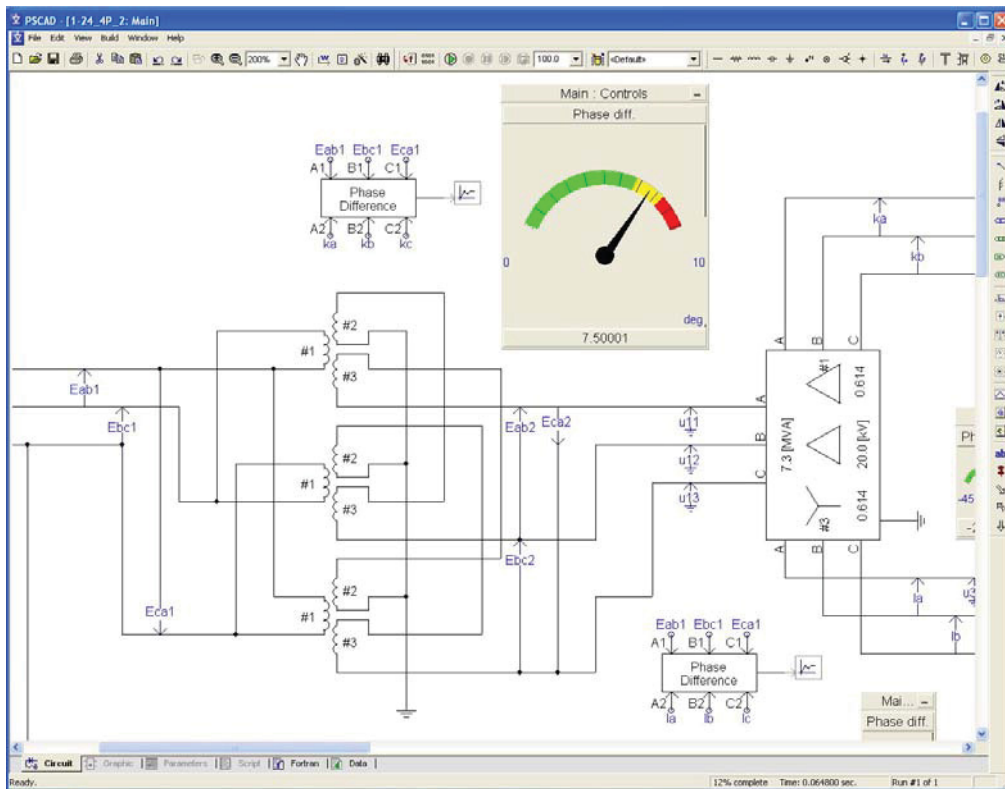


Figure 3-10 Simulation Result (Degree)**

3.2.3 24-Pulse Rectifier

The 24-pulse rectification can greatly improve the quality of output voltage. There are four connection methods to get the 24-pulse rectification with two commutation transformers which going through 2 groups of Diode Bridges in the output side (Figure 3-11). We calculate the current through each diode in the four parallel connections with the basic parameter as following:

$$\begin{aligned} \text{DC side: } U_{0AV} &= 1\,500\text{ V} & P_N &= 6\text{ MW} & \cos(\varphi) &= 0,91 \\ I_{0AV} &= 4\,000\text{ A} & S_N &= 6,6\text{ MVA} \\ I_{FAV} / I_{0AV} &= 0,167 & U_{RRM} / U_{0AV} &= 1,05 \end{aligned}$$

$$\text{So: } I_{FAV} = 668\text{ A} < 1\,310\text{ A} \quad U_{RRM} = 1\,575\text{ V} < 1\,700\text{ V}$$

(Refer to Appendix A: Avalanche Rectifier Diode 5SDA 11D1702 from ABB AG)

Then, regarding the other three connecting versions, we use the same type of diode. In order to prevent commutation failure or conduction-through, ($2 * I_{FAV} = 1\,336\text{ A} > 1\,310\text{ A}$) the design uses put two or four diodes in parallel. (Figure 3-11) Therefore, series-parallel, parallel-series type must use $2 * 4 * 6=48$ diodes, and series type must use $4 * 4 * 6=96$ diodes.

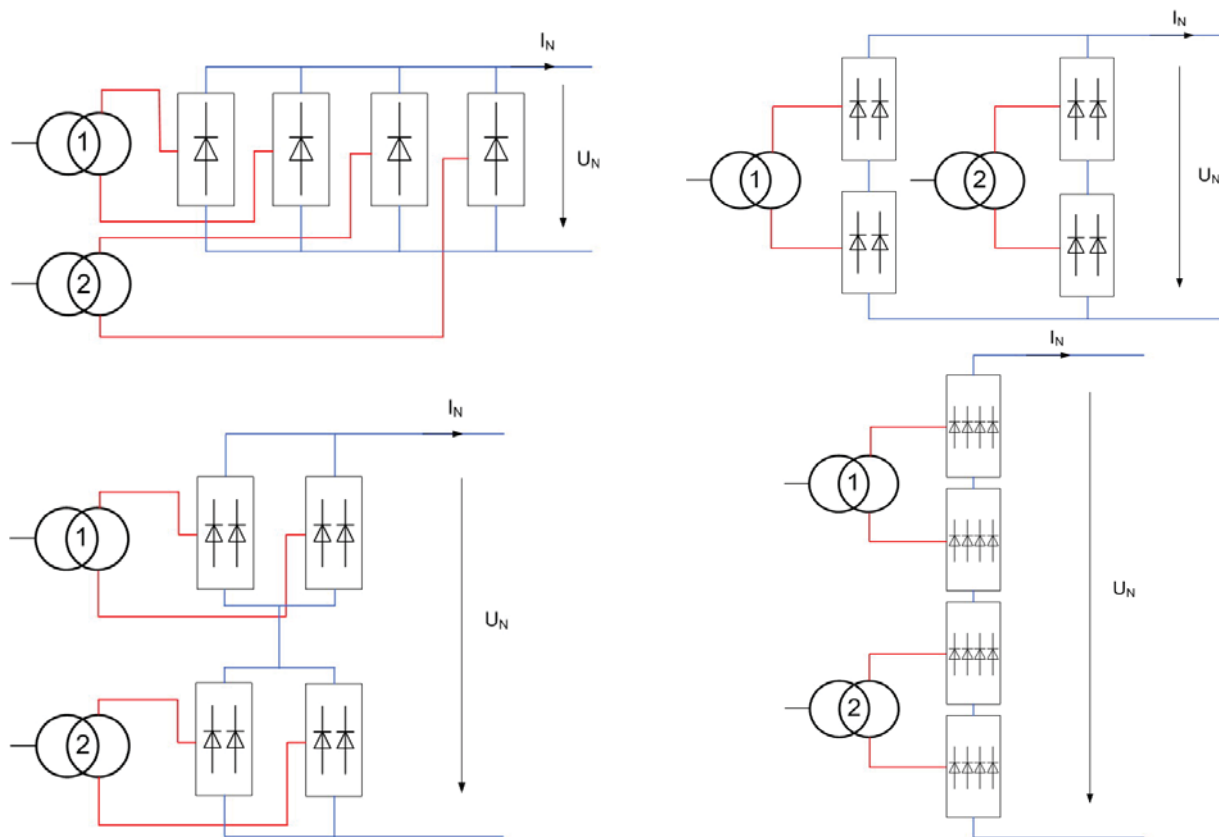


Figure 3-11 Four different connecting methods**

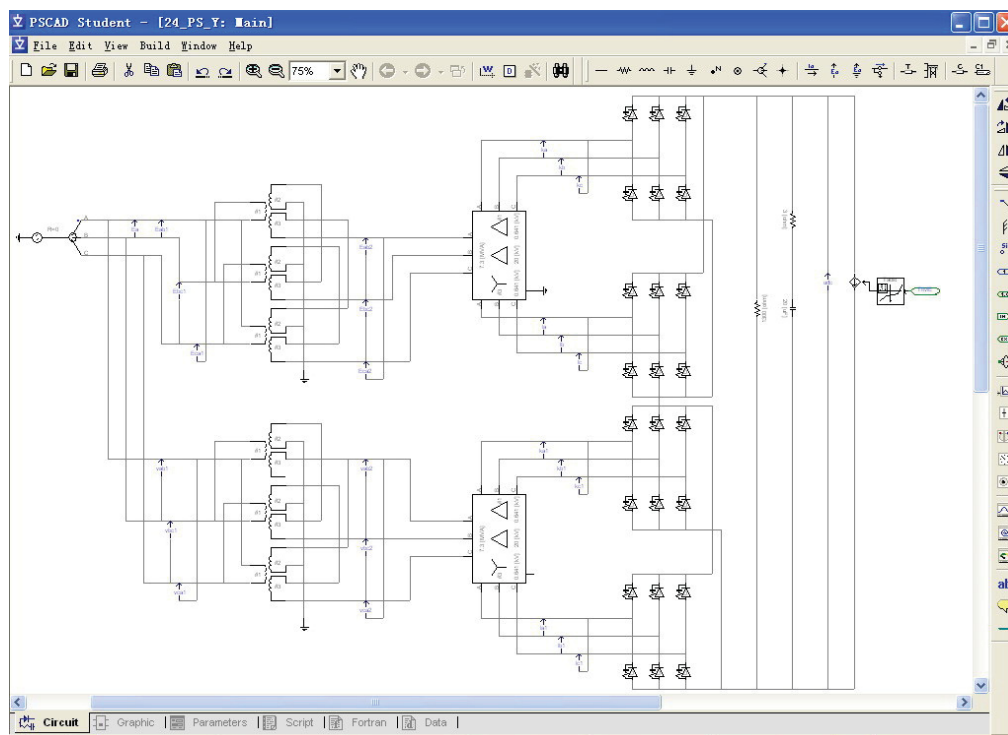


Figure 3-12 (6BU)2P2S AC/DC Rectification Simulation**

In order to obtain a stable direct current, to eliminate higher harmonic components as far as possible and to reduce ripple and harmonics in DC side. We can select the Delta/Zigzag (Dz-Transformer) and Delta/Delta/Star winding connection (Ddy-Transformer) to obtain

24-pulse direct current, (Figure 3-12) with four groups at rectification bridges, each one being composed of six diodes. These two groups three-phase Z-transformer should produce sinus output waves with respectively difference phasing (leading or lagging) with $-22,5^\circ$; $-7,5^\circ$; $7,5^\circ$ and $22,5^\circ$.

3.2.4 24-Pulse Profile

From the above information described we know that both the ripple factor and the total harmonic distortion (THD) of the 24-Pulse DC voltage profile are better than the values of the 12-Pulse AC/DC converter's output voltage coming from the traditional star and delta (Yd) transformer.

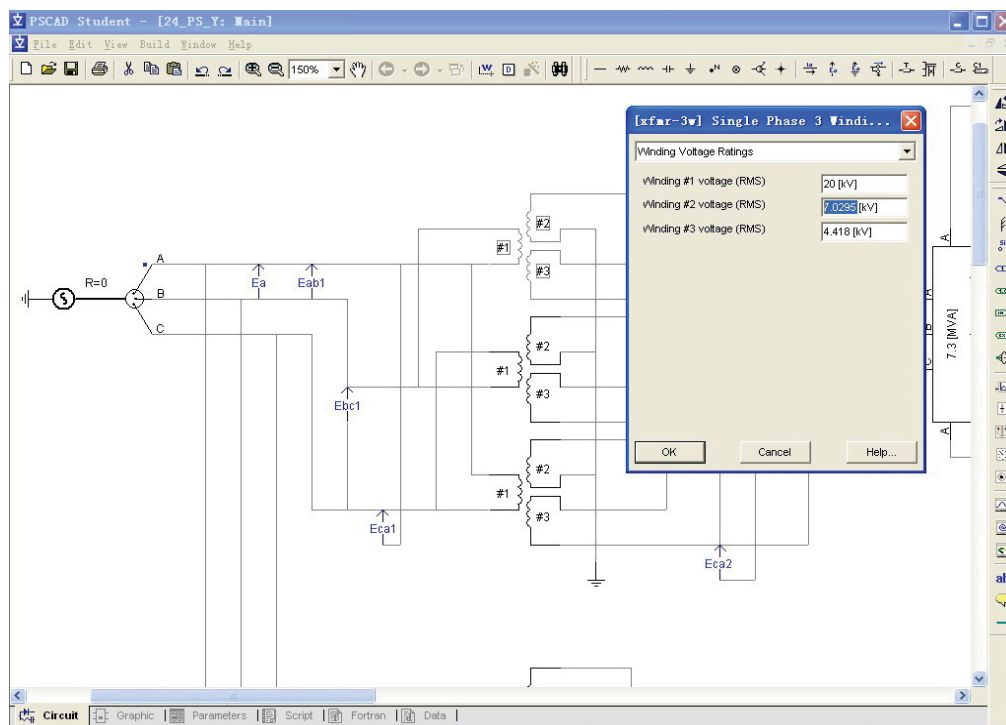


Figure 3-13 Write in Parameter**

We introduce the winding parameters into the zigzag transformer parameter list (Figure 3-13). The numbers of windings are calculated by the software MathCAD (Figure 3-9). Then we obtain the output DC voltage curve (Figure 3-14), counting the numbers of pulse in each interval of 5 ms. When frequency is 50Hz, there are 24 pulses in 20 ms (Figure 3-15).

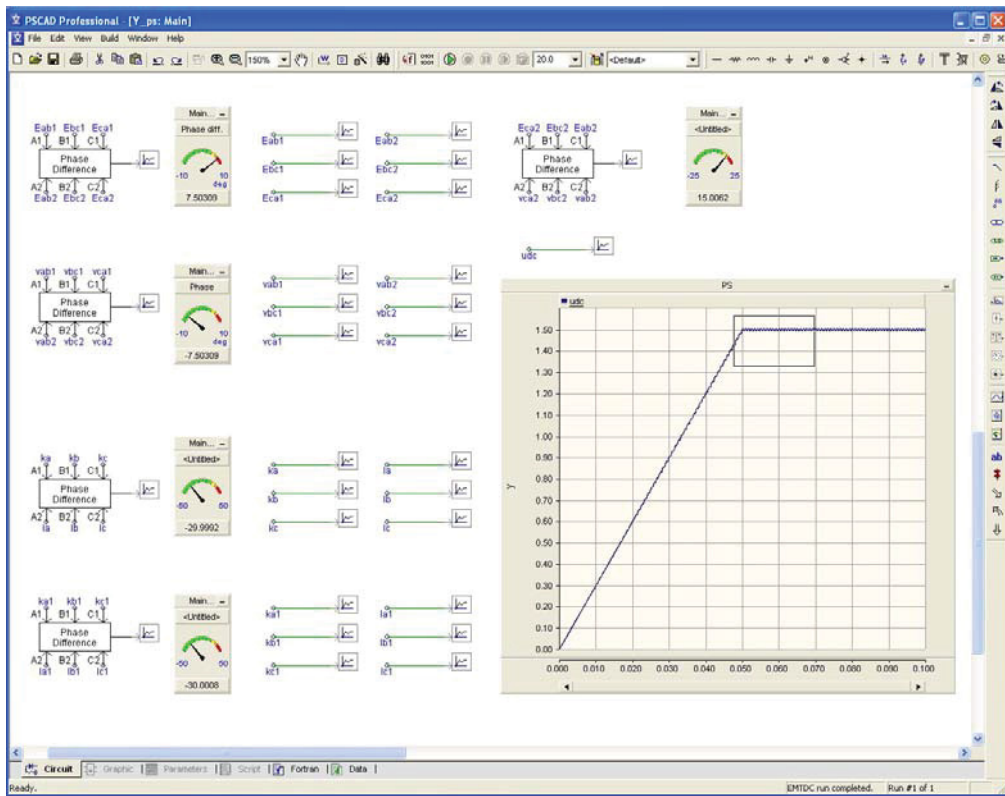


Figure 3-14 DC voltage curve**

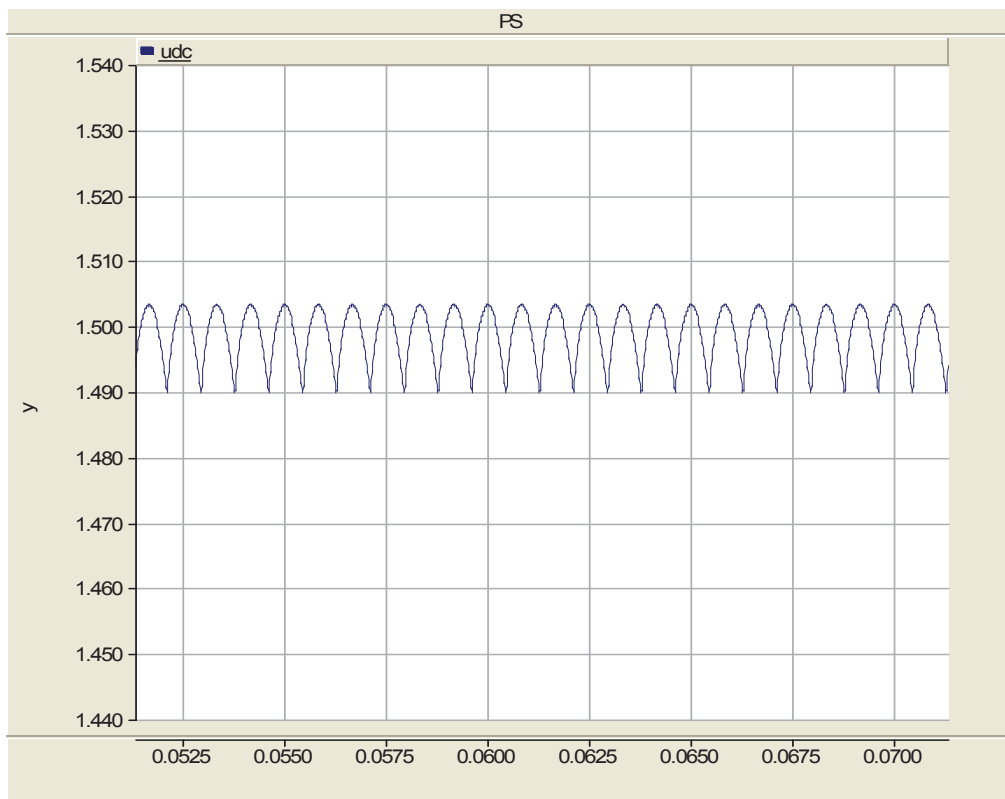


Figure 3-15 Voltage curve Zoom in**

3.3 Characteristics

The characteristics are compared in tables as follows, including 6-pulse, 12-pulse and 24-pulse rectifiers with different connections. The simulations choose the important ones but not all possible connections.

3.3.1 Basic Characteristics

Table 3-2 24-pulse Transformer Power**

| | Parallel | Parallel-Series | Series-Parallel | Series |
|-----------------|----------|-----------------|-----------------|--------|
| P_{IN} (MW) | 6,179 | 6,477 | 6,352 | 7,251 |
| Q_{IN} (Mvar) | 2,130 | 1,775 | 1,695 | 1,476 |
| φ | 19,96° | 15,78° | 12,05° | 10,98° |
| $\cos(\varphi)$ | 0,940 | 0,962 | 0,978 | 0,982 |

Table 3-3 24-pulse Voltage Regulation**

| | | Parallel | Parallel-Series | Series-Parallel | Series |
|-------|-----------|----------|-----------------|-----------------|----------|
| U_0 | | 1,560 kV | 1,576 kV | 1,570 kV | 1,569 kV |
| VR(%) | I_{dN} | 4,00 | 5,07 | 4,67 | 4,60 |
| | $3I_{dN}$ | 20,46 | 31,33 | 30,83 | 84,59 |

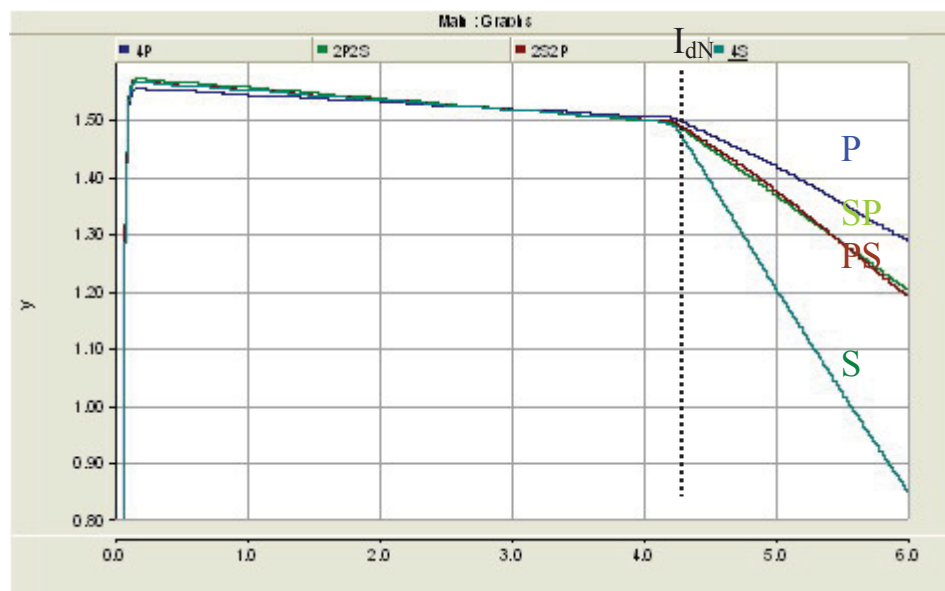


Figure 3-16 Curves of Voltage Regulation**

The curves in Figure 3-16 are obtained with rated voltage of 1,5 kV and rated current of 4,0 kA. The load runs from no-load to 300% I_{dN} ($t < 60s$, IEC 60146-1).

Table 3-4 24-pulse Transformer Losses**

| | $P_0=P_{Fe}$ (kW) | $P_K=P_{Cu}$ (kW) | P_N (MW) | η (%) |
|-----------------|-------------------|-------------------|------------|------------|
| Parallel | 3,67 | 69,01 | 6,0 | 98,80 |
| Parallel-Series | 3,76 | 65,89 | 6,0 | 98,85 |
| Series-Parallel | 3,74 | 94,74 | 6,0 | 98,39 |
| Series | 3,90 | 109,95 | 6,0 | 98,14 |

Table 3-5 24-pulse Short Current**

| | Parallel | Parallel-Series | Series-Parallel | Series |
|--------|----------|-----------------|-----------------|--------|
| I (kA) | 33,92 | 33,16 | 33,24 | 23,76 |

Table 3-6 THD in no-load**

| Pulse | 3 | 6 | 12 | 24 |
|-----------------------------------|-----------|-----------|------------|-----------|
| Theoretical THD | 18,271 % | 4,197 % | 1,028 % | 0,256 % |
| Simulation the 24-Pulse Rectifier | | | | |
| Full load | Series | Series-P | Parallel-S | Parallel |
| THD | 0,11255 % | 0,11255 % | 0,11255 % | 0,11267 % |

Table 3-7 Ripple factor for d.c.**

| Pulse | 6 | 12 | | 24 | | | |
|---------------|--------|--------|--------|--------|--------|--------|--------|
| Ripple factor | 7,18 % | 1,73 % | | 0,43 % | | | |
| Simulation | 7,19 % | 2S | 2P | 4S | 2S2P | 2P2S | 4P |
| | | 1,75 % | 1,53 % | 0,55 % | 0,61 % | 0,57 % | 1,17 % |

Table 3-8 Commutation ratio**

| Pulse | 6 | 12 | | 24 | | | |
|-------------------|------|------|------|------|------|------|------|
| connect | / | 2S | 2P | 4S | 2S2P | 2P2S | 4P |
| q | 3 | 3 | 3 | 3 | 3 | 3 | 3 |
| s | 2 | 4 | 2 | 8 | 4 | 4 | 2 |
| U_{di} / U_{V0} | 1,35 | 2,70 | 1,35 | 5,40 | 2,70 | 2,70 | 1,35 |
| measure | 1,35 | 2,70 | 1,35 | 5,40 | 2,72 | 2,79 | 1,40 |

3.3.2 Harmonics on AC and DC Side

Table 3-9 Superposed AC voltage on DC side**

| Pulse | k | h | U_h / U_{di} | Simulation | | | |
|-------|---|----|----------------|------------|---------|---------|---------|
| | | | | 4S | 2S2P | 2P2S | 4P |
| 24 | 1 | 24 | 0,246 % | 0,762 % | 0,719 % | 0,777 % | 0,970 % |
| | 2 | 48 | 0,061 % | 0,342 % | 0,448 % | 0,354 % | 0,315 % |

Table 3-10 Harmonic current on AC side**

| Pulse | k | h | I_h / I_{i1} | Simulation | | | |
|-------|---|----|----------------|------------|---------|---------|---------|
| | | | | 4S | 2S2P | 2P2S | 4P |
| 24 | 1 | 23 | 0,043 % | 1,109 % | 2,761 % | 0,690 % | 1,293 % |
| | | 25 | 0,040 % | 0,826 % | 2,037 % | 0,409 % | 0,350 % |
| | 2 | 47 | 0,021 % | 0,263 % | 0,485 % | 0,186 % | 0,374 % |
| | | 49 | 0,020 % | 0,219 % | 0,297 % | 0,089 % | 0,118 % |

Now after PSCAD simulation we can get the harmonic analysis for the four different connections. The results are the same as the theoretical value. (Figure 3-17) Referring to the figures in Appendix C we see that harmonics on the AC side contain not only the frequencies $(24n \pm 1)f$ but also exhibit the frequencies $(6n \pm 1)f$, because the 24-pulse circuit is built by B6U with different topology.

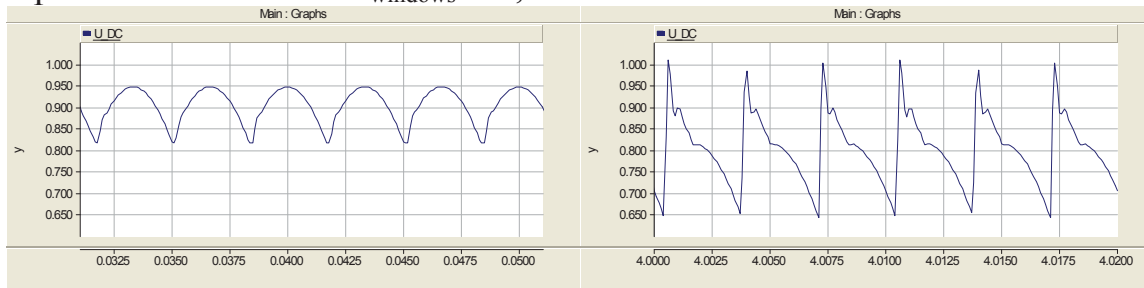


Figure 3-17 FFT analysis for Harmonics**
Superposed alternating voltage on the DC side (above)
harmonic current on the AC side (below)

3.3.3 THD and Voltage Profile

The comparison of the different types of rectifiers (6-pulse, 12-pulse uncontrolled, 12-pulse with firing angle controlled, and 24-pulse uncontrolled) yields:

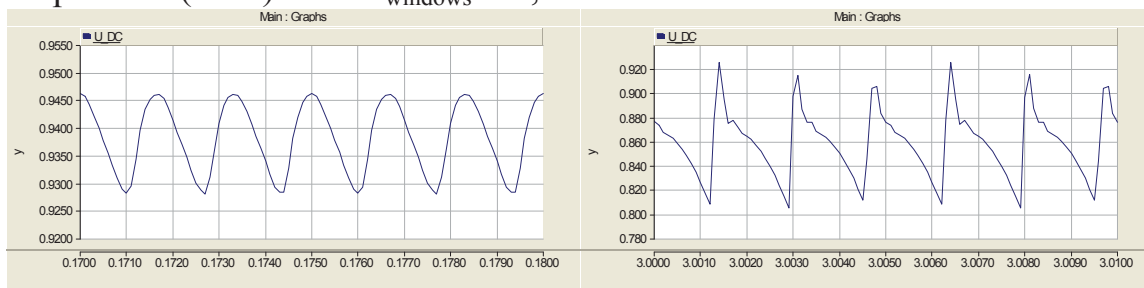
6 pulse in **B6U** $T_{windows} = 0,02s$



THD = 2%

THD = 10%

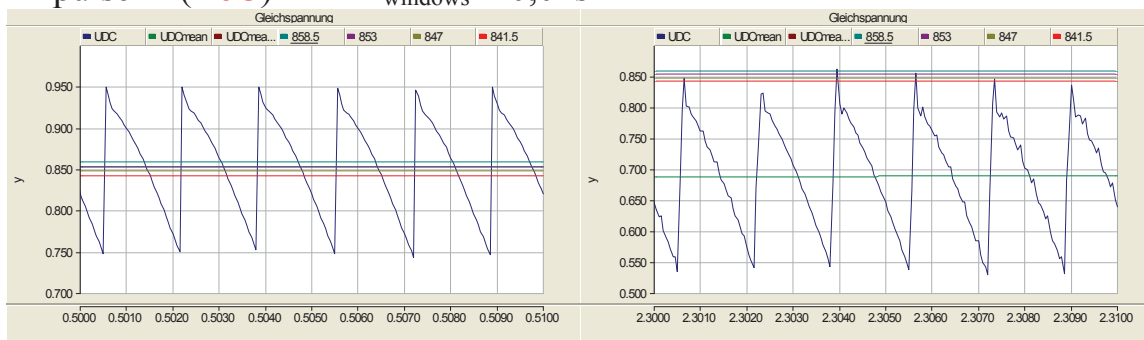
12 pulse in **(B6U)2P** $T_{windows} = 0,01s$



THD = 2%

THD = 4%

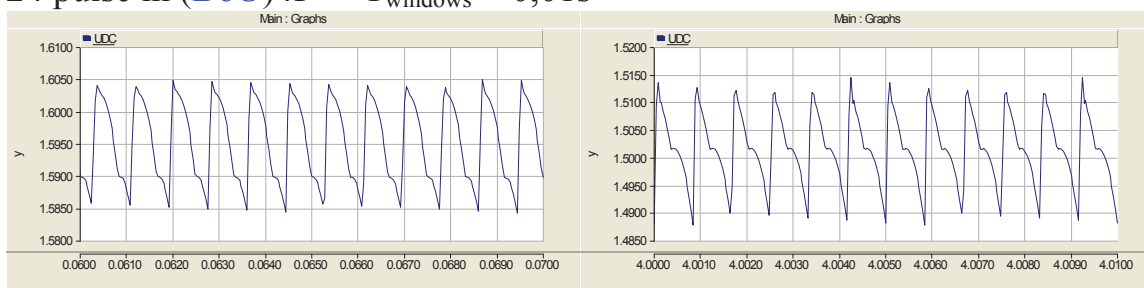
12 pulse in **(B6C)2P** $T_{windows} = 0,01s$



THD = 6%

THD = 5%

24 pulse in **(B6U)4P** $T_{windows} = 0,01s$



THD = 2%

THD = 3,5%

Figure 3-18 Left: no-load (idling) operation; Right: operated at rated current.

3.3.4 Inductive Direct Voltage Drop (d_x)

The inductive direct voltage drop is related to the output voltage and current by following formula:

$$d_x = f(I_d) = (U_{Imp} / 2I_{dN}) * I_d \quad (3.1)$$

$$U_d = f(d_x) = U_{d0} * (1 - d_x) \quad (3.2)$$

We get the I - d_x curve with 24 pulse rectifier in different connections (Figure 3-19).

Next we calculate the relation between d_x and THD for a load varying from zero to 300% rated load (during short interval of less than one minute). (Figure 3-20)

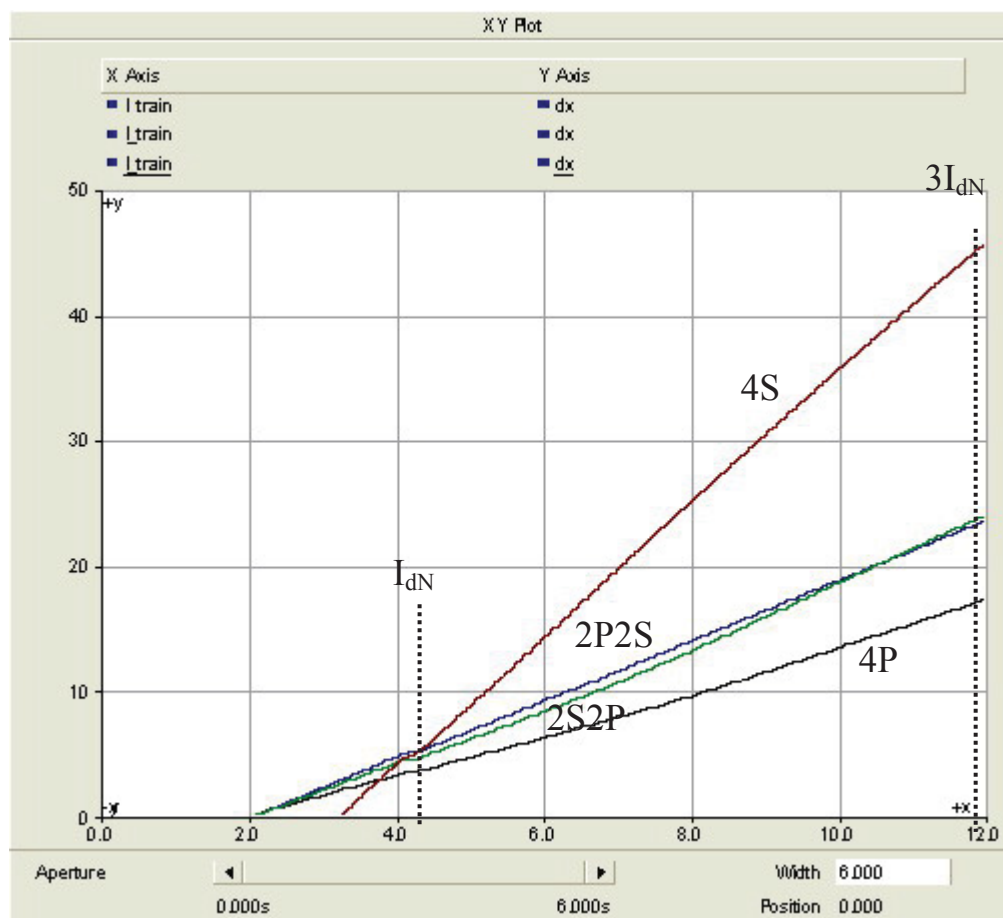


Figure 3-19 24pulse I_d - d_x Curve*

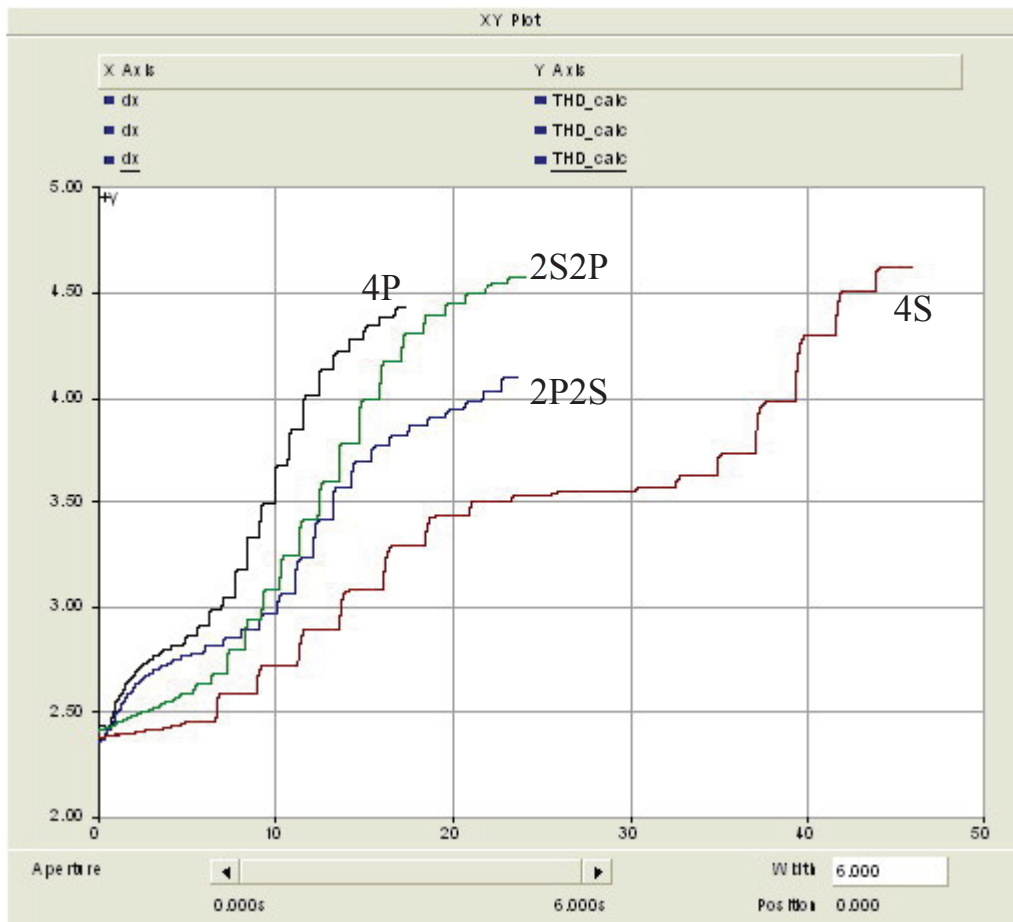


Figure 3-20 24 pulse d_x -THD Curve*

3.4 Summary

Table 3-11 General Evaluation*

| Pulse | 6 | 12 | | 24 | | | | Reference |
|-------------------------|----|----|----|----|------|------|----|--------------------------|
| | | 2P | 2S | 4P | 2P2S | 2S2P | 4S | |
| cos (ω) | | | | + | ++ | ++ | ++ | Table 3-2 |
| voltage regulation | | | | ++ | + | + | -- | Table 3-3 Figure 3-16 |
| η | | | | + | + | + | + | Table 3-4 |
| Short current | | | | + | + | + | + | Table 3-5 |
| Ripple factor | -- | + | + | + | ++ | ++ | ++ | Table 3-6 |
| U_{di} / U_{V0} | ++ | ++ | + | ++ | + | + | -- | Table 3-8 |
| THD | -- | + | | + | | | | Chapter 3.3.3 |
| d_x | | | | ++ | + | + | -- | Chapter 3.3.4 |
| Robustness | -- | + | - | ++ | + | + | - | Chapter 4 |
| anti-harmonics from net | | | | ++ | ++ | - | -- | Chapter 4.3 |
| Economic | ++ | + | | - | | | | |

Note: ++ very good; + good; - not good; -- bad; empty no assessment.

3.5 36-Pulse Rectification and Improvement

3.5.1 Normal 36-Pulse rectification

Using a similar method to get 36-pulse rectification as in 3.2 we may construct 36-pulse rectification using the PSCAD rectification transformer. (Figure 3-21). In this figure, each red dashed line ellipse is a transformer. We have to use six three-phase Zigzag transformers for this method. Regarding the transmission energy for track transportation the transformer rating may reach Mega Volt-Amp level. So it is not cheap that we add such number of transformers in the system. Furthermore, it affects not only the system reliability but also robustness in operation.

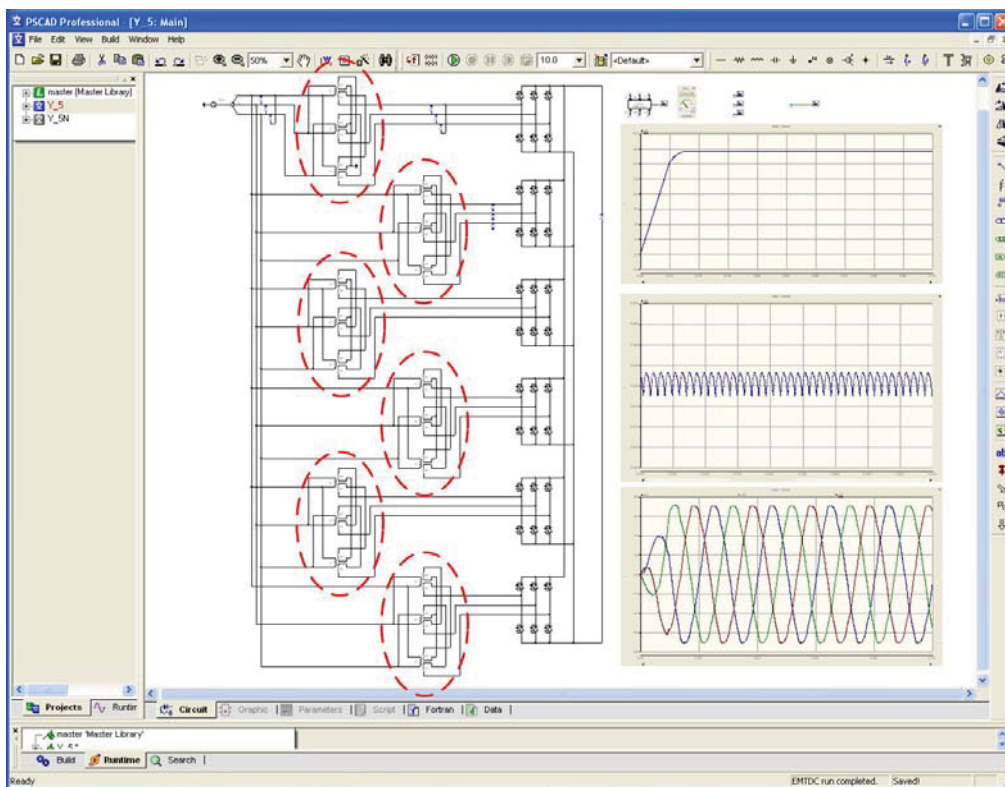


Figure 3-21 Normal 36-Pulse Rectification**

When comparing the normal 36-pulse rectification with the 24-pulse rectification, there is no obvious advantage on the harmonic elimination. Especially when we use inexpensive and more reliable RC filter loops on the 24-pulse rectifier there is no value to apply 36-pulse rectification.

3.5.2 Principle of Advancing Rectification

We discuss increasing the numbers of windings only at limited extent and reduce the numbers of transformer (the later is less than four, because the 24-pulse rectification must use two Zigzag transformers and two Y/D transformers together).

For this topology, we can reduce the filter loop and get a rectification performance enhancement without high expenditure (cost is naturally reduced). With this kind of idea, we described one improvement method for the 36-pulse rectification.

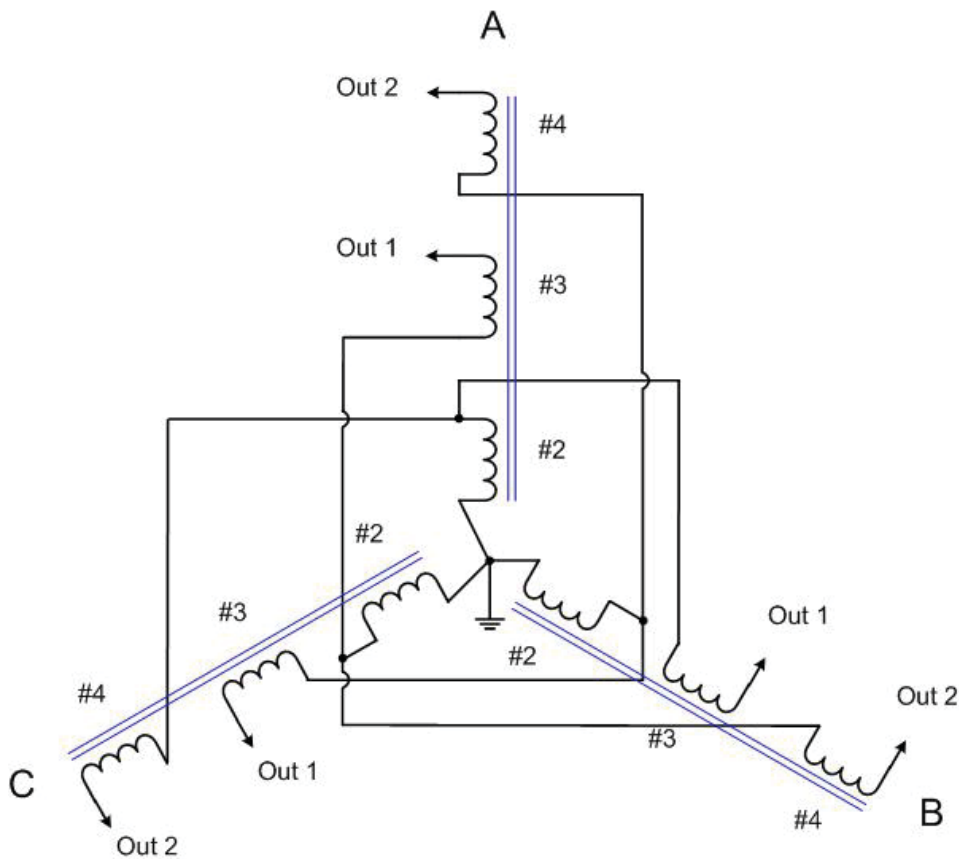


Figure 3-22 Secondary side of Four Windings Zigzag Transformer**

The analysis of the voltage vector is given in Chapter 3.2. We can obtain the direction of current in the secondary side of Zigzag transformer directly deciding the output voltage vector direction.

When we add the groups of coils (#4) at the secondary side (Figure 3-22), then the #2-#3 and the #2-#4 separately compose one Zigzag transformer in secondary side. Afterwards we exchange the phase of #4 coil into clockwise direction and then connect it to the #2 coil. (Figure 3-23)

The phase shift angle of #2-#3 transformer is equal to the phase shift angle of #2-#4 transformer (supposing the numbers of winding in #3 and #4 coils being the same), also the length of voltage vector is equal. We take the direction of voltage vector in primary side as 12 o'clock. (Figure 3-23)

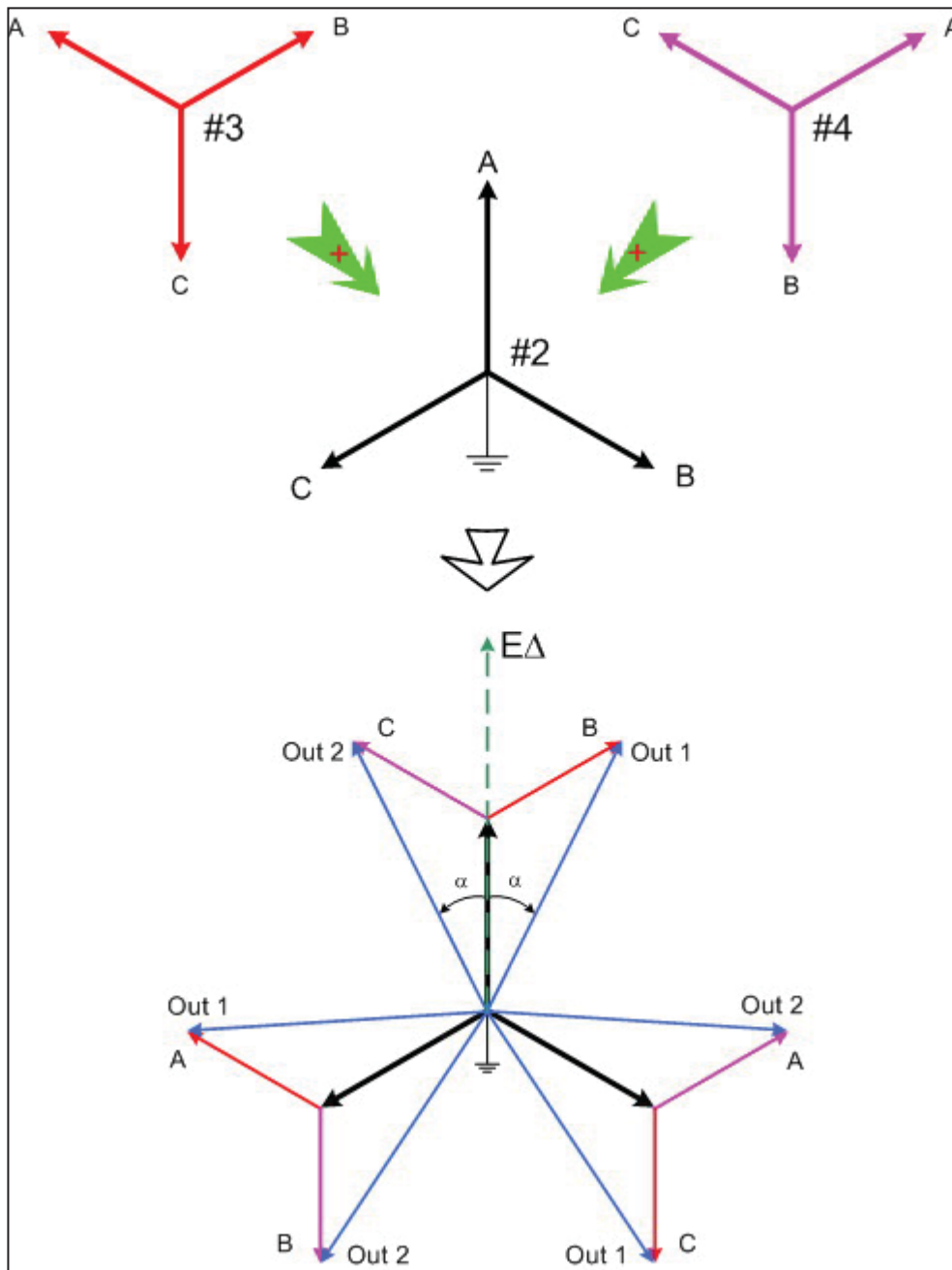


Figure 3-23 36-Pulse Voltage Vector Analysis**

From Table 3-1, we know that if the phase shift angles are $\pm 5^\circ$, $\pm 15^\circ$, $\pm 25^\circ$, the output DC voltage after the rectification bridge can be taken. (the 36-pulse rectifier bridge) In the Figure 3-24, each blue dashed line ellipse represents a four-winding Zigzag transformer. This new system produces smoother DC output.

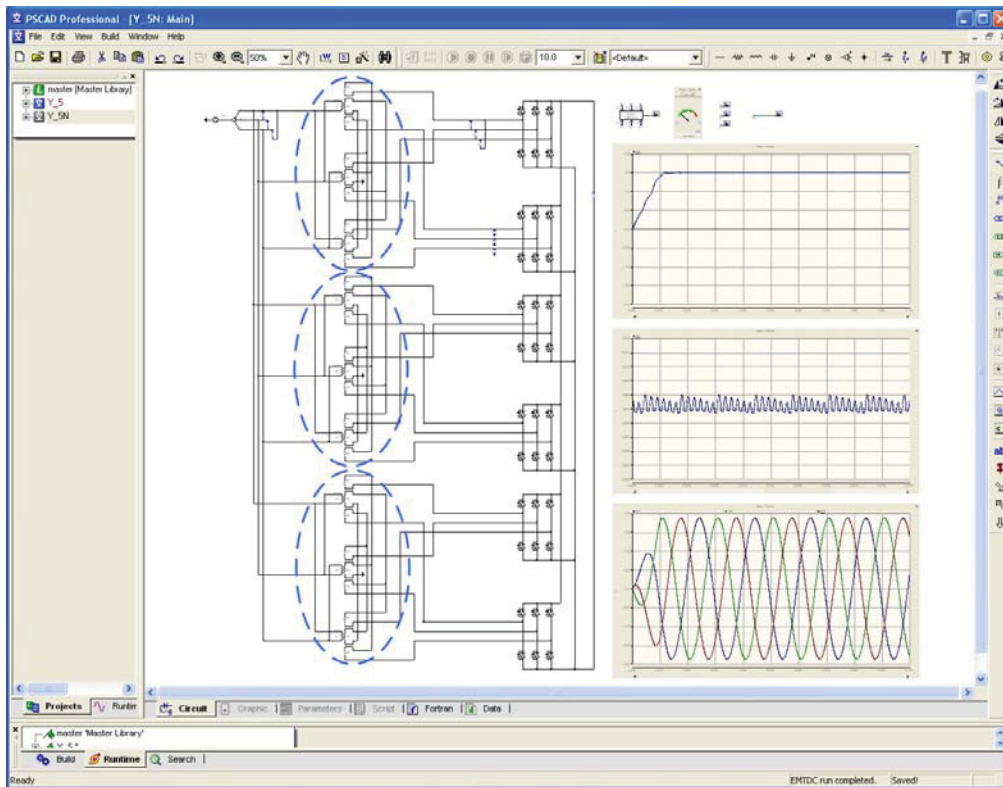


Figure 3-24 Advanced 36-Pulse Rectification**

3.5.3 Assessment

On the right side of Figure 3-21 and Figure 3-24, there are the simulation output results obtained by PSCAD in normal configuration and new configuration respectively. The middle of three result-windows in these two figures is enlarged so we can see the results clearly. At the bottom of three windows there is the three phase voltage wave in front of the rectification bridge.

Compared to two modals output voltage profiles, there is no large difference between both designs. However, we should test all kinds of magnetic and electrical characteristics before we can say good or not. Presently, we just did the first step.

4 Faults and Harms

4.1 Short-circuit on Diode

We insert two kinds of faults in rectification as supposition to simulate on the diode D4 of Rectifier Bridge 1 as shows on Figure 4-1:

1. Short-circuit over D4.
2. Disconnect on the welding points of D4. (Chapter 4.2)

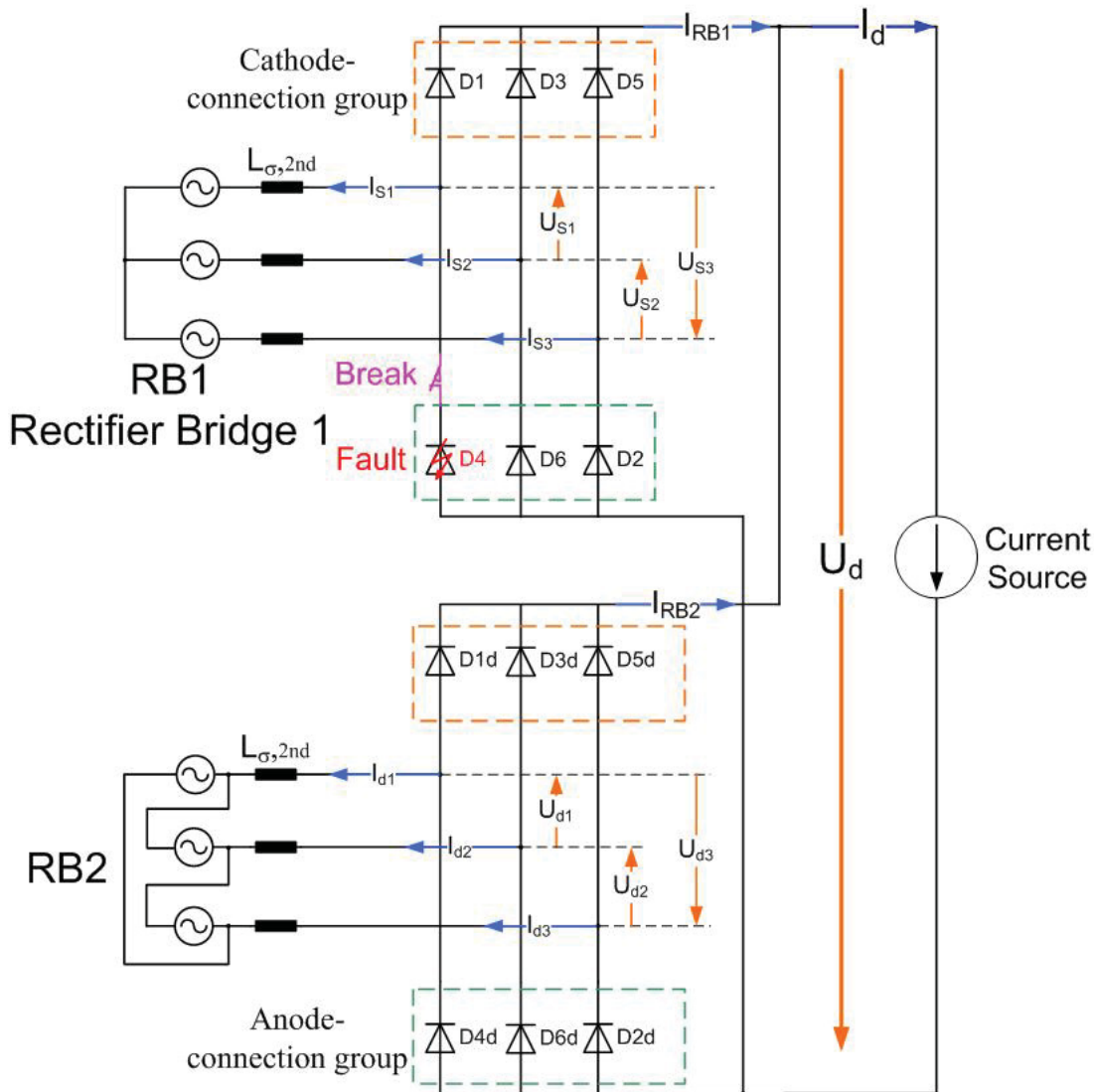


Figure 4-1 Diagram for Diode Faults**

At first we suppose D4 to produce an anode-to-cathode short-circuit the resistance is nearly zero. The whole system has to survive of a short interval time (no longer than 1 second). We see the results of the currents and voltages on each branch. (Figure 4-2)

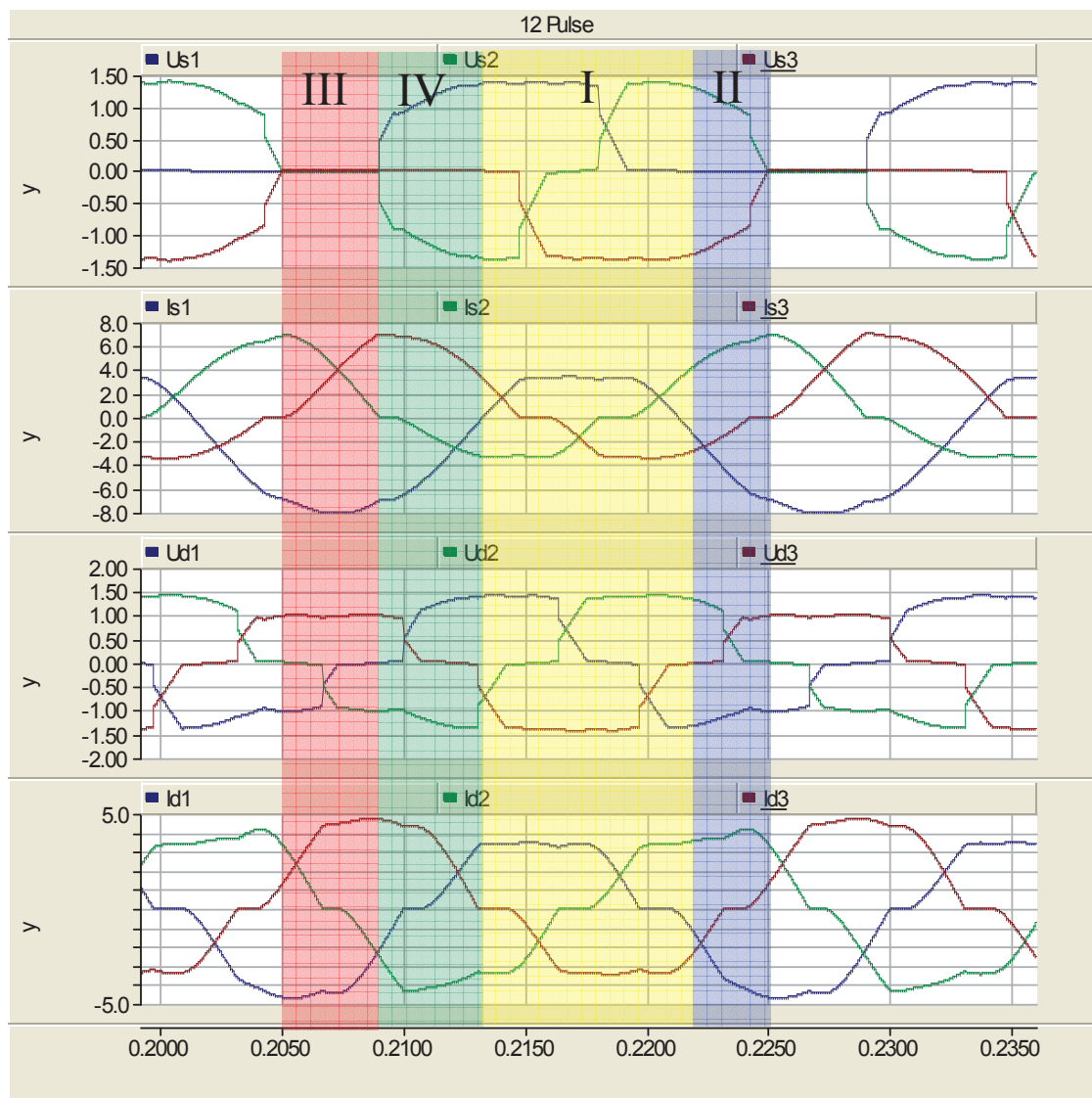


Figure 4-2 Results on the each branch when diode short-circuit*

Here we can recognize four areas on one period. (Figure 4-2)

Area I: In this time area the rectifier bridge 1 (RB1) behaves as in normal operation. The short-circuit branch of the diode D4 provides a conducting path over the course of its branch voltage. Therefore, the diode short-circuit within this range does not have an influence on the operational behavior of the group of static inverters. The entire load current I_d divides itself (except for the circle current) in equal parts on the ways of the two rectifier bridge I_{d1} and I_{d2} . The voltage U_d over both parallel connected rectifier bridges are equal to nominal DC voltage. At present the operating condition is symmetrical.

Area II: There are two-poles short-circuit between the diode D4 and the diode D6 in the anode-connection group of commutations. Thereby D4 works as short-circuit.

In this area during normal operation (without diode short-circuit) the diode D4 is conducted. Since the two-pole short-circuit in the anode-point group of

commutations is not kept and the voltage difference of the branch with diode D6 continues to drop, the currents I_{S1} and I_{S2} increase because of the voltage over the diode group more than the rated value thereby.

To the end of Area 2 the value of current I_{S3} is zero (D5 is in conducting state). Two branches of short-circuit carry the entire prospective current of a circuit. The voltage as well as the current in the RB2 rises in this time. The RB2 carry the total current I_d at the end of A2.

Through the two-pole short-circuit between the secondary windings the voltage over the short-circuit winding (star-connection) drops to zero. The current adjusts itself in those short-circuit windings in each case which compensates the voltage in those secondary winding according to the Lenz's rule. Thus current drops in two sides of the iron core within the transformer 1.

Area III: There are three-pole short-circuits in this area. In the secondary winding of the Transformer 1 flow only the short-circuit current.

The RB2 transfers the entire load current I_d in this area. The voltage over the RB2 has double the nominal value due to increasing voltage over the secondary winding of the transformer 2. Through parallel connection of the two rectifier bridges at the DC bus-bar of the substation DC voltage U_d increases likewise to the double nominal value. Current conditions are the same as Area II applies.

The characteristics with the fault are that the short-circuit current in the RB1 does not come into effect due to the misalignment short-circuit character in primary side. The characteristics lie with constant load in the traction network in the order of magnitude of double the rated current. This realization has remarkable influence on the protection concept of the plant.

Area IV: The three-poles short-circuit in the RB1 is decreasing. One reason is that the current in the branch of D6 at the end of Area III goes to zero. If the current on D6 is zero, the diode turns off and this makes a positive voltage over the D3 automatically.

There is a two-poles short-circuit in the anode-connection group of commutations of the RB1 between the D2 and D4. At the half-time of Area 4 the diode D3 works due to the positive voltage, the current in the cathode-connection group of commutations rises. Thus the current in the diodes D2 and D4 sink. Over these two branches a negative voltage emerges by itself. The RB1 takes over a portion of the load current I_d .

Since the voltage does not over the RB1 and thus the voltage on the secondary winding of the Transformer 1(T1) is nearly zero the current on the T1's iron core

increases. The voltage over the primary winding of this transformer rises consequently. The voltage difference between the T1 and T2 is reducing.

At the end of Area IV the voltage difference nearly goes to zero over the two rectifier bridges and thus both windings of the transformers have the equal voltage. Both rectifier bridges lead the half load current. The voltage on the bus corresponds to its nominal value.

From analyze of the fault process we want to disconnect immediately when the fault happens. One possibility of fault recognition lies in the monitoring of the output DC voltage U_d . It is clear that when the voltage is raised beyond the nominal value, the reason with highest probability is a diode fault. Over a data link between the protective devices at the distance branches and the protective devices and/or directly to the circuit-breaker of the primary voltage side an "OFF" signal can be transmitted in the case of a clear increase of the voltage U_d . Thus the fault can be switched off.

4.2 Interruption on a Diode

Usual faults generally erect a forward and reverse conducting element with semiconductor used for rectifiers. However, also an interruption shall be considered. When the diode junction is not working any more because it receives heavy stress or the diode operation heating produces a deformation such a diode disconnection fault can occur. Thus establishing a break (D4 branch opens when we give a signal) on the D4 branch we simulate the condition of an interruption of diode D4. (Figure 4-1)

Now we obtain the current and voltage results on each branch and recognize two areas on every period from Figure 4-3.

Area I: In this area the rectifier bridge 1 (RB1) behaves as in the normal operation. The voltage on break branch of D4 is negative, so as a standard D4 is off and the other diodes work without being influenced by the conduction loss.

Area II: In this range, when there is no break fault on the diode, the voltage on line C rises and drops on line A so the current naturally flows in a transient from D2 to D4. After this transient, the voltage between phase A and B is constant.

But now D4 is broken, the current I_d flows back only through D2. The path is from D3 to the load then back over D2. The abnormal current flowing way is taken until the current on the line C drops to zero. At this time the voltage between AC also unceasingly reduces to the normal value.

After some time meaning that we have to wait for a voltage rise high enough to open the diode D6 again, the current now on cathode-connection group of RB1 flows commuting from D3 to D5. The current flows through D5 to the load then

back over D6. The voltage on line B (U_{S2}) continuously drops. The abnormal current commutation on D4 is over at this time the voltage on line B (U_{S2}) is lower than on line A (U_{S1}).

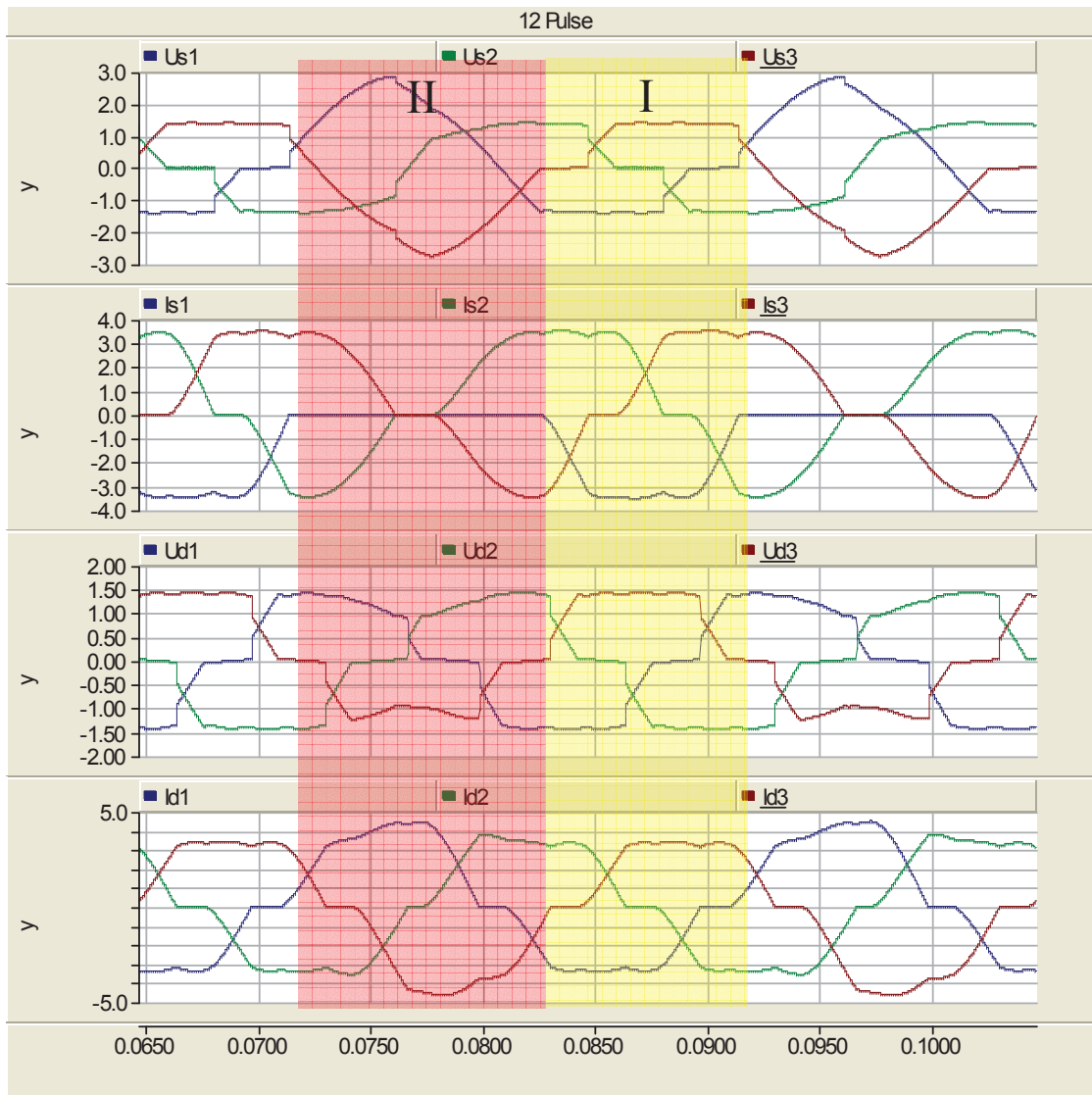


Figure 4-3 Results on branch when diode conduction is interrupted*

In Area II, the currents on RB2 increase when I_{RB1} is decreasing because the output current I_d is maintained due to the current source at the load side. Simultaneously, the voltage U_d is going down to maintain the power output.

Now we can compare the fault of the short-circuit and the break fault. Although the fault current with break-fault is not as large as the short-circuit current the voltage on D2 and D6 which are in the same group of the broken diode D4 exhibit a crest value of nearly double the normal value. Such a condition was not intended.

4.3 Harmonics from Net

In actual operation the transformer for electric locomotive trains gain the energy from the electrical network. Anyhow, it is impossible that only one user is on this electrical network. When the harmonics made by other users on-line are transferred through the transformer substation, in the same way the harmonics can come from the AC side to the DC side through the rectifier-diodes. We want to obtain the outcome by simulating with these harmonics on the AC side as input source. The parameters refer to Table 4-1 for peak harmonics levels defined with EN50160.

Table 4-1 Odd-numbered Harmonics (non-multiple to 3)*

| | | | | | | | | |
|----------------|-----|-----|-----|-----|-----|-----|-----|-----|
| Order number v | 5 | 7 | 11 | 13 | 17 | 19 | 23 | 25 |
| U_v % | 6,0 | 5,0 | 3,5 | 3,0 | 2,0 | 1,5 | 1,5 | 1,5 |

(Source from EN 50160:1999)

Operating at full load we measure THD at AC and DC side, the active power, the reactive power and the power factor. Results are presented in Table 4-2.

Details are given in Appendix B. Comparing the FFT results on both AC side and DC side it is clear to observe that Parallel and Parallel-Series connections are better than the others and the Parallel connection has the smallest effect by the harmonics from outside.

Referring to the power factor $\cos(\varphi)$, these four connection types have no large difference between each other.

Table 4-2 Full load with harmonics from net**

| | | Parallel | Parallel-Series | Series-Parallel | Series |
|----------------|-----|----------|-----------------|-----------------|--------|
| THD % | In | 4,67 | 4,58 | 7,23 | 9,40 |
| | Out | 6,49 | 6,10 | 4,40 | 4,49 |
| $\cos(\omega)$ | | 0,945 | 0,965 | 0,966 | 0,955 |
| P (MW) | | 4,884 | 5,065 | 4,994 | 4,827 |
| Q (MVar) | | 1,654 | 1,351 | 1,293 | 1,165 |

5 Harmonic Analysis for SNCF

Along with the equipment renewal, SNCF (Société Nationale des Chemins de fer Français, en: French National Railway Company) wants the new transformer which can fulfil the specification while operating. At the same time, investment should not be high. Generally, the locomotives in the southern area of France use the 1,5 kV direct voltage net for electric trains. Therefore, the AC/DC rectification transformer is an important component in energy transmission.

5.1 SNCF Requirements on rectifier

SNCF defined as standard for rectification and transformation the 20-kV-line-ground voltage 50Hz 3-phase AC input and 1,5 kV / 6,6 MVA DC output. According to Chapter 3 about 24-pulse Zigzag transformer rectification, we can observe that the voltage quality in the transformer's primary side is obviously influenced directly when the load changing. On the other side, the transformer itself also has the limitation in operation when an overload happens or a short-circuit current occurs by a lighting at the load side. These two aspects for the same transformer are contradictory. The engineers in SIEMENS initially defined the transformer simulation parameter scope as follows:

- a) The parameters for the 24-pulse rectifier and short circuit impedance, together with voltage and current ratings of the transformer are:
- Line voltage: 20 kV
 - DC side no load voltage: 1 742 V
 - Rated DC current: 4 000 A
 - Coupling between secondary windings of one transformer: no larger than 0,20 (typically 0,15)

The following conditions have to be fulfilled, and we give an explanation of reasons when these conditions are not met:

- DC voltage at 4 kA: not smaller than 1 650 V
- DC short circuit current: not larger than 40 kA

At the beginning we expect that the short circuit impedance respectively leakage inductance voltage will be around 7% to 8%. In any case we need the exact value. It could also be possible that both conditions could not be fulfilled together.

- b) We make a FFT analysis of the current with resistor as load at the following conditions:
- Change the number of turns (equivalent the voltage) of the delta windings of the zigzag-transformer about - 5 %, - 2,5 %, +2,5 % and +5 %
 - Adjust the mains voltage (20 kV) but the load current must be constant at 4,4 kA

In addition the Z transformer caused a certain fluctuation of the output voltage when the input changes. These results should be compared with the results of the rated input voltage situation. The 24-pulse Z transformer rectifies the input energy and has 4 different kinds of output connections, which are parallel, parallel-series, series-parallel and series connection. Therefore, we also compare the results with each other at those 4 types of situations.

5.2 Software Familiarization and Preparation before Simulation

We familiarize with the simulation software and get on understanding how the actual electric circuit works. The Harmonic FFT analysis element is built in PSCAD software. (Refer to Chapter 1.2.2) With the help of the FFT output window we can read the FFT analysis results not only in data table but like Figure 5-1. (PSCAD puts the basic wave as 100%; in Figure 5-1 “[23] 1,02253 ” means the 23rd harmonic is 1,02253 %)

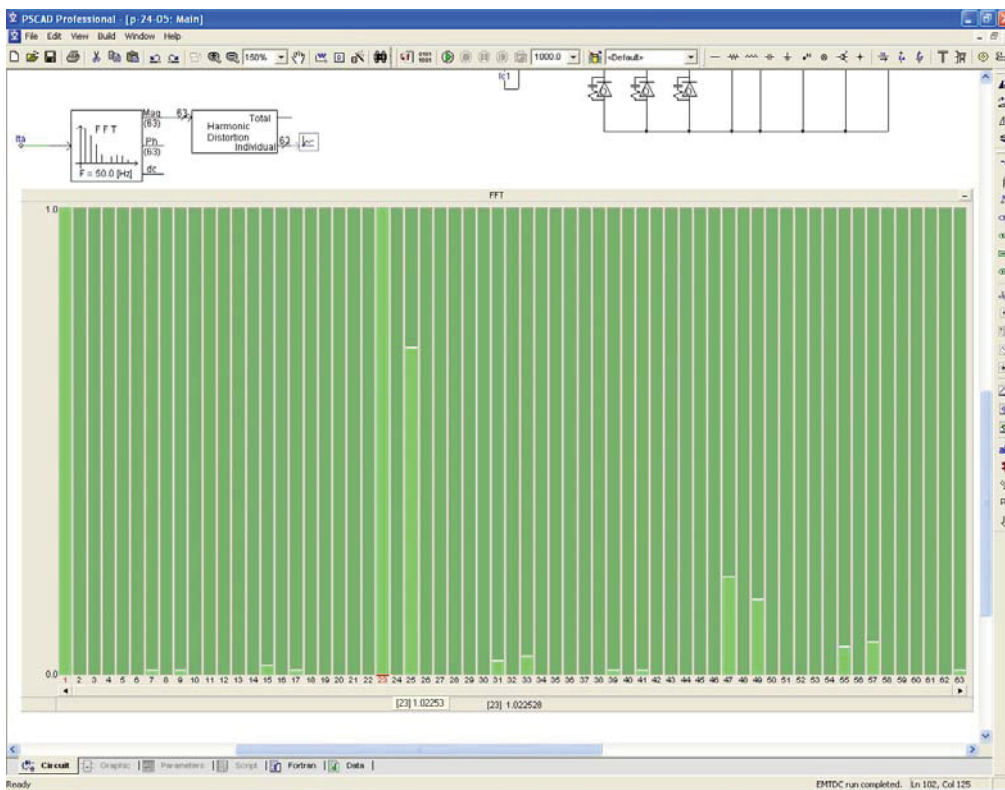


Figure 5-1 Harmonic FFT analysis Output**

Deciding on the transformer parameter in simulation, we can refer to the Direct Current Rectifier Character on-line software (DCRC, Figure 5-2 and Figure 5-3) which is an extremely practical software designed by SIEMENS engineers, and establishes the parameters in advance. However, this software originally chooses the parameters in 6 pulse rectifiers or 12 pulse rectifiers.

Figure 5-2 On-line software for DC Rectifier Character (1)*

Therefore, using it for 24 pulse rectifier analysis, we have to modify a little. Considering the 24-pulse rectification method similarly as two groups of 12-pulse rectifiers in parallel connection, simultaneously we select the voltage value as given. The output current value of each system is half of the rated value.

We also have to consider the connection type at the output. When using parallel connection, the values of voltage and current must be a quarter compared to the series connection.

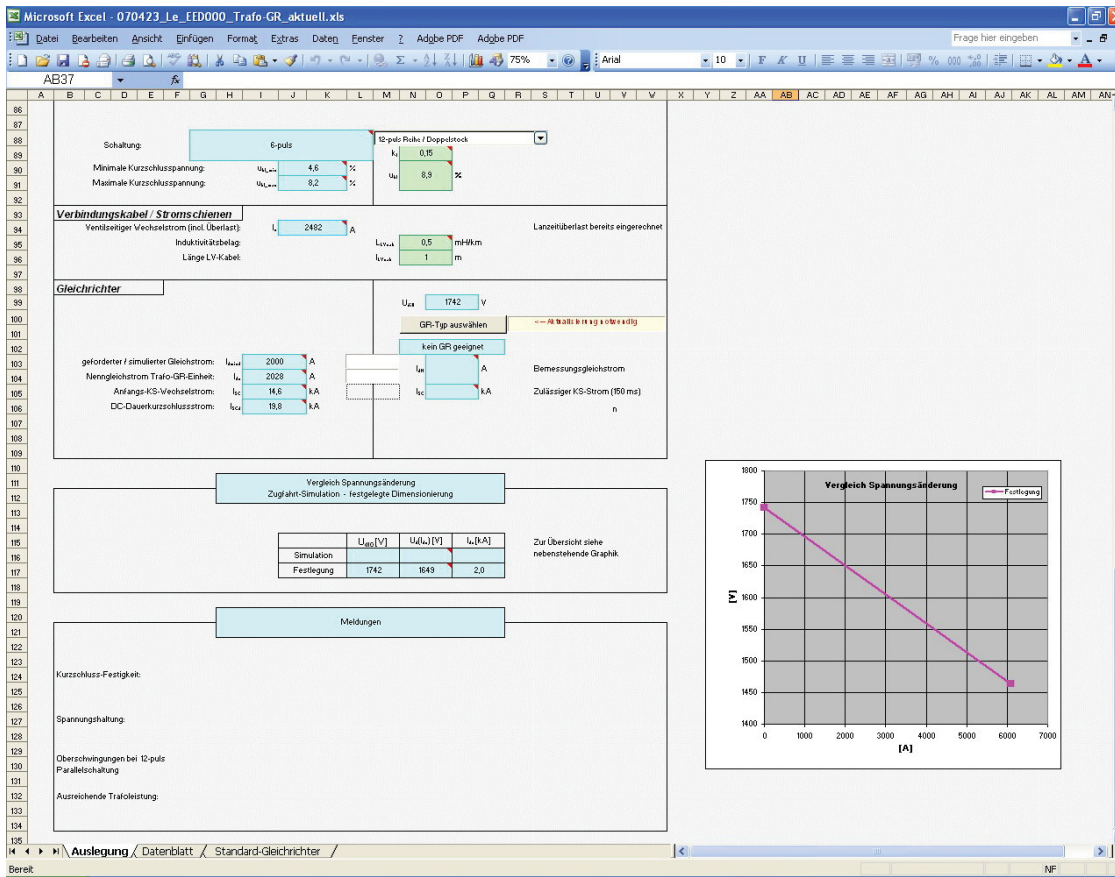


Figure 5-3 On-line software for DC Rectifier Character (2)*

This software has a great advantage because there is an automatic output of all other important parameters of the transformer. According to the different standards (IEC 60146 class IV, class V, class VI), all of these are chosen according to the operation condition. So we take these parameters as the ideal value. After running the PSCAD simulation we obtain results immediately.

Comparing the results to the ideal value and finding that they are inconsistent we have to adjust that the parameters put into PSCAD simulation. It is even possible that the simulation method designed is unreasonable and must be re-designed.

5.3 Assessment

The first task is to establish the simulation environment and input data array. After insertion of all parameters into PSCAD circuit (as in Figure 3-17), we run program and obtain the results. The FFT analysis data are shown with reference to the standard pattern. The so-called standard pattern refers to the rated output current 4 kA at output power 6,6 MVA.

From the table we know the even numbers of harmonic waves obviously should be neglected and a part of odd numbers of harmonic waves also reach such small values so we need not consider them. We compare different input voltages but all of them use the same output connection (parallel-connection). Results are displayed in Table 5-1 for easy

comparison and analysis. Further, the data of series, series-parallel and parallel-series connection in Appendix D are also done in three forms allowing to give an overview.

Considering data in the Table 5-1 we should divide these data into 3 groups.

Table 5-1 Harmonic Analysis by FFT**

| Parallel | Standard ¹ | - 5 % | - 2,5 % | 2,5 % | 5 % |
|----------|-----------------------|--------|---------|--------|--------|
| 3rd | 0,0000 ² | 0,0155 | 0,0395 | 0,0408 | 0,0144 |
| 5th | 0,0000 | 0,0113 | 0,0196 | 0,0195 | 0,0062 |
| 7th | 0,0564 | 0,0206 | 0,0115 | 0,0161 | 0,0137 |
| 9th | 0,0572 | 0,0157 | 0,0026 | 0,0101 | 0,0107 |
| 11th | 0,0004 | 0,7871 | 0,3955 | 0,3790 | 0,7165 |
| 13th | 0,0004 | 0,3099 | 0,1568 | 0,1492 | 0,2891 |
| 15th | 0,0264 | 0,0021 | 0,0105 | 0,0147 | 0,0156 |
| 17th | 0,0262 | 0,0059 | 0,0052 | 0,0082 | 0,0134 |
| 19th | 0,0000 | 0,0133 | 0,0230 | 0,0149 | 0,0172 |
| 21st | 0,0000 | 0,0167 | 0,0210 | 0,0185 | 0,0000 |
| 23rd | 1,2211 | 1,0083 | 1,0387 | 1,0260 | 1,0225 |
| 25th | 1,0350 | 0,6613 | 0,6907 | 0,6891 | 0,6962 |
| 31st | 0,0585 | 0,0218 | 0,0124 | 0,0203 | 0,0179 |
| 33rd | 0,0596 | 0,0252 | 0,0164 | 0,0239 | 0,0177 |
| 35th | 0,0001 | 0,1793 | 0,0904 | 0,0871 | 0,1714 |
| 37th | 0,0001 | 0,1330 | 0,0690 | 0,0669 | 0,1244 |
| 39th | 0,0142 | 0,0059 | 0,0088 | 0,0083 | 0,0090 |
| 41st | 0,0198 | 0,0041 | 0,0064 | 0,0059 | 0,0066 |
| 43rd | 0,0001 | 0,0313 | 0,0202 | 0,0204 | 0,0353 |
| 45th | 0,0001 | 0,0365 | 0,0274 | 0,0270 | 0,0420 |
| 47th | 0,2690 | 0,1633 | 0,1915 | 0,1946 | 0,1657 |
| 49th | 0,2159 | 0,1227 | 0,1434 | 0,1493 | 0,1302 |

First group includes harmonic waves ($f = 3k$, $k = 1,2,3\dots$) which are neglected under the standard pattern, but those waves increase obviously when the output voltage is changed, such as the 3rd, 9th, 15th, 21st, 27th, 33rd, 39th and 45th wave.

The second group concerns harmonic waves that not neglected under standard pattern, but they are being reduced when the output voltage is changed, like the 17th, 19th, 29th, 31st, 35th, 37th, 41st and 43rd wave. Those are the secondary goals for harmonic elimination.

1 with 4 kA / 1,5 kV / 6,6 MVA in output

2 value scale is per cent

The last group, which we have to pay attention to higher degree ($f = k \pm 1$, $k = 6, 12, 24, 48$), is the harmonic sources in our 24-pulse rectification, which are the 5th, 7th, 11th, 13th, 23rd, 25th, 47th and 49th wave. But no matter which connection we are choosing the results in our analysis are similar. (Refer to Appendix D for details)

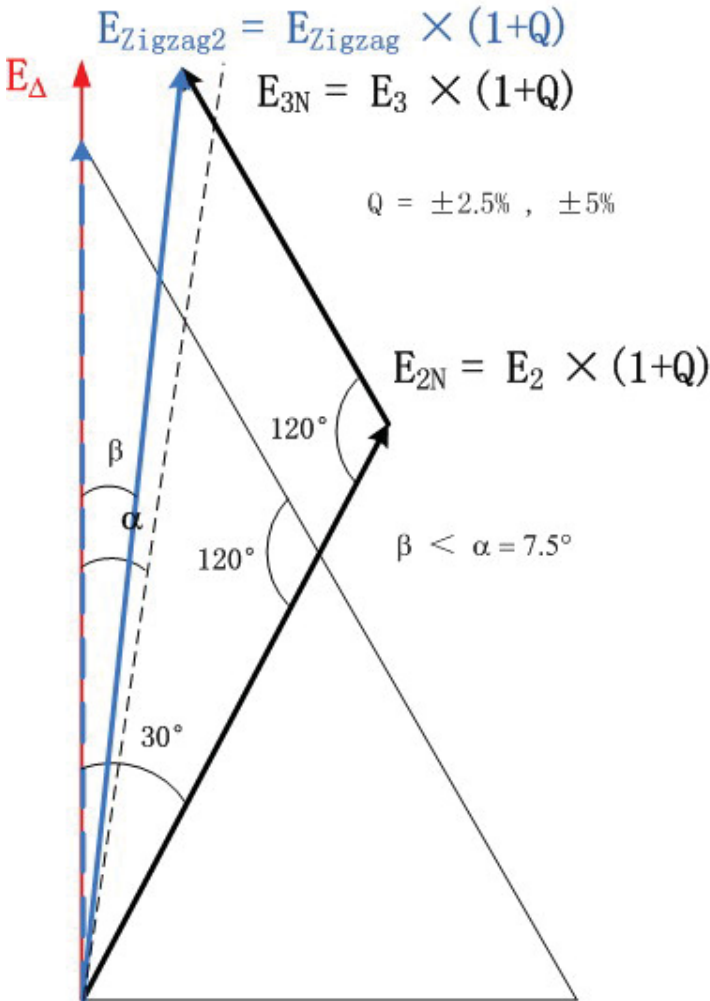


Figure 5-4 Voltage Vector Analysis (4)**

The reason for the harmonic increase when the output voltage is changing can be answered by the Figure 5-4. The voltage value E_{zigzag} is changing leads to the vector angle change. Figure 5-4 has already been calculated at an voltage increase of 5%. The vector angle reduces by $\beta = 6,092$ degree. Comparing the angle $\alpha = 7,5^\circ$ as normal value, the deteriorating effect from the harmonics is inevitable.

Our next task is to obtain the transformer non-load output voltage (idling voltage) under the condition of the output current maintaining 4 kA and the output DC voltage being 1 650 V, while the input line-ground voltage fixed to 20 kV. Then we connect the positive terminal and negative terminal directly to measure the impedance voltage value.

Of course we have to change the input voltage when the secondary side is short-circuited by a wire in order to get the output current as rated output current. By now the ratio of this input voltage value and rated input voltage is the impedance voltage. This

ratio is an important characteristic value to a transformer necessary for the design and technical realization of the transformers.

After the PSCAD simulation data are written in Table 5-2. The comparison of these results from PSCAD yields that the connection method in series has the largest impedance voltage (worse). Other three have nearly the same impedance voltage but the Parallel connection has the smallest short-circuit current and the smallest no-load voltage which means it is hardly affected by load variation and harmed from short current only in a minor way. Choosing the parallel connection is favorable.

Table 5-2 SNCF simulation results**

| Connection | Parallel | Parallel-Series | Series-Parallel | Series |
|----------------------------|-----------|------------------|------------------|------------------|
| U_s^3 | 1 443 V | 2×756 V | 2×758 V | 4×431 V |
| No load U_d | 1 758,3 V | 1 826,6 V | 1 783,9 V | 2 011,4V |
| Short-current | 32,75 kA | 34,22 kA | 34,26 kA | 25,27 kA |
| DC short-circuit Impedance | 6,15 % | 5,90 % | 5,89 % | 7,96 % |

3 Line voltage: 20 kV DC side (rated value): 1 650 V / 4 000 A

6 Metro Test in Phoenix

6.1 Introduction

Phoenix is the capital and the most populous city of the U.S. state of Arizona. SIEMENS TS has realized a metro project since 2004. Now a group in SIEMENS TS has a task to test and optimize this system.

At first the system should be checked in no-load state which means that the train does not run and the pantograph is down. The operation with auxiliary system on will be discussed in Chapter 6.3.

We use the digital measuring instrument (DEWE4010) to survey the voltages and/or currents at the AC side and DC side during rectification operation, and then get the survey curve on the instrument's window. The measure connection diagram and Traction Power Supply Substation (TPSS) refers to Appendix E.

The TPSS Rectifier topology is shown in Figure 6-1.

When the pulse signal is Red it means that in this time the pulse signal is set at 1; when it is Orange it means waiting now for the pulse signal to be set at 0 and after 60° later ($0,167 T$) it will be set at 1; green means waiting and the pulse signal set at 0. Because the secondary winding voltage in triangle connection and the star connection which have 30° degree lagging difference on the voltage phase, all pulse signals for the RB2 delay 30° ($0,083 T$).

In the survey there are some strange signal courses which are not explained at the moment. After analyzing them it will be solved. Then the user will be given a report about a reasonable explanation and the solution, therefore some software can help to get those important parameters. PSCAD has the powerful function to simulate the train operation in different status.

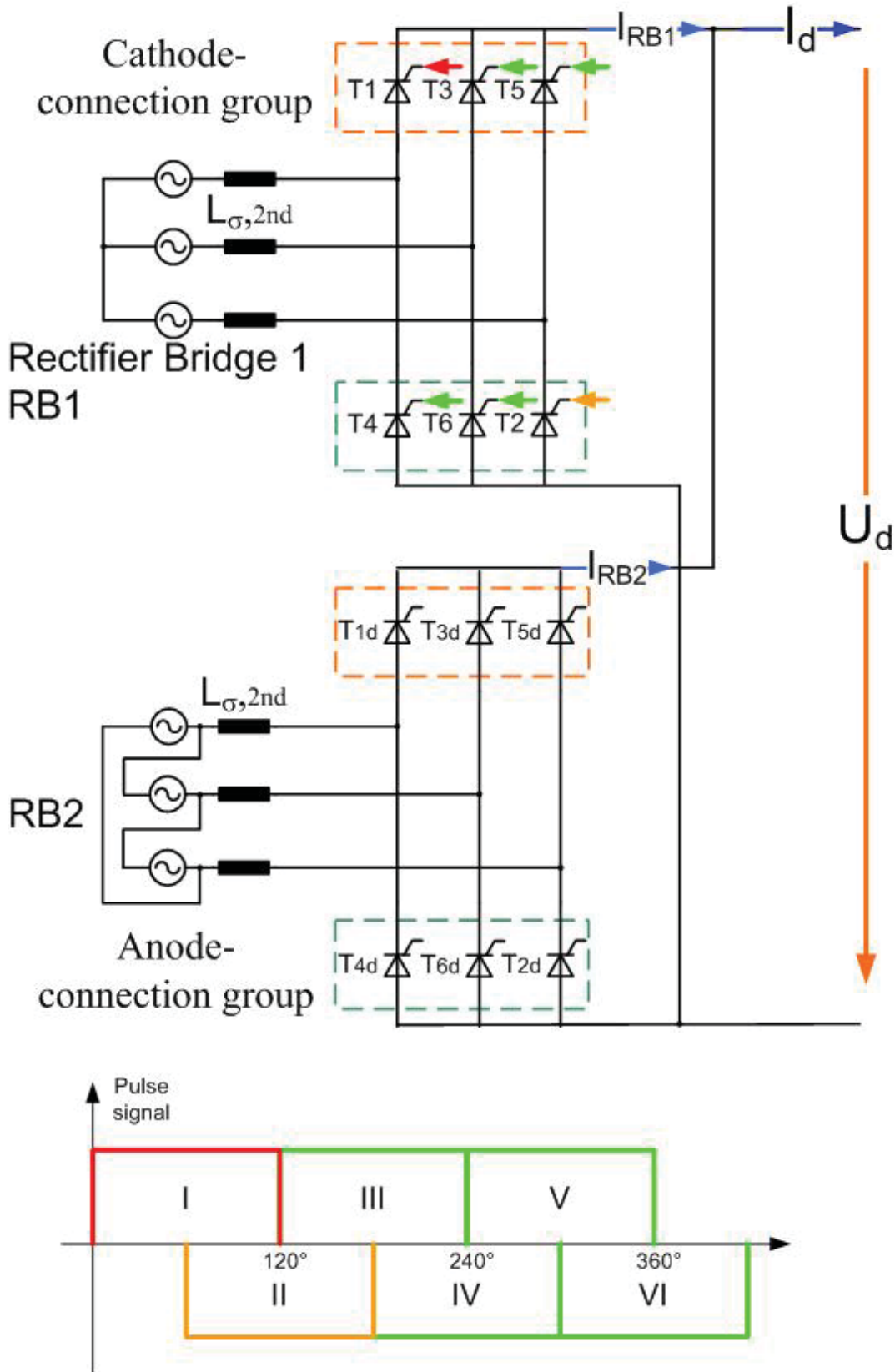


Figure 6-1 TPSS circuit Topology**

6.2 No-load Operation

As known the rectification in B6 means pulsing on the semiconductors in a cycle. Now we just focus on the time (from 60° to 120° on the Figure 6-1) when the Thyristors T1 and T2 turn on simultaneously. During this time the shunt capacitors and resistors on RB2 can be seen as load parallel to the RB1 output. (Figure 6-2 above) We simplify the circuit on the triangle connection (RB2) to the star branch (RB1) and here we have $C = 0,75 \mu\text{F}$, $R = 29,33 \Omega$. (Figure 6-2 middle)

Then we simplify all the shunt capacitors and resistors on the branches of T3, T4, T5 and T6, and at this time the T1 and T2 turn on, these two branches can be regarded as wire ($R = 0 \Omega$) connected, the capacitors discharge respectively just over the branch. Finishing all simplifications mentioned above we get the single phase AC circuit with $C = 2\mu\text{F}$ and $R = 9,78 \Omega$.

With the ideal conditions the train stops while not considering auxiliary system operation can be regarded as the no-load operation. However, some resistors in parallel as load ($2R$ or $4R$) must be put in to measure the output current I_d . (Figure 6-2 bottom) Because of the tolerance on each product four resistors of same value in parallel connection as load ($4R$) are better than two resistors ($2R$). The total value is same $R_{\text{load}} = 1 \text{ k}\Omega$.

The value on snubber (Figure 6-2) as $C = 20\mu\text{F}$ and $R = 3\Omega$ is given.

The output voltage shows 12 pluses as we know. With this operation the output current is about 1 Ampere. But in real time the rectification thyristors will make a current crest value (I_{peak}) when they are turned on because this current charges the capacitors and resistors on RB1 and RB2 (when snubbers are also charged) to make a voltage crest value (U_{peak}) on RC charge line. (Figure 6-3)

After the crest value (U_{peak}) has passed by all the capacitors discharge and the voltage U_d drops exponentially from U_{peak} towards 0 on RC discharge line.

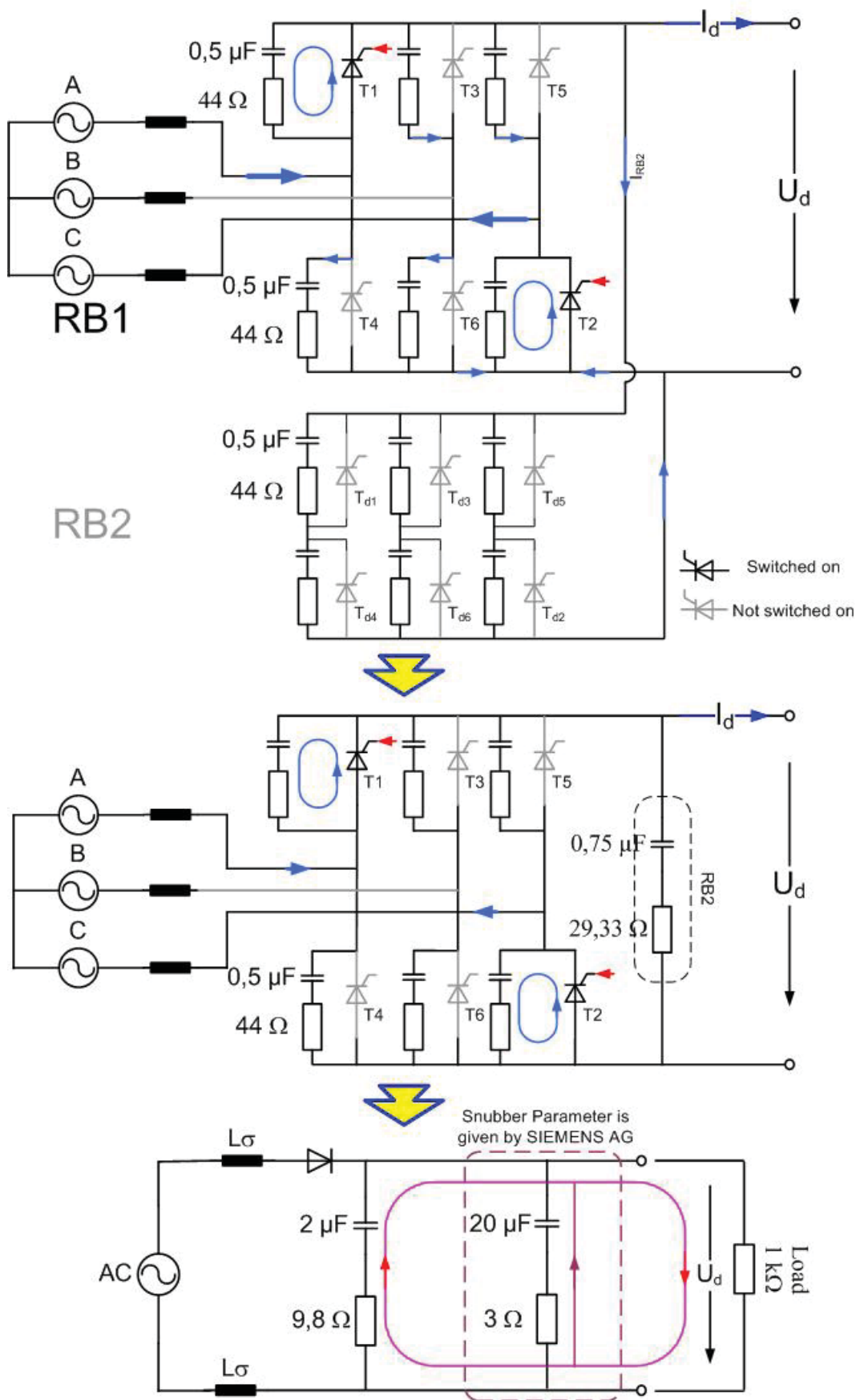


Figure 6-2 No-load operation**

Here we calculate the output voltage curve without snubber.

- 1 Given the firing angle: $\alpha = 38,7^\circ$
- 2 $U_{\text{high}} = 1,414U_{\text{eff}} * \sin(\alpha + 60^\circ) = 936,6\text{V};$ ($U_{\text{eff}} = 670\text{V}$)
 $U_{\text{low}} = 1,414U_{\text{eff}} * \sin(\alpha + 90^\circ) = 739,5\text{V}$
- 3 When the thyristor turns on the voltage difference on the shunt capacitance is about 197,1V
- 4 The crest current I_{peak} is $197,1 \text{ V} / 44 \Omega = 4,48 \text{ A}$
- 5 This current drops to 1A, as short circuit on the Thyristor branch, at a time constant.
 $T_i = R * C = 44 \Omega * 0,5 \mu\text{F} = 0,022 \text{ ms}$, within
 $\Delta T = -0,022 * \ln(1 / 4,48) = 0,033 \text{ ms}$ (Figure 6-3)
- 6 In this time the output voltage from 936,6V increases to the crest voltage
 $T_v = R * C = 9,78 \Omega * 2 \mu\text{F} = 0,020 \text{ ms}$ (Figure 6-3 red Charge line)
 $\Delta U = I_{\text{peak}} * 9,78 \Omega * (1 - e^{-\Delta T / T_v}) = 35,4 \text{ V}$
 $U_{\text{peak1}} = 936,6 \text{ V} + 35,4 \text{ V} = 972 \text{ V}$
- 7 the voltage discharge on the R_{load} circuit (without snubber) yields
 $T = R * C = 1\,009,8 \Omega * 2 \mu\text{F} = 2,020 \text{ ms}$.
 the time for one Thyristor turn on is $T_s = 1 / (60 \text{ Hz} * 12) = 1,389 \text{ ms}$
 as American use 60Hz frequency and the rectification is (B6)2P.

$$(T_s - \Delta T) / T = 67,1 \% = 0,671 \tau,$$

which means discharging just continuing for 1,356 ms. After that time the next voltage pulse will occur.

$$U_R(t) = U_{\text{peak1}} * e^{-0,671\tau} = 972 \text{ V} * 0,511 = 496,9 \text{ V} < U_{\text{low}} = 739,5 \text{ V}$$

The output voltage drops on the line II instead on the line III (Figure 6-3 bottom), after 1,356 ms the next pulse comes on from the RB2 branch.

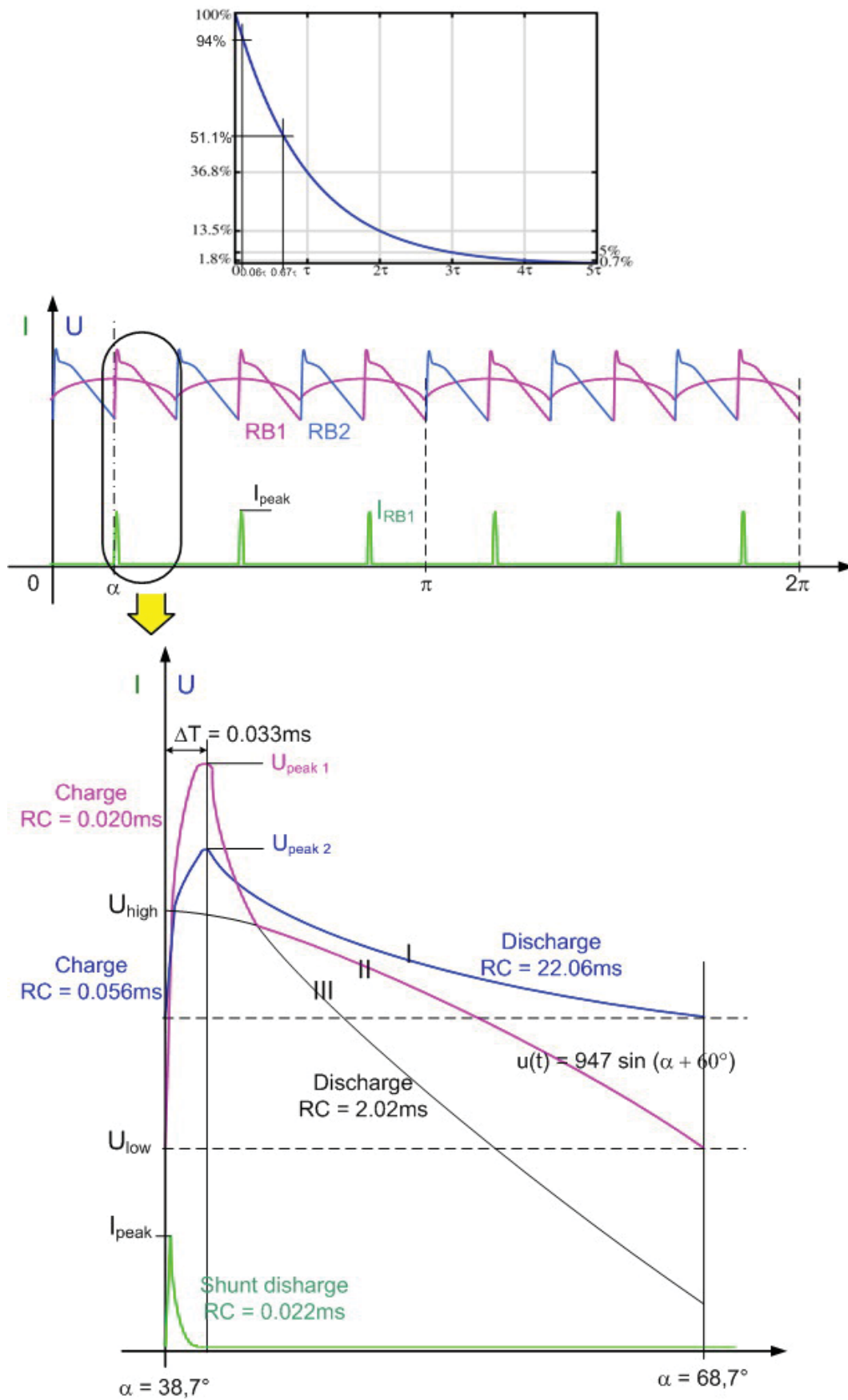


Figure 6-3 Crest Voltage by Pulse Current**

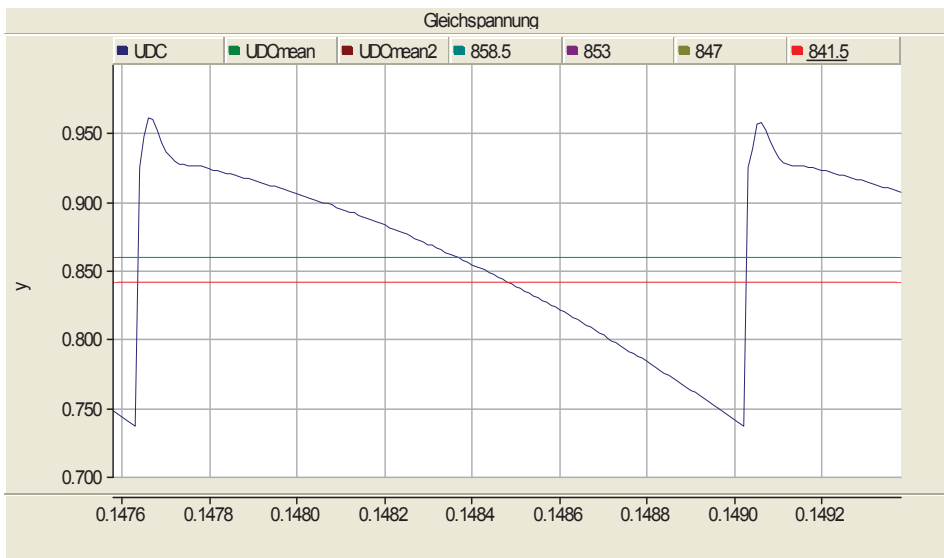


Figure 6-4 No-load output Voltage (without snubber)

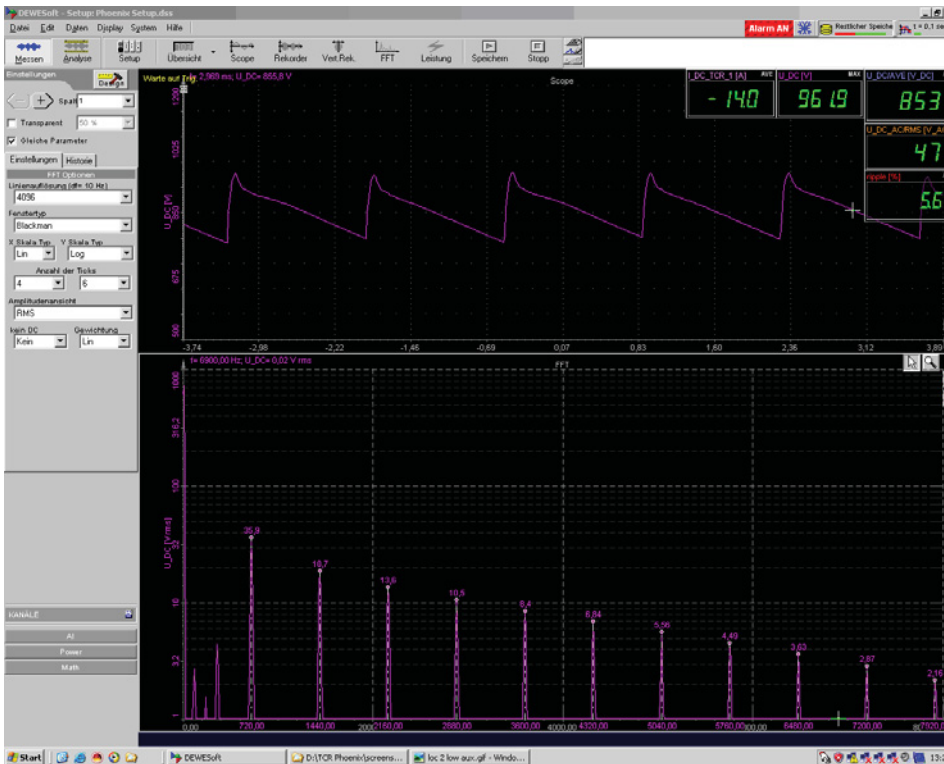


Figure 6-5 No-load Measure Result*

Comparing the simulation Figure 6-4 with the survey Figure 6-5, we see that both are completely same and it has been proven by the calculation above.

Using the snubber maybe limits the crest current, so trying to put the RC branch as a snubber in the topology. (Figure 6-2)

Then we calculate the output voltage curve with snubber.

- 1 Same firing angle: $\alpha = 38,7^\circ$
- 2 $U_{\text{high}} = 1,414U_{\text{eff}} * \sin(\alpha + 60^\circ) = 936,6 \text{ V};$ ($U_{\text{eff}} = 670 \text{ V}$)
 $U_{\text{low}} = 1,414U_{\text{eff}} * \sin(\alpha + 90^\circ) = 739,5 \text{ V}$
- 3 The voltage difference on the shunt capacitance is 197,1 V
- 4 The crest current I_{peak} is $197,1 \text{ V} / 44 \Omega = 4,48 \text{ A}$
- 5 This current drops to 1 A, as short circuit on the Thyristor branch.
 $T_i = R * C = 44 \Omega * 0,5 \mu\text{F} = 0,022 \text{ ms}$
 $\Delta T = -0,022 * \ln(1 / 4,48) = 0,033 \text{ ms}$ (Figure 6-3)
- 6 In this time the output voltage from 936,6 V increase to the crest voltage
 $T_v = R * C = 2,56 \Omega * 22 \mu\text{F} = 0,056 \text{ ms}$ (Figure 6-3 blue charge line)
 $\Delta U = I_{\text{peak}} * 2,56 \Omega * (1 - e^{-\Delta T / T_v}) = 5,1 \text{ V}$
 $U_{\text{peak2}} = 936,6 \text{ V} + 5,1 \text{ V} = 941,7 \text{ V}$
- 7 The voltage discharge on the R_{load} circuit (with snubber)
 $T = R * C = 1\,002,56 \Omega * 22 \mu\text{F} = 22,06 \text{ ms}$.
 Within same $T_s = 1 / (60 \text{ Hz} * 12) = 1,389 \text{ ms}$

 $(T_s - \Delta T) / T = 6,15 \% = 0,0615 \tau,$
 $U_R(t) = U_{\text{peak2}} * e^{-0,0615\tau} = 941,7 \text{ V} * 0,94 = 885,6 \text{ V} > U_{\text{low}} = 739,6 \text{ V}$

The output voltage drops on the line I instead on the line II (Figure 6-3), after 1,356 ms the next pulse comes on from the RB2 branch.

In Figure 6-6 it seems to be not better than the configuration without snubber. At this point we do not go in detail as the snubber's function is discussed in Chapter 6.3.

We want the crest voltage to be smaller. Analyzing Figure 6-3 the voltage crest depends on the pulse current. Increasing the resistance on shunt will decrease the current. Trying to make $R_{\text{shunt-new}} = 88 \Omega$ we get the new curve. (Figure 6-7) It has a smaller crest voltage than in Figure 6-4 but the resistor is a protection when the current on the thyristor is too large. Large R_{shunt} will decrease the current for protection.

Assessment is that the way to get a small crest voltage through increase of R_{shunt} is not good. The PSCAD topology refers to Appendix E.

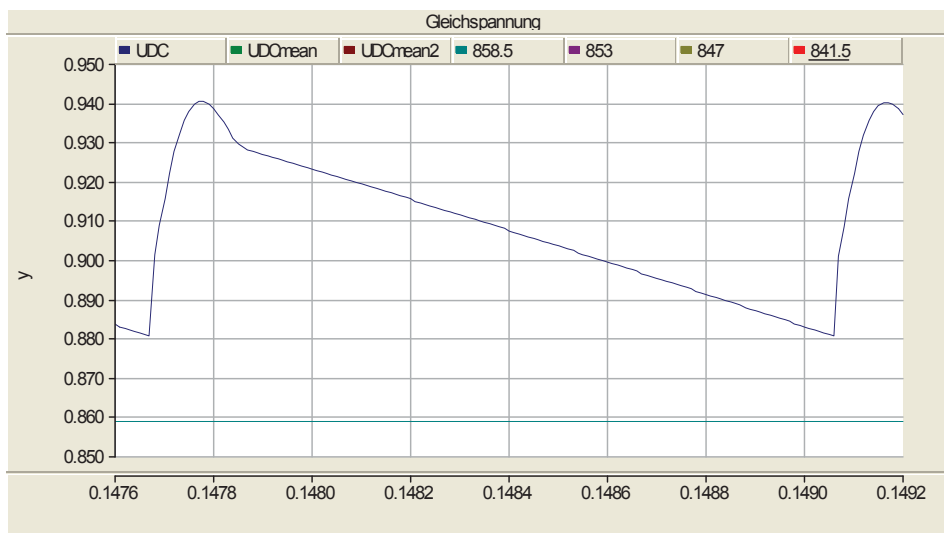


Figure 6-6 No-load output Voltage (with snubber)

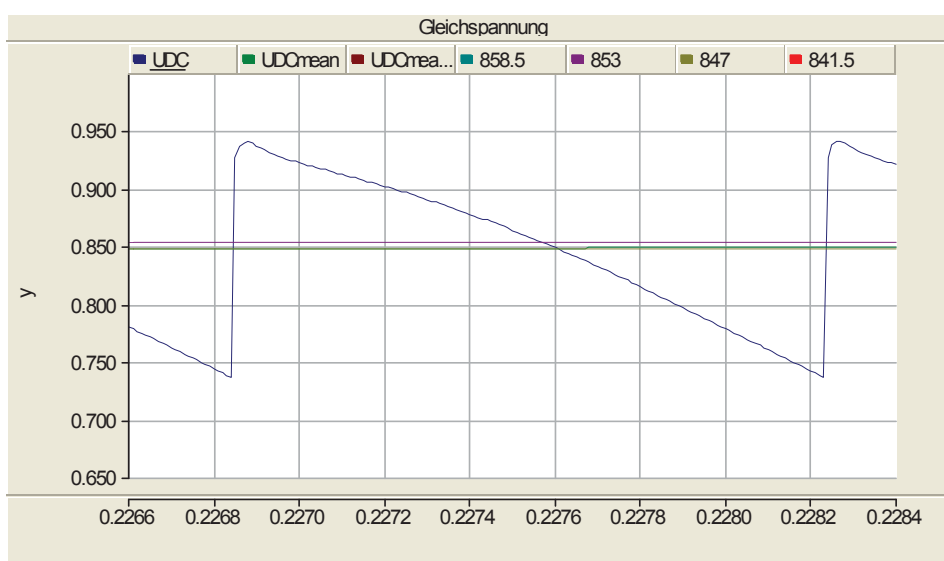


Figure 6-7 Output Voltage (without snubber) $R_{shunt} = 88\Omega$

6.3 Operation with Auxiliary system

When the locomotive stops and the auxiliary system (Aux-system) on the train is in operation simultaneously, the capacitance in Aux-system and the inductance on the overhead line make a resonance circuit and influence the output voltage.

The Aux-system consists of the air conditioning and ventilation system, the lighting system, and the vehicle operation control system. When these systems are running in full or partial operation according to the needs a different influence on the output voltage can be observed. By changing the current value from 20 A (low level) to 100 A (high level) the simulation produces two different operation results. (Figure 6-8)

In this chapter, we consider what will happen when the auxiliary system works. Thus we turn off the switch 1(Power system) and turn on the switch 2 (Aux-system). With or without the snubber yields total different voltage profiles on TPSS output side.

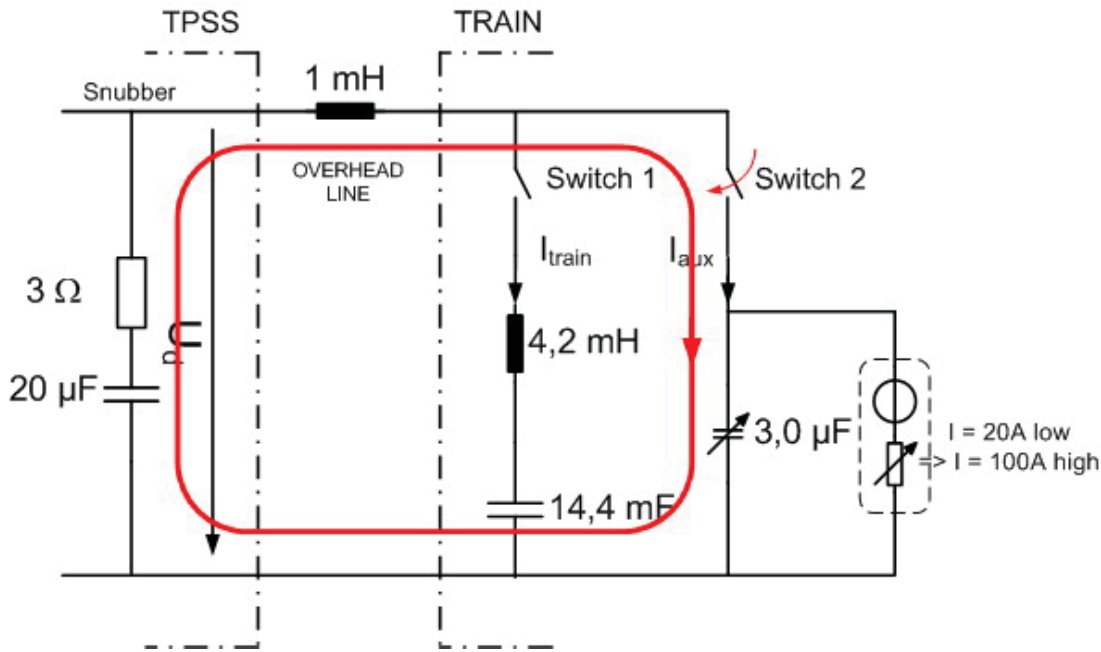


Figure 6-8 Power system and Aux system Topology**

6.3.1 Low Level Auxiliary Operation

We simulate with the switch 2 on and put $C = 3 \mu\text{F}$ as the inductance on the overhead line is 1mH which is estimated through the distance between two substations being about 1km as normal and at 1mH/km (Refer to [1]). The current is $I = 20 \text{ A}$ as the Aux-system works in low level. Figure 6-9 and Figure 6-11 are simulation curves without/with snubber respectively.

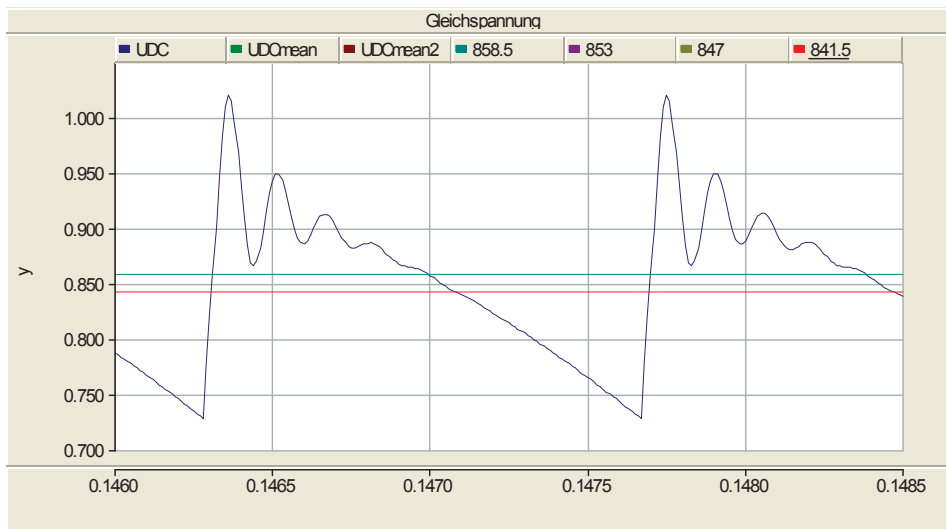


Figure 6-9 Low aux $I = 20 \text{ A}$ (without snubber)

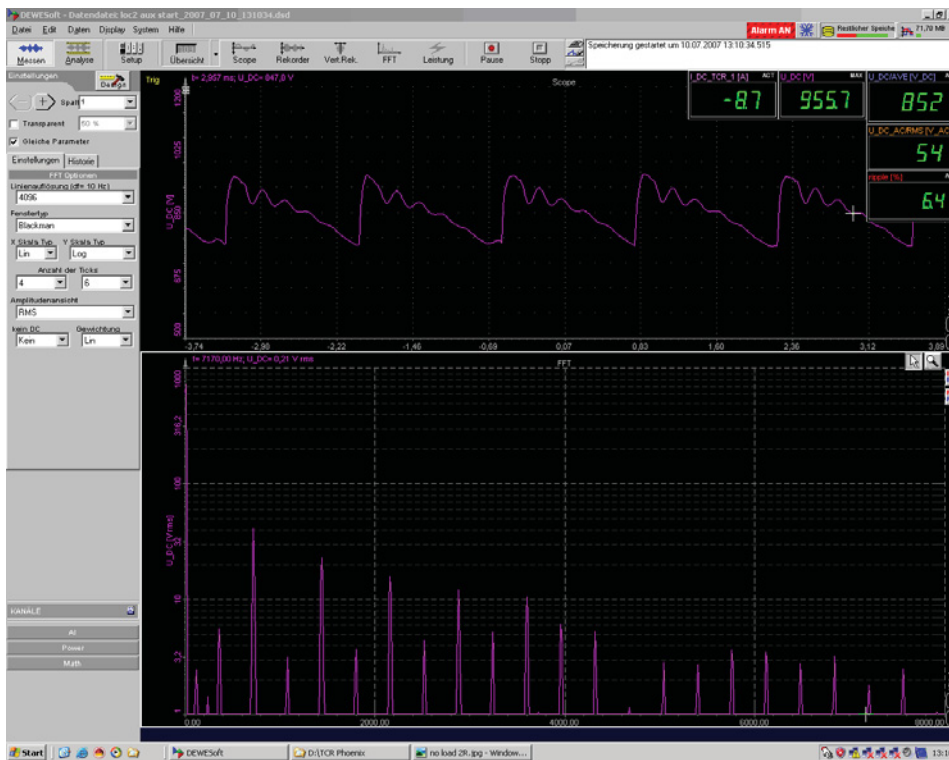


Figure 6-10 Low Auxiliary System Running*

Then we compare it to the measurement results on Figure 6-9. It appears that the time course profile with the snubber is smoother than without it. The simulation with snubber is more similar to the measurement which proves that the snubber has a good effect for operation.

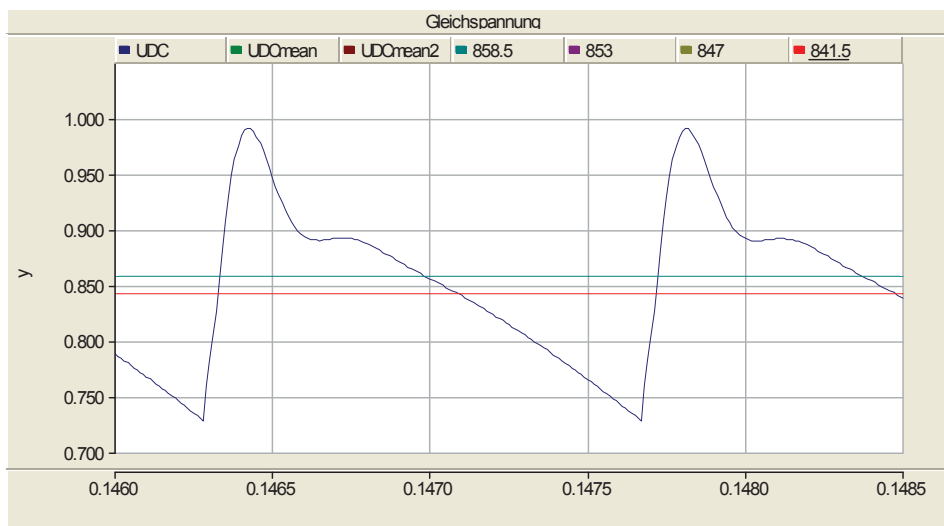


Figure 6-11 Low aux I = 20 A (with snubber)

6.3.2 High Level Auxiliary Operation

Then the Aux-system runs at heavy load level which means that all systems (belonging to Aux-system) are in full load running. The parameters are set as $L = 1,0 \text{ mH}$ (overhead), $C = 3,0 \text{ }\mu\text{F}$ and the current is increased to $I = 100 \text{ A}$. First without snubber we get Figure 6-12.

Then simulation with the snubber produces Figure 6-14.

Comparing the output voltage profiles in Figure 6-12 and 6-14, we see they are the same as for low level operation. The snubber can smooth the output voltage.

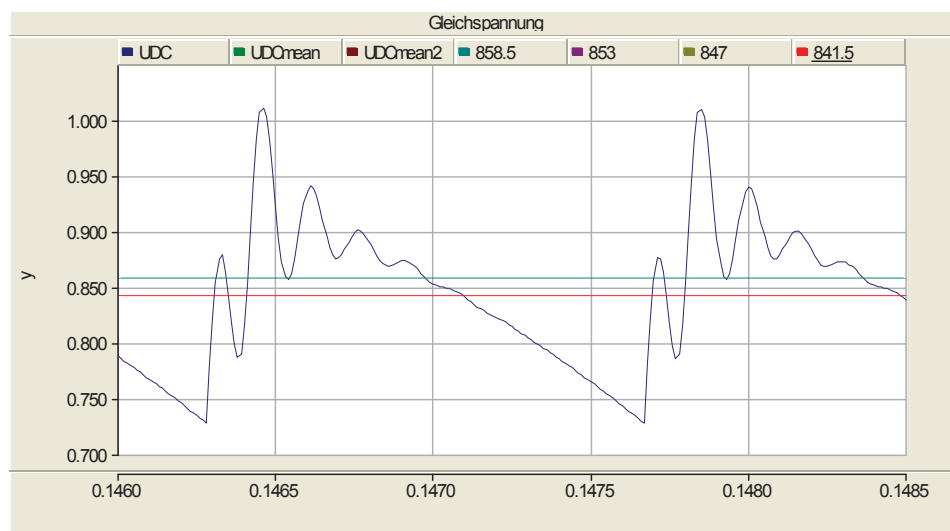


Figure 6-12 Heavy aux I = 100 A (without snubber)

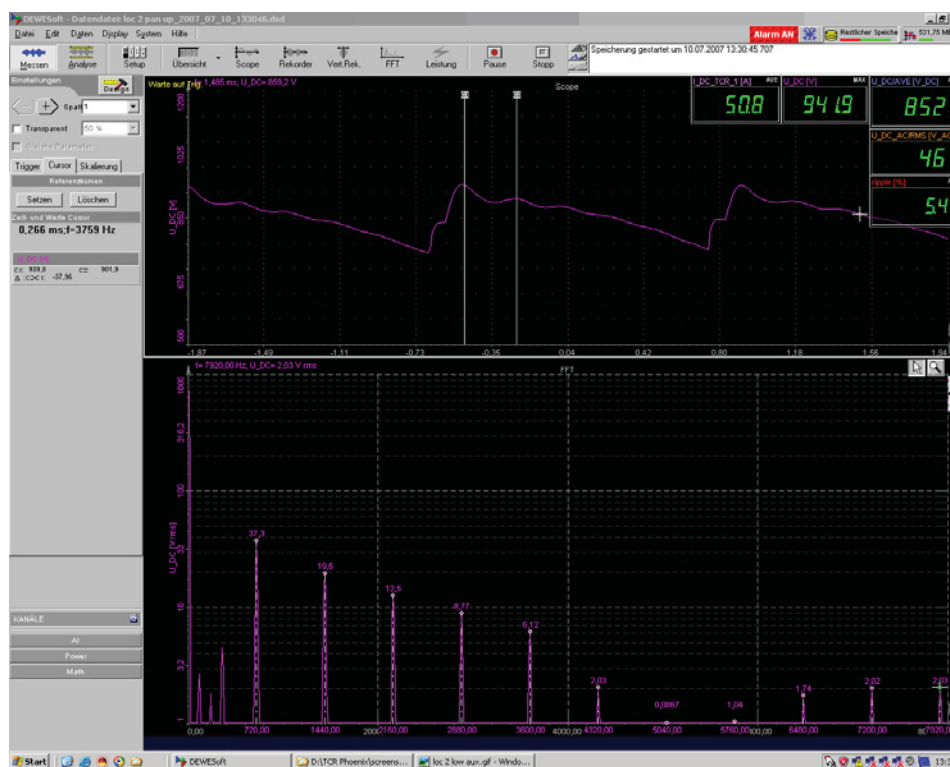


Figure 6-13 Heavy Auxiliary System Running*

Interpreting the profile displayed in Figure 6-10, 6-13 and 6-5 it is obvious that the no-load operation voltage is nearly a triangle and the low level voltage is smoother than for heavy load. This means that the heavy level operation produces more harmonics that could cause a distortion back to the total system.

However, the ripple factors in Figure 6-10 (low level is 6,4% , which is at the right side of this picture), in Figure 6-13 (heavy level is 5,4%) and in Figure 6-5 (no-load ripple factor

is 5,6%) are very similar. So just reading the ripple factors does not provide a way to analyze which is better. It means the time course may give the result more clearly than the ripple factor value.

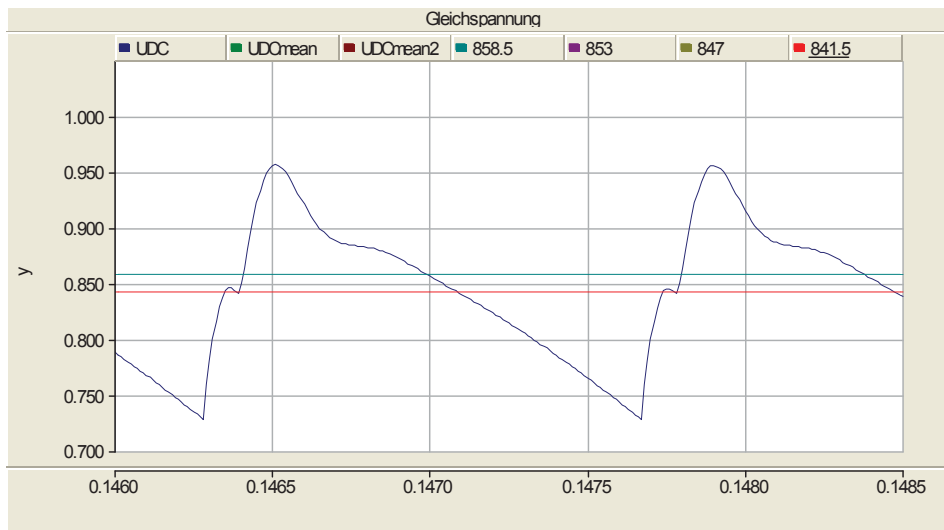


Figure 6-14 Heavy aux I = 100 A (with snubber)

6.4 Characteristic in Crossing Feeder

The locomotive has the pantograph on its top, which is a device that connects between the overhead line and electric train and collects the current from overhead lines for electric train or tram. Anyhow, the overhead line does not have an unlimited length between feeding points. Therefore, we have to the feeders (or say feeder stations) between two sections as the connection (See section SL in Traction Power Sectionalization Diagram in Appendix E).

With the locomotive running the pantograph also goes from one section (Figure 6-15) to another section over the feeder. The feeder includes an overhead line switch and gives connection generally only to one power supply substation.

When the current flowing from the substation to the pantograph is changed, the resulting impedance (Z) over the line is changing, too. The DC voltage is affected by the inductance and capacitance on the line. As we know the maximal change happens at this time instant when the train cross the feeder point. (Figure 6-16)

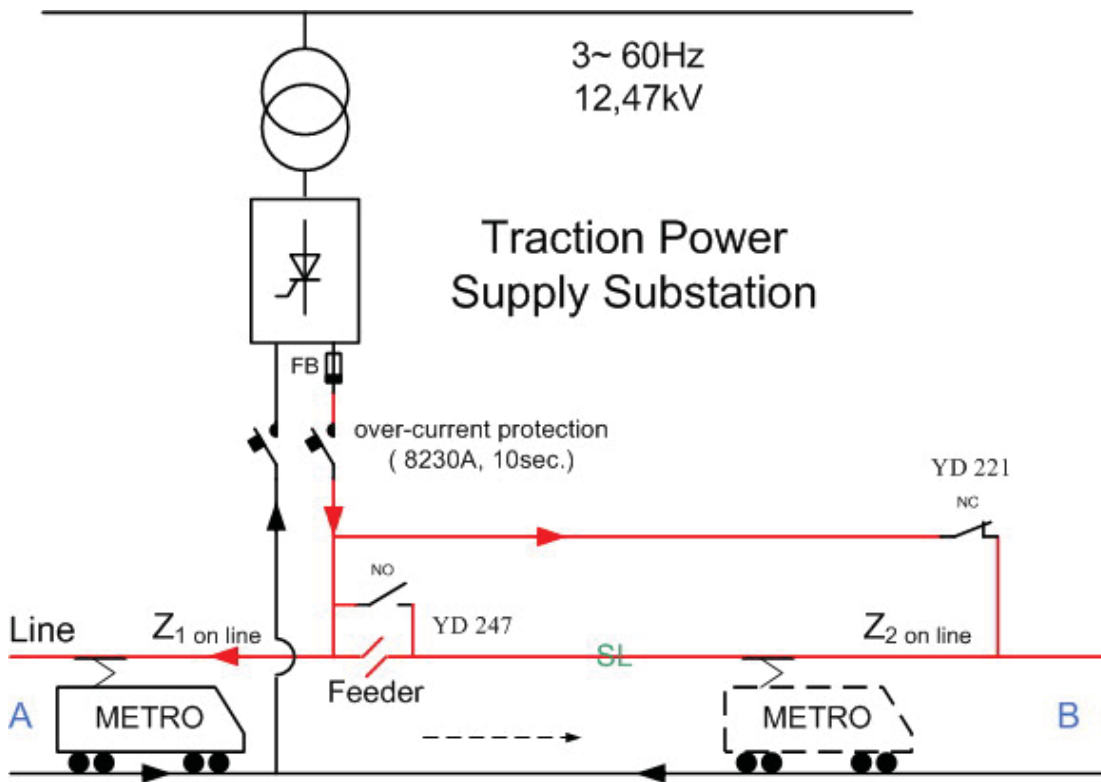


Figure 6-15 Feeder Crossing**



Figure 6-16 Feeder on contact line*

We consider the train going from A near to the feeder station direct to B. When the train passes through the feeder (Figure 6-15) the inductance and capacitance have a large change from minimum to maximum.

The simulation with the inductance (L) on line change from 1,0 mH to 1,5 mH and the capacitance (C) on line from 3 μ F to 5 μ F yields Figure 6-17.

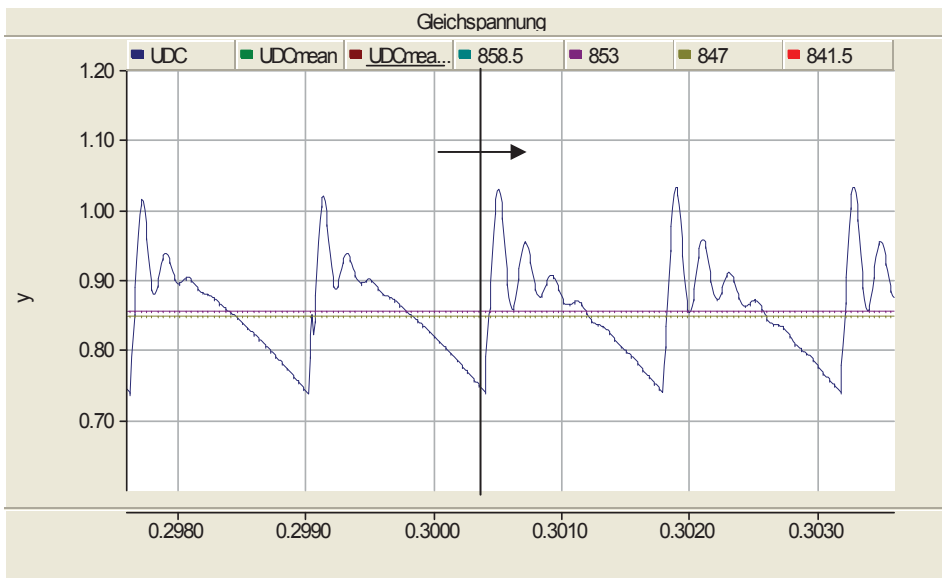


Figure 6-17 Cross Feeder ($L=1\text{ mH}\Rightarrow 1,5\text{ mH}$, $C=3\text{ }\mu\text{F}\Rightarrow 5\text{ }\mu\text{F}$)

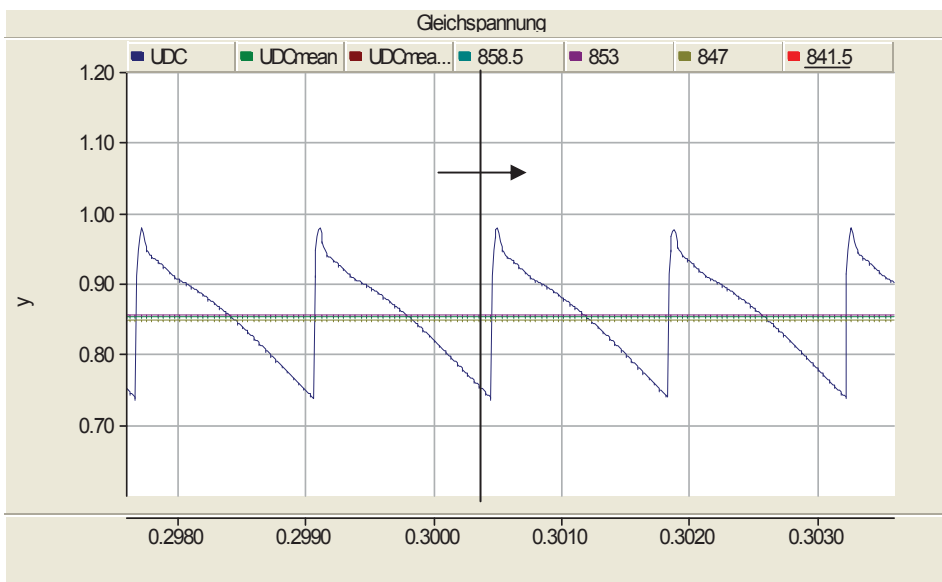


Figure 6-18 Cross Feeder ignorance L,C on overhead line

It seems the time course of voltage will change at the moment of crossing the feeder. But the exact profile at changing depends on the parameters of the train running which include the length of one section line, the outside temperature, the train's speed and more.

Figure 6-18 is shows the result of ignoring the inductance (L) and the capacitance (C) on overhead line. The harmonics in Figure 6-17 depend on the overhead line and not on the substation system itself.

Figure 6-19 is obtained in measurement when crossing the feeder. The simulation proves the measured time course. In Figure 6-17 the curve is smoother when we introduce smaller inductances and capacitances on the line. This situation has to be noticed when the user wants to know the feeder's influence online.

Using the snubber can effectively smooth the crossing change effects as displayed in Figure 6-20.

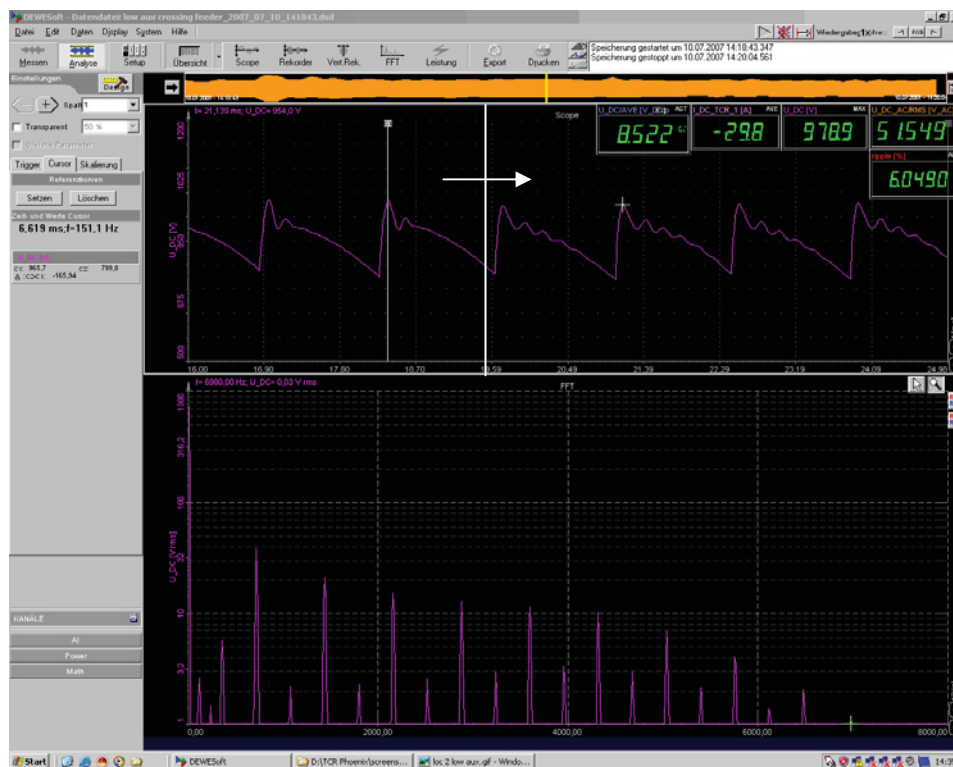


Figure 6-19 Crossing Feeder measure*

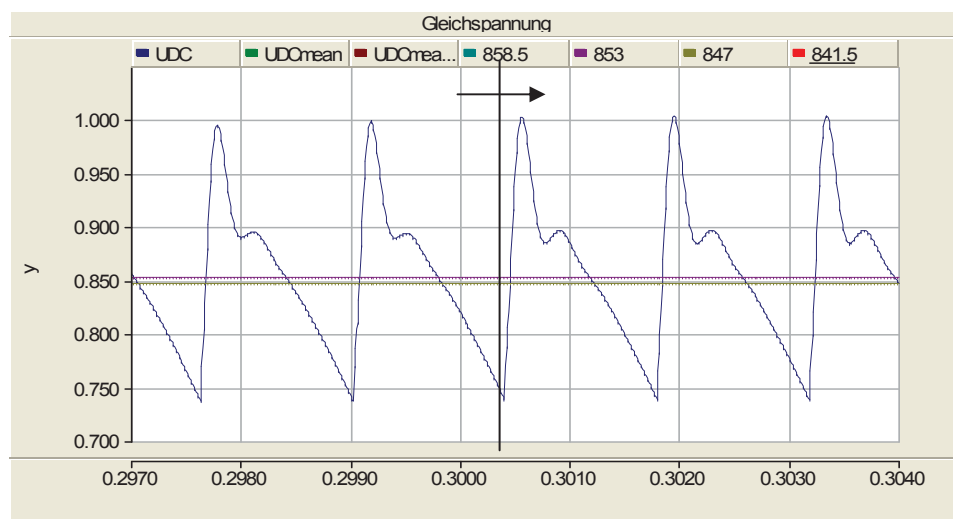


Figure 6-20 Cross Feeder (with snubber)

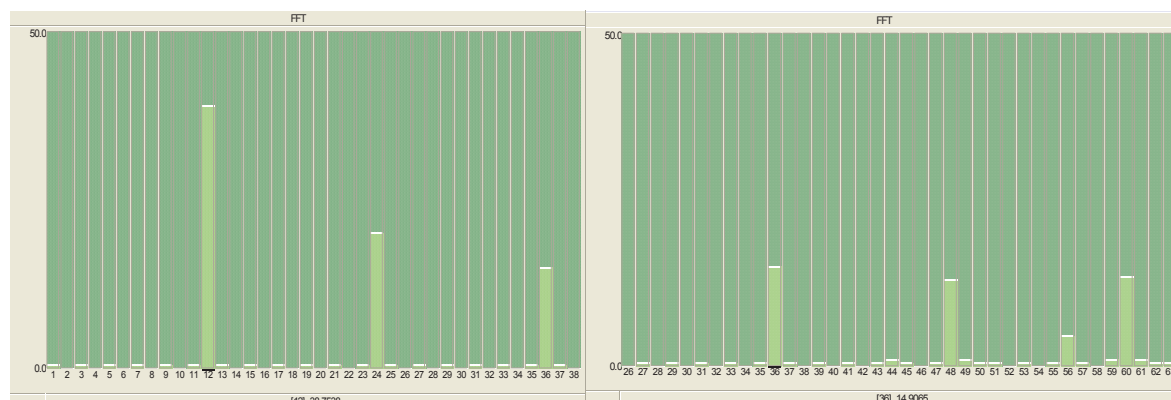


Figure 6-21 FFT on DC side without Snubber



Figure 6-22 FFT on DC side with Snubber

FFT value can be read in Figure 6-19 directly. We compare it with the simulation value in Table 6-1 which are with and without the snubber. (Figure 6-21 and 6-22)

Table 6-1 Harmonics on DC side**

| 60Hz * 12 * n | | 720 Hz (N=1) | 1 440 Hz (N=2) | 2 180 Hz (N=3) | 2 880 Hz (N=4) | 3 600 Hz (N=5) |
|---------------|-----------------|-----------------|-------------------|-------------------|-------------------|-------------------|
| Measure | | 37,89V | 20,95V | 15,08V | 12,56V | 11,24V |
| PSCAD | without Snubber | 38,75V | 20,21V | 14,91V | 13,14V | 13,43V |
| | with Snubber | 31,99V | 19,24V | 16,35V | 11,85V | 6,34V |

We have to notice that the values are changed at 3 600 Hz. The reason is calculated as follows. The resonance frequency for snubber is

$$f_c = 1 / (2 * \pi * R * C) = 3 183 \text{ Hz} (R = 2,5 \Omega, C = 20 \mu\text{F})$$

Bandwidth for snubber (Filter) has f_1 and f_2 as boundary value. (Figure 6-23)

$$\log (f_2 / f_c) = \log (f_c / f_1) = -3 \text{ dB}$$

$f_1 = 1\,595 \text{ Hz}$ and $f_2 = 6\,351 \text{ Hz}$

The $3\,600 \text{ Hz}$ value is obviously affected by the snubber.

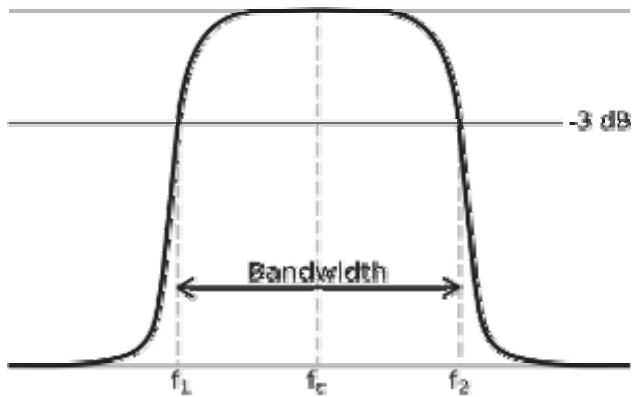


Figure 6-23 Filter's gain magnitude*

6.5 Unbalancment of the Output

Known from the TPSS topology, two groups of B6 rectifiers are used in parallel connection and obtain the DC output in 12 pulses. The output current I_d is sum of the two commutated currents (I_{GR1} , I_{GR2}).

As a result of some fault condition such as the Thyristor pulse triggers are not in synchronization the two currents output will be unequal. This means unbalanced operation and also affects the really voltage output.

Actually this kind of condition will happen but not accidentally. The reason is that all products in devices exhibit a certain tolerance. As these will be below acceptance imagines and are to be tolerated under the permission scope it will raise the problem during the debugging and operators do not know what happens exactly. Therefore it is important to know which influence will be introduced.

The simulation in no-load low Aux-level operation with the two commutated currents being not the same is realized through giving two rectification groups different commutate firing angles.

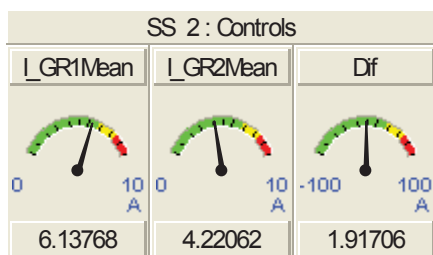


Figure 6-24 Firing angle control

Adjusting firing angle difference value to $7,2^\circ$ we start the simulation. Two rectified currents output (Figure 6-24) and the value difference is 1,92 A.

We also get the voltage output time course in Figure 6-25. It is similar to the measured value of Figure 6-26.

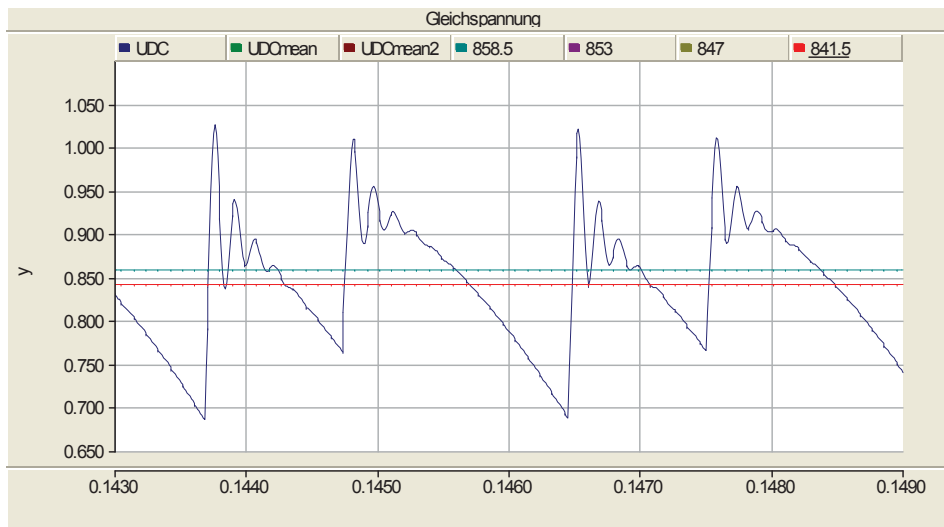


Figure 6-25 Asymmetry Operation with Low Aux

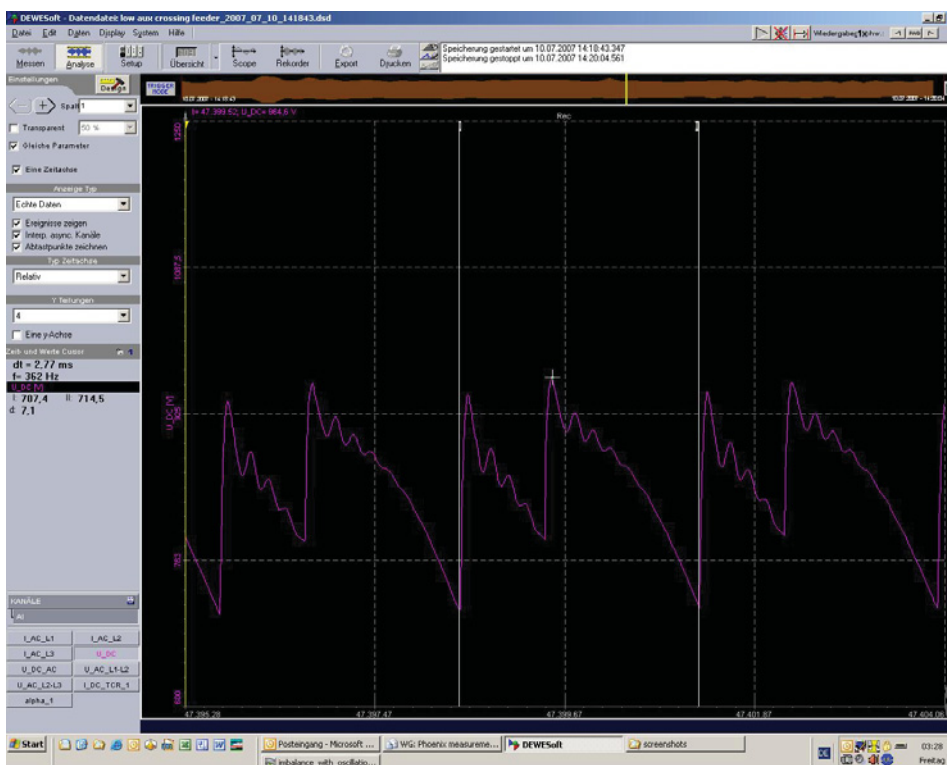


Figure 6-26 Asymmetry Operation Measurement*

6.6 Assessment

From all the comparisons done above we desire that PSCAD can simulate the different train operations and we really get results that are nicely fitting to the measured curves done on July, 2007 at Phoenix, U.S.A.

When measurement and simulation are consistent with each other the parameters can be read on simulation software. In case it is not at first attempt we have to adjust the parameters until results are the same.

In order to get those parameters it is important that we can analyze and find some ways to solve the problems and questions which are met.

An assessment report written by engineers at SIEMENS AG gives a satisfying answer to the customer. The simulation part as described includes the content and data of this diploma thesis (master thesis) report especially out of this chapter.

7 DC/AC Inversion

After a deeper understanding of the principle of AC/DC rectification function, a next work shall use PSCAD simulating DC/AC inversion.

7.1 Rectifier-Inverter Operation

In train operation especially for metro applications there are always deceleration and braking interval at about each 2 kilometers. Thus the motor of the train works as generator when the train is braking and at this time the energy flows from train to substation through the overhead line.

In earlier time the braking energy was dissipated in heating at the resistor which is then connected in parallel to the motor. Now we use the inverter to feed the energy back to the substation grid. Though this way we can reuse about 70% of braking energy and this is very effective for metro operation in the city.

7.1.1 Prerequisites

To reuse the energy from regenerative braking the effective method is opening way for the energy that can let the current flow from train back to the substation. The inverter just is this way. (Figure 7-1) We call this a double converter connection.

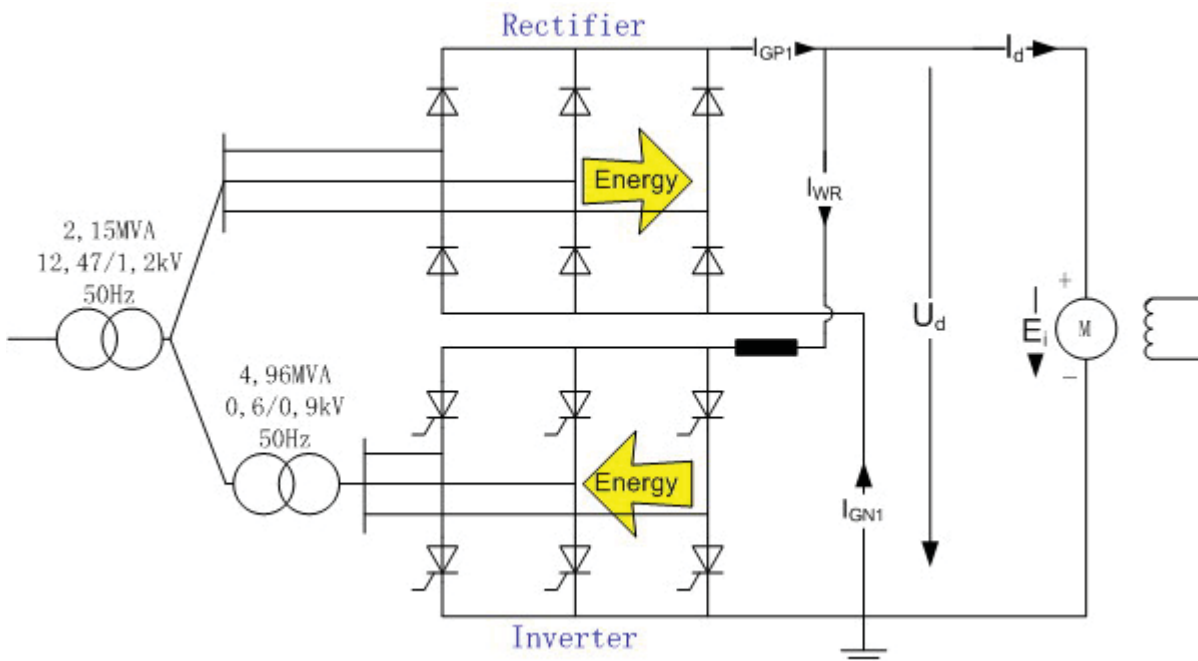


Figure 7-1 Double converter topology**

Theoretical regulation curves for a double converter connection for different control angles α_1 for one converter and α_2 for the other converter are shown in Figure 7-2. In this

paper we use two B6 groups in anti-parallel connection. One acts as rectifier ($\alpha_1 = 0$) and the other Thyristor group works as inverter. (α_2 is controlled by voltage and current on overhead line, refer to Chapter 7.1.2)

For the metro, the power on the overhead line is constant which can give the drive motor a more stable condition of operation. The red line in Figure 7-3 means the power line. When the substation works in the inverter operation region the current can be seen to flow in different direction as in rectifier operation. However, the commutation limit line delay angle α_2 is between 135° to about 160° .

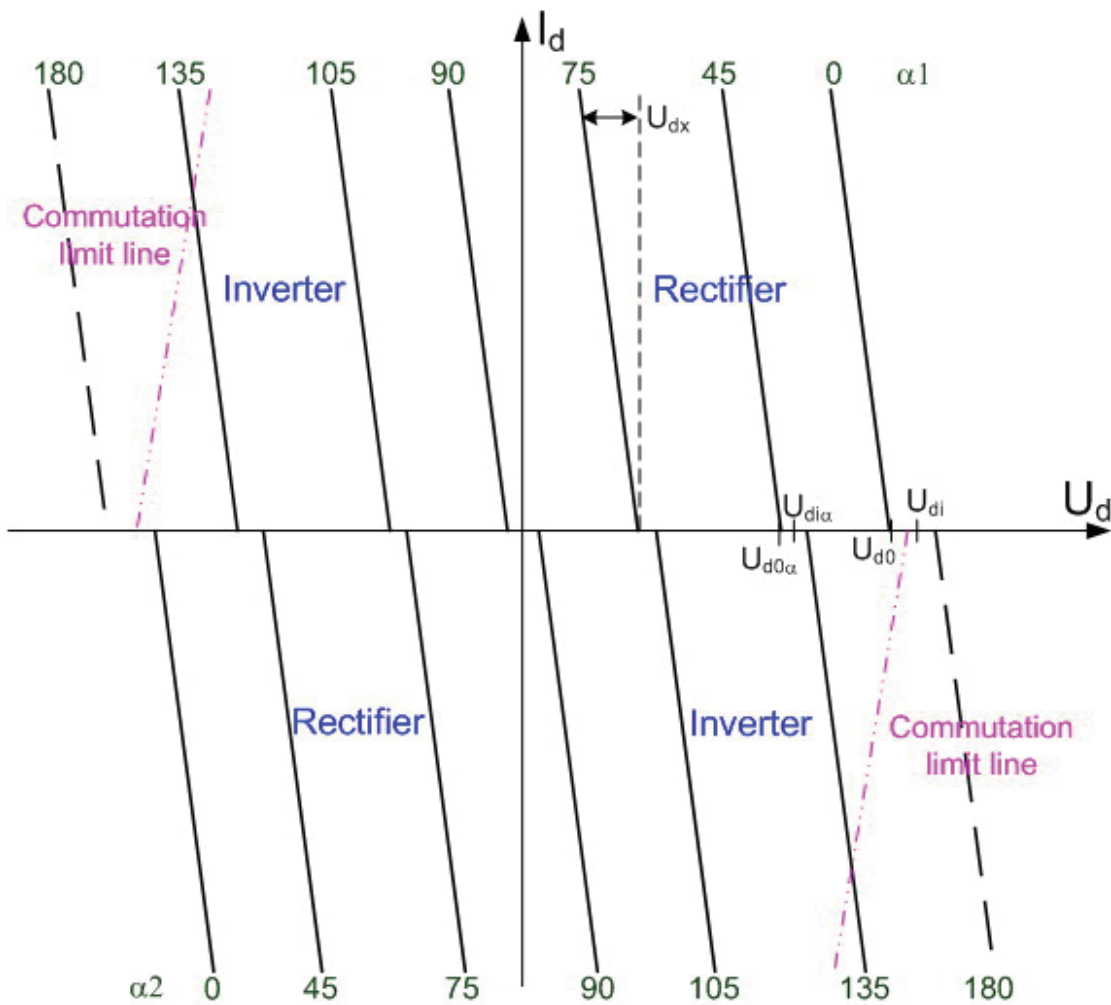


Figure 7-2 Direct voltage limits in inverter operation
(Source from IEC 60146-2)

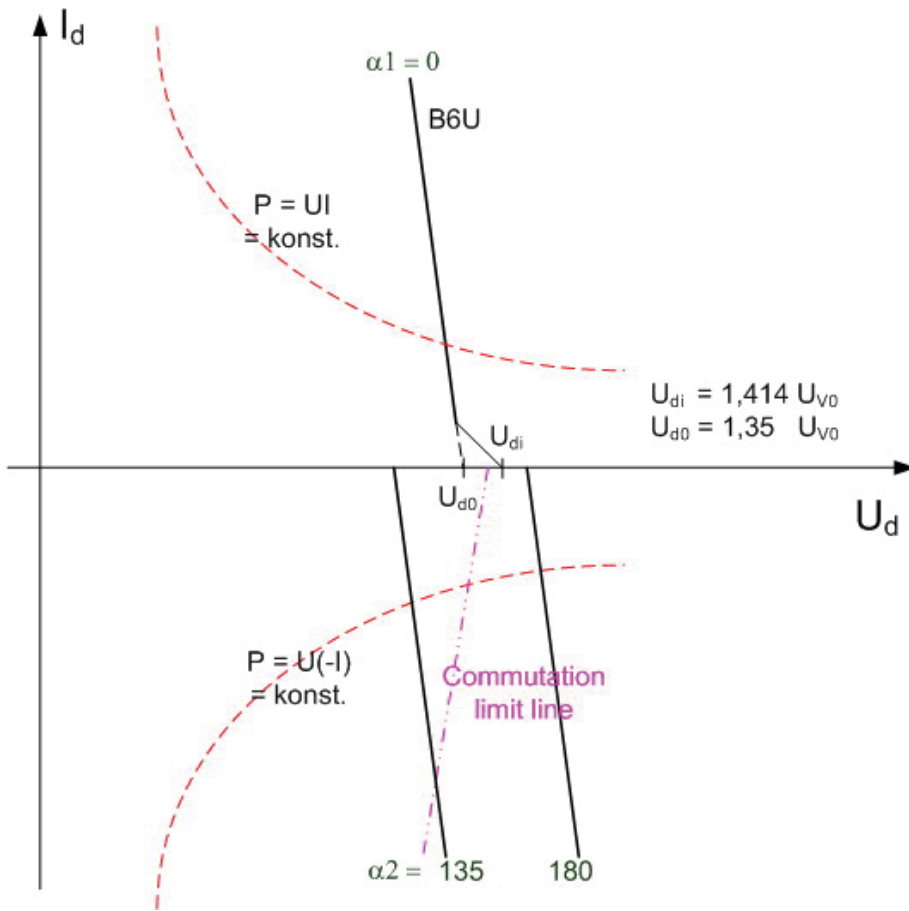
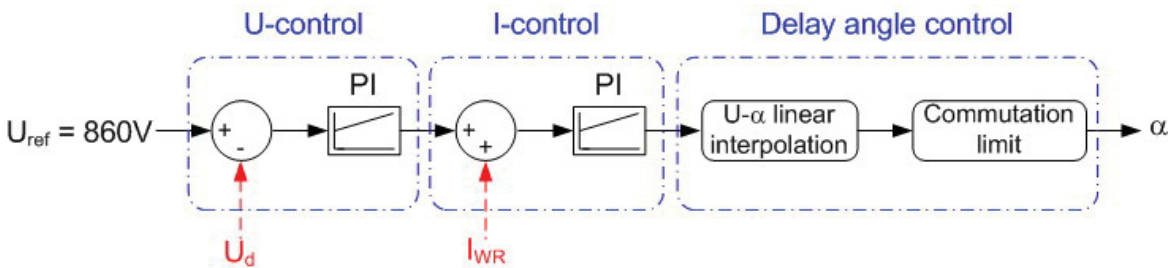


Figure 7-3 U-I curve in Braking**

Appendix F describes how to change the operation sequences between motor and generator by converting the current on a armature circuit reversible d.c. motor.

7.1.2 Dynamic control

The commutation limit lines indicated in Figure 7-3 give the highest admissible direct current for inverter operation at which the critical value of the extinction angle (circuit commutated recovery time) $\gamma = 180^\circ - \alpha$ is reached. For a given set of operating conditions (direct current and d.c. voltage) an unfavorable conduction through will occur if the delay angle α is increased beyond this limit.



Although the working limit for rectifier operation region in this paper is no used ($\alpha = 0^\circ$), it may be necessary for inverter operation region to limit the minimum value of the delay angle to control direct current circulation.

It is important to give an ideal delay angle value to the inverter so that more regenerative energy can flow back and at the same time less impact on system is occurring. Therefore, the double loop control as shown above is used.

The reference voltage is given with 860 V DC according to IEC 60850 standards. We take the voltage on the overhead line and the current flowing in the inverter as two feed-back values. Then the delay angle control will calculate an angle depending on the input which will avoid faulty Thyristors operating.

7.1.3 Results and Assessment

Let us discuss the current results in Figure 7-4. The current I_d is negative because its direction is different from original setting on Figure 7-1. From this figure we can easily get the relation between current as: $I_{WR} = I_d + (I_{GP1} - I_{GN1})$.

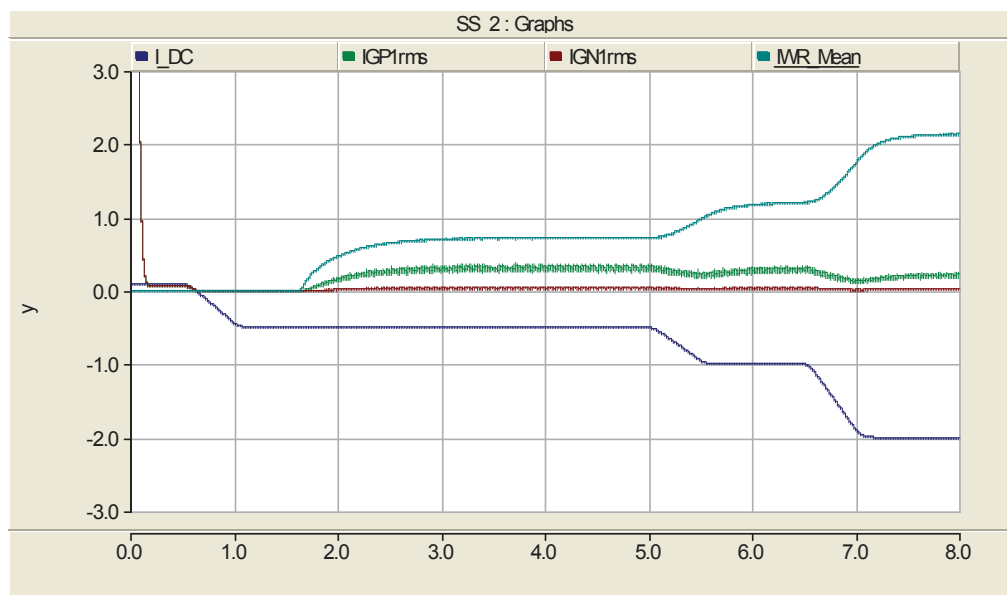


Figure 7-4 Currents in double converter

At the same time, we see in Figure 7-5 that the voltage at the overhead line is between 860 V and 890 V (time zone from 5s to 8s).

During the time zone from 0s to 2s the voltage crest is over 950 V because of the capacitance parallel on the load as a chopper.

The voltage difference between U_d and E_i (Figure 7-1) is U_{LkrM} which is displayed in Figure 7-5.

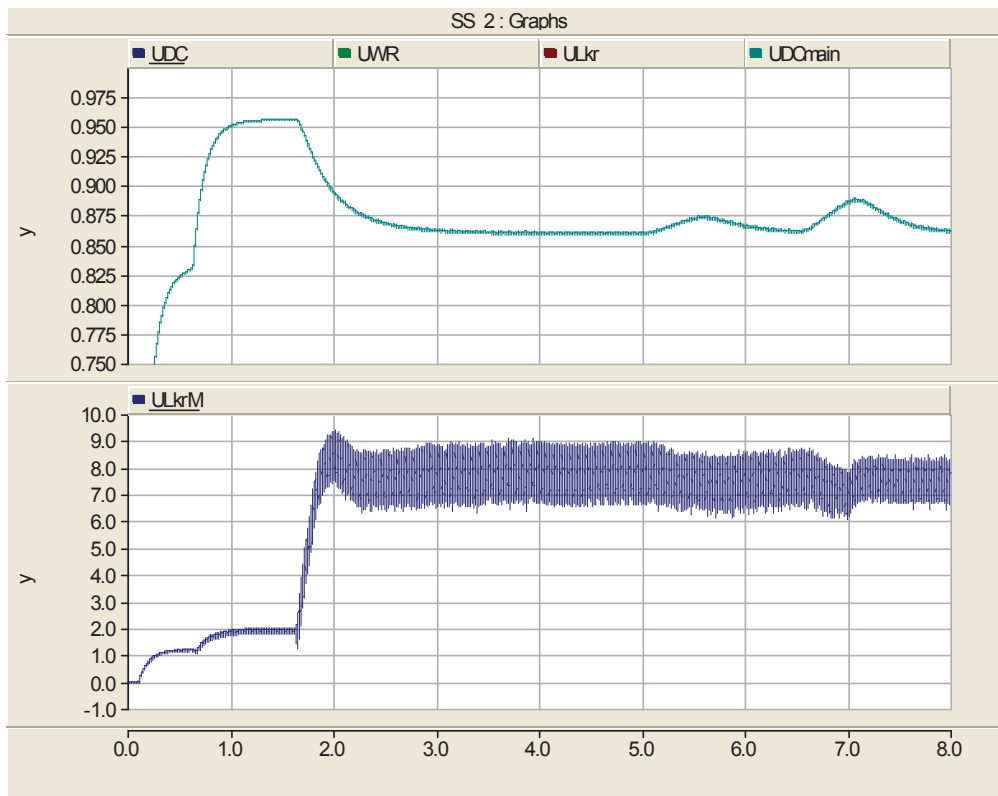


Figure 7-5 Voltage in Overhead line

In time zone 0s to 2s the voltage difference increases from 2 V to 8 V and then is nearly constant at 8 V with the current I_{DC} changing from -0,5 A to -2 A. It means that the double feed-back loop causing the voltage difference on the line does not create a too large voltage. By this we can avoid the over-current stress at the system.

Combining Figure 7-4 and 7-5 it shows that the voltage increases when the braking current increases. This means that the energy really flows back when braking and it proves the method to be effective.

7.2 Inverter with PWM

Pulse-width modulation (PWM) uses a square wave whose duty cycle is modulated resulting in the variation of the average value of the voltage. If we consider a square waveform $f(t)$ with a low value Y_{min} , a high value Y_{max} and a duty cycle D (Figure 7-6); the average value of the waveform is given by:

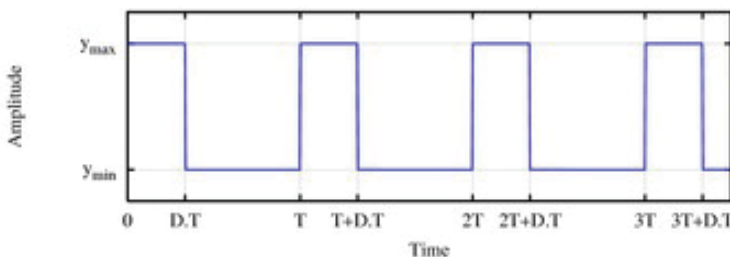


Figure 7-6 Square Wave*

$$\bar{y} = \frac{1}{T} \int f(t) dt \quad (7.1)$$

The PWM control set gives the time pulse signals for GTOs or IGBTs. GTOs are used for the lower frequency switching (less than 500 Hz). IGBTs have smaller turn on-off loss than GTOs. Therefore IGBTs are commonly used with higher switching frequencies.

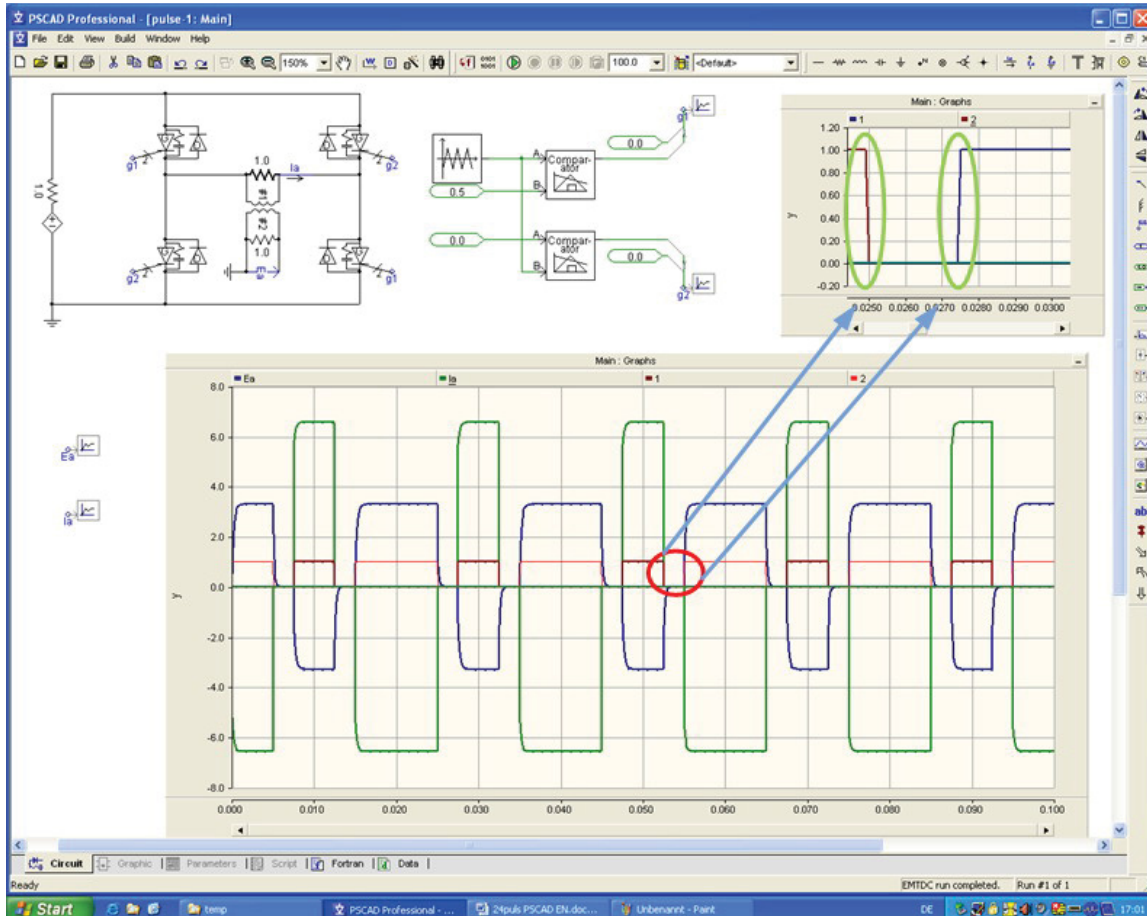


Figure 7-7 The Push-Pull Inversion**

In Figure 7-7, we can see the push-pull type inversion that is made by four GTOs. On the right side of this picture the pulse signal is shown with zoom in the original curve. The region at the edges of the pulse signal the line slopes because of the time delays.

PSCAD software lets the user the choice whether or not put the shunt capacitance and the resistance (value may adjusted freely) in GTO/IGBT elements. Insertion means that we can simulate the real condition more adequately.

For the three-phase PWM inversion simulation (Figure 7-8), we can change the phase and the width of pulse signals through adjustment of the firing angle. The AC output voltage and current are all shaped in the steps.

But they have a difference in phase. If we put the pulse signal like waveform (magenta) in Figure 7-9, we can obtain a waveform approximated better to a sinus curve. Then we are able to control the output voltage frequency and the peak-to-peak voltage value. Those

methods are proved in theory and practical applications completely.

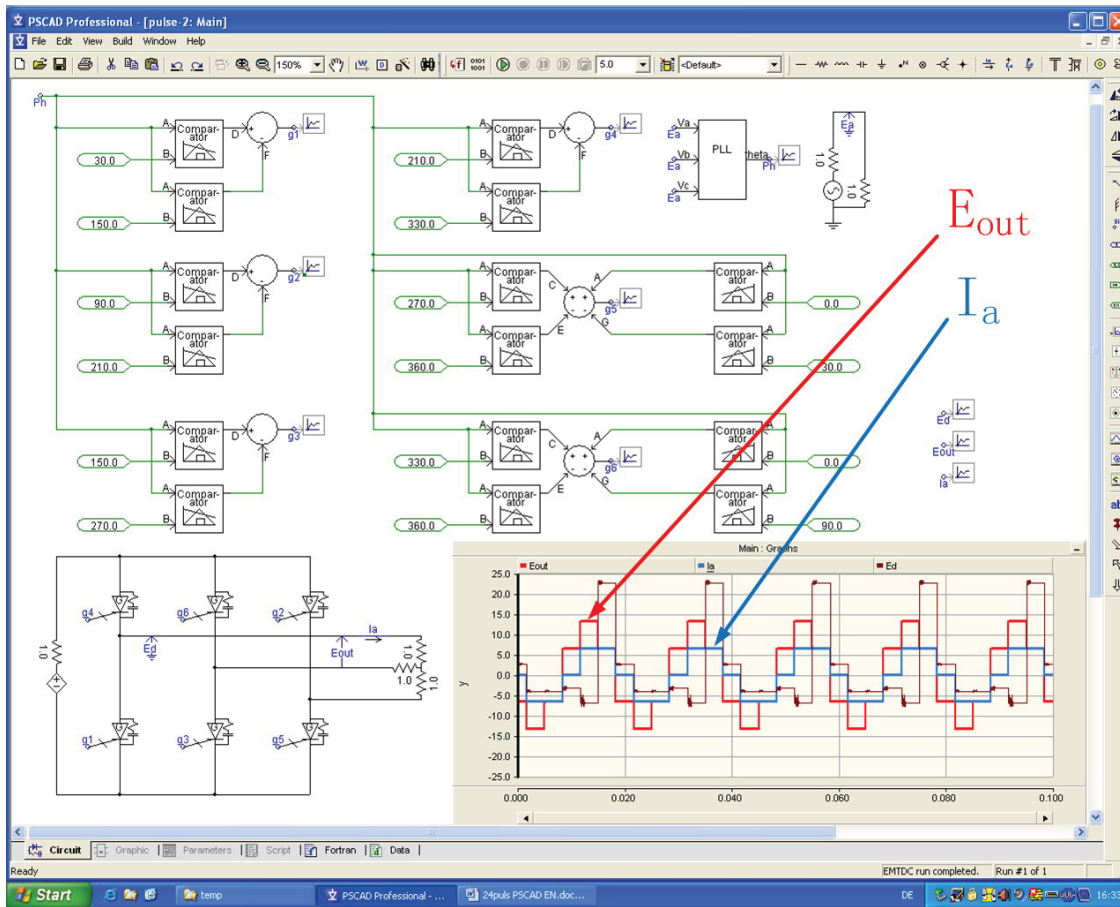


Figure 7-8 Three Phase DC/AC Invert**

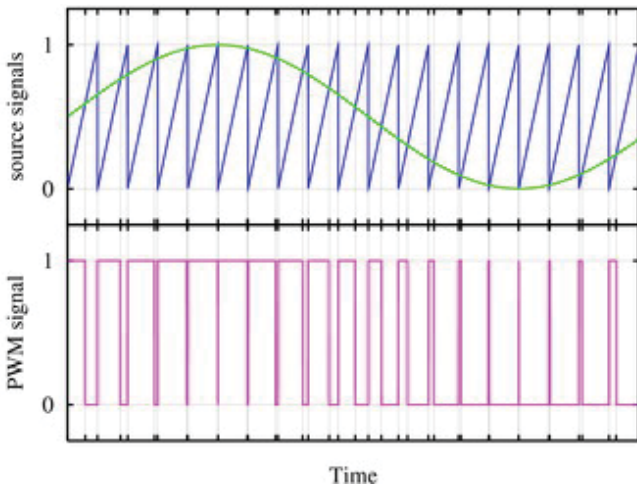


Figure 7-9 PWM Pulse Made*

Now a new problem happens. In this process of rectification and inversion the flow of energy is unidirectional. For a more effective use of energy the regenerative power flow with feedback of power to the grid or to a storage device leads to new idea in technological areas.

Now SIEMENS AG TS develops a method for accelerating track transportation applications to store the braking energy and reuse it for the train directly afterwards. The efficiency will reach 40 % which is a very advanced in the world. (Figure 7-10)

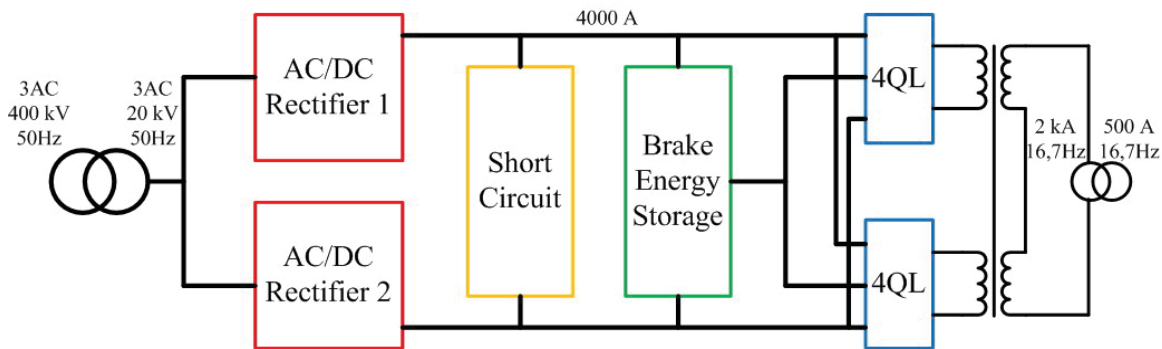


Figure 7-10 New method*

For an assessment in this chapter the PWM method is succeeded by PSCAD simulation. The further activities would be a discussion if, for example, whether we should provide a finer energy control model to simulate on PSCAD software.

8 Conclusion and Future

Practice should mean intensive work to achieve a goal. During these months of practice at the SIEMENS AG I reached more than one goal.

8.1 Conclusion

First, I became familiar using PSCAD software to simulate circuits such as AC/DC rectifier, DC/AC inverter or transformer in the traction power supply system.

Then I obtained an actual understanding about composition in rectification and inverter systems, the history of development and the principle of operation. It truly is an extremely beneficial experience for me that I can use in the future.

From all assessments in each part in this paper it can be concluded that simulations play a significant role in substation operation analysis, especially in the SNCF project and the Phoenix project.

So I am very satisfied with my practice work for obtaining many useful experiences during this time.

8.2 Further work

Work done after this thesis consists of a follow-up substation operation simulation by PSCAD that shall include three points as follows:

- 1 We can use PSCAD with every kind of built-in module to simulate all details in the actual operation in substations. This helps us to obtain a more precise operation curve and parameters which all are important for the advanced designs. This initiative also would enhance the efficiency in the design process, just in the way I did in Chapter 5 SNCF project.
- 2 After thoroughly discussing 24-pulse and/or 36-pulse substation we found a feasible plan comparing by results with each other to find advantages. The new winding connection way is described in Chapter 3.5. However, up to now I have no assessment on this substation design about magnetic and various electrical requirements to be found by simulation including all suitable test methods for the transformer.
- 3 During the inverter research I just simulate the inverter in the PWM way in Chapter 7. Now there is another kind of inverter control feasible by Space Vector PWM. When these two methods can be realized by PSCAD and compared for advantages and disadvantages, it will benefit provide a great for the motor designer. This development can be anticipated.

References

- [1] *Biesenack, H.; George, G.; Hofmann, G.; Schmieder, A.*: Energieversorgung elektrischer Bahnen. B.G. Teubner, Wiesbaden 2006.
- [2] IEC 60850 “Railway applications – Supply voltage of traction systems” 02/2007
- [3] *Helmut Weiß; Markus Lampersberger*: Sta In: Elektrische Bahnen 105(2007), S.260-264. tische und rotierende Netzkupplungs- umformer mit GTO- und IGC-Thyristoren- eine Gegenüberstellung. ZEV+DET Glas. Ann.122, 9/10 1998.
- [4] IEC 146-1 “Semiconductor converters – General requirements and line commutated converters” 03/1991
- [5] *Carsten Söffker; Rene Tutzauer*: Bahn-Antriebstechnik für sensible Streckenabschnitte und zur Energierückgewinnung. In: Elektrische Bahnen 105(2007)7,S.403-411.
- [6] DIN EN 50160 “Merkmale der Spannung in öffentlichen Elektrizitätsversorgungsnetzen” 01/1999
- [7] IEC 60076-8 “Power transformers – Application guide” 10/1997
- [8] *Thomas Groh; Martin Lemke*: Instandhaltung bei der DB Energie. In: Elektrische Bahnen 105(2007)4-5,S.260-264.
- [9] DIN 41750 “Begriffe für Stromrichter” 07/1986
- [10] *Schlunegger, H.*: Wechselrichterwerk bei DC-Bahnen. In: Elektrische Bahnen 101(2003)11,S.500-506.
- [11] *Puritz, K.-J.; Schwarzer, M.*: Konzept für Gleichrichterwerke der S-Bahn. In: Elektrische Bahnen 98(2000)7, S.259-265.
- [12] *Petterson, G. A.; Swenson, S.*: Störungskompensation durch Gleise, Rückleiter und Saugtransformatoren an elektrischen Bahnen. In: Tele (1961)2, pp.61 to 92.
- [13] *Kötnitz, H.; Pundt, H.*: Berechnung elektrischer Energieversorgungsnetze, Mathematische Grundlagen und Netzparameter. Verlag Grundstoffindustrie, Leipzig, 1968.
- [14] *Bethge, W.*: Return of traction current on the German Railway’s new high-speed

- lines. In: ETR 31(1982)12, pp.901 to 908.
- [15] *Berends, D.; Brodkorb, A.; Hofmann, G.*: Berechnungsverfahren für Fahrleitungsimpedanzen. In: Elektrische Bahnen 92(1994)4, pp. 114 to 122.
- [16] *Rainer Jäger; Edgar Stein*: Leistungselektronik – Grundlagen und Anwendungen. VDE VERLAG, Berlin, 2000.
- [17] IEC 76-1 “Power transformers” 03/1993
- [18] *Jäger, A.; Baechler, U.; Brom, B.*: Maßnahmen zur Verbesserung des Netzverhaltens von Stromrichter-Triebfahrzeugen. Brown Boveri Mitt.60 (1973) S.501.
- [19] *Kehrmann, H.; Lienau, W.; Nill, R.*: Vierquadrantensteller. Elektr. Bahnen 45(1974) S.135.
- [20] *Samuli, T.*: Technical Specification for Controlled Thyristor Double Converter. Adtranz Sweden, 1996.
- [21] *Thiwanka Wijekoon; Christian Klumpner; Patrick Wheeler*: Active Compensation for Supply Voltage Unbalance on Two-stage Direct Power Converter. EPE Journal Vol.17 2007 Page 5 to 12. ISSN 0939-8368
- [22] DC-Leistungsnetzgeräte mit Energie-Rückspeisung Energy Recovery-System. Elektronik Report oktober 2007, Page 27.
- [23] *Marquardt, R.*: GTO-Gleichstromsteller für Nahverkehrsbahnen. Elektr. Bahnen 85 (1987) S.336.
- [24] *Milko Paolucci; Lutz Görgens*: Neue MOSFETs für grüne DC/DC-Wandler. Elektronik 21/2007, Page 46 to 49.
- [25] *Gitta Rohling*: Virtuell auf Hochtouren. Pictures of the Future Die Zeitschrift für Forschung und Innovation / Herbst 2007 SIEMENS, Page 30 to 32.
- [26] *Bernhard Gerl*: Schnelle Stromdepots. Pictures of the Future Die Zeitschrift für Forschung und Innovation / Herbst 2007 SIEMENS, Page 74 to 75.
- [27] *Stein, W.*: Stufenschalter mit Thyristor Lastumschalter für Wechselstrom-Triebfahrzeuge. Siemens-Z.39 (1965) S.269.
- [28] *Edel, R.; Schneider, E.; Schweller, M.*: Systemauslegung der Bahnstromversorgung von Gleichstrom- und Wechselstrombahnen. eb-Elektrische Bahnen, 1998.
- [29] *Schneider, E.; Zachmeier, M.*: Bahnrückstromführung und Erdung bei Bahnanlagen

- Teil 3: Gleichstrombahnen. eb-Elektrische Bahnen, 1998.
- [30] *Junsheng, L.; Zimmert, G.*: Electrification of the line Harbin-Dalian within the P.R.C. In Elektrische Bahnen 3, pp.107 to 120
- [31] *Halfmann, U.; Hein, G.; Olsen, H.; Röhlig, S.*: Wirtschaftliche Optimierung von Stadtbahnen durch Nutzung der Bremsenergie in Energiespeichern. In: VDE-Bericht zum VDE Kongress 2002 NetWorlds, Band 1, VDE-Verlag Berlin (2002), S.419-425.
- [32] *Lindner, H.; Brauer, H.; Lehmann, C.*: Taschenbuch der Elektrotechnik und Elektronik. VEB Fachbuchverlag Leipzig 1989.
- [33] *Erich Braun*: Fünfzig Jahre Doppelerdschluss-Automatik im DB-Unterwerk Steinbach. Elektrische Bahnen 8/2007, Page 436 to 439.
- [34] *Helmut Lehmann*: Energiesparende Fahrweise bei der Deutschen Bahn. Elektrische Bahnen 7/2007, Page 397 to 402.

List of Nomenclature

(in order of appearance)

List of subscripts

| | |
|----------|--|
| 0 (zero) | at no load |
| h | pertaining to harmonic component of order h |
| i | ideal |
| N | rated value (nominal value) |
| x | inductive |
| α | angle of delay of phase control (firing angle) |

List of symbols

| | |
|---------------------|--|
| DC | direct current |
| AC | alternating current |
| FFT | Fast Fourier Transform |
| B6U | 6 pulse bridge converter connection with diode |
| B6C | 6 pulse bridge converter connection with controlled thyristor |
| U_{0AV} (U_d) | average output voltage on DC side |
| I_{0AV} | average output current on DC side |
| f | frequency |
| P_N | rated real power |
| Q_N | rated reactive power |
| S_N | rated apparent power |
| $\cos(\omega)$ | power factor |
| THD | total harmonic distortion |
| $U_{di\text{ eff}}$ | effective value for ideal output voltage on DC side |
| P_0 (P_{Fe}) | iron core losses |
| P_K (P_{Cu}) | copper losses |
| U_{V0} | no-load line-to-line voltage (RMS) on the line side of the converter or on the valve side of the transformer, if any |

| | |
|--------------|--|
| I_{1i} | ideal fundamental component of current on line side |
| I_{di} | ideal direct current |
| q | commutation number |
| s | number of series connected commutating groups |
| p | pulse number |
| U_h | harmonics voltage (per unit to rated input voltage) |
| I_h | harmonic order of current on line side |
| d_x | inductive direct voltage regulation at rated load in per unit of U_{d0} |
| U_{Imp} | impedance voltage in per unit of U_N on transformer primary side |
| E_{ZigZag} | vector value for transformer output voltage |
| I_{FAV} | maximum average on-state current of diode or thyristor |
| U_{RRM} | maximum momentary value of periodic reverse voltage impulses in form of a sine half oscillation with defined duration or frequency |
| I_{WR} | current on inverter |
| I_{GP1} | current from rectifier positive point |
| I_{GN1} | current back to rectifier negative point |
| U_{ref} | reference voltage value |
| RB | Rectifier Bridge |
| T | time constant of RC circuit |

List of Illustrations

| | | |
|--------------------|---|----|
| Figure 1-1 | 2007 The HeXie train running* | 4 |
| Figure 1-2 | Railway Plan “8 vertical 8 horizontal” in China | 5 |
| Figure 1-3 | AC power supply* | 6 |
| Figure 1-4 | DC power supply* | 6 |
| Figure 1-5 | U-I Line for GTO/IGBT | 7 |
| Figure 1-6 | U-I Line for GTO/IGBT | 8 |
| Figure 1-7 | New Train developments by SIEMENS* | 10 |
| Figure 2-1 | Measurement of Power | 11 |
| Figure 2-2 | Power factor measurement in PSCAD** | 11 |
| Figure 2-3 | Voltage Regulation [4] | 12 |
| Figure 2-4 | DC voltage values with arbitrary pulse [16] | 14 |
| Figure 2-5 | Ripple factor measurement in PSCAD | 14 |
| Figure 2-6 | THD measure in PSCAD | 15 |
| Figure 2-7 | DC output Voltage profile [16] | 16 |
| Figure 3-1 | 6-pulse rectifier by B6U** | 18 |
| Figure 3-2 | Zigzag Transformer** | 19 |
| Figure 3-3 | Z-Transformer (1)** | 20 |
| Figure 3-4 | Voltage Vector Analysis (1)** | 20 |
| Figure 3-5 | Z-Transformer (2)** | 21 |
| Figure 3-6 | Voltage Vector Analysis (2)** | 21 |
| Figure 3-7 | Z-Transformer (3)** | 22 |
| Figure 3-8 | Voltage Vector Analysis (3)** | 22 |
| Figure 3-9 | Calculate Shift Angle with MathCAD Software** | 23 |
| Figure 3-10 | Simulation Result (Degree)** | 24 |
| Figure 3-11 | Four different connecting methods** | 25 |
| Figure 3-12 | (6BU)2P2S AC/DC Rectification Simulation** | 25 |
| Figure 3-13 | Write in Parameter** | 26 |
| Figure 3-14 | DC voltage curve** | 27 |
| Figure 3-15 | Voltage curve Zoom in** | 27 |
| Figure 3-16 | Curves of Voltage Regulation** | 28 |
| Figure 3-17 | FFT analysis for Harmonics** | 30 |
| Figure 3-18 | Left: no-load (idling) operation; Right: operated at rated current | 31 |

| | | |
|--------------------|--|----|
| Figure 3-19 | 24pulse I_d-d_X Curve* | 32 |
| Figure 3-20 | 24 pulse d_X-THD Curve* | 33 |
| Figure 3-21 | Normal 36-Pulse Rectification** | 35 |
| Figure 3-22 | Secondary side of Four Windings Zigzag Transformer** | 36 |
| Figure 3-23 | 36-Pulse Voltage Vector Analysis** | 37 |
| Figure 3-24 | Advanced 36-Pulse Rectification** | 38 |
| Figure 4-1 | Diagram for Diode Faults** | 39 |
| Figure 4-2 | Results on the each branch when diode short-circuit* | 40 |
| Figure 4-3 | Results on branch when diode conduction is interrupted* | 43 |
| Figure 5-1 | Harmonic FFT analysis Output** | 46 |
| Figure 5-2 | On-line software for DC Rectifier Character (1)* | 47 |
| Figure 5-3 | On-line software for DC Rectifier Character (2)* | 48 |
| Figure 5-4 | Voltage Vector Analysis (4)** | 50 |
| Figure 6-1 | TPSS circuit Topology** | 53 |
| Figure 6-2 | No-load operation** | 55 |
| Figure 6-3 | Crest Voltage by Pulse Current** | 57 |
| Figure 6-4 | No-load output Voltage (without snubber) | 58 |
| Figure 6-5 | No-load Measure Result* | 58 |
| Figure 6-6 | No-load output Voltage (with snubber) | 60 |
| Figure 6-7 | Output Voltage (without snubber) $R_{shunt} = 88\Omega$ | 60 |
| Figure 6-8 | Power system and Aux system Topology** | 61 |
| Figure 6-9 | Low aux $I = 20$ A (without snubber) | 61 |
| Figure 6-10 | Low Auxiliary System Running* | 62 |
| Figure 6-11 | Low aux $I = 20$ A (with snubber) | 62 |
| Figure 6-12 | Heavy aux $I = 100$ A (without snubber) | 63 |
| Figure 6-13 | Heavy Auxiliary System Running* | 63 |
| Figure 6-14 | Heavy aux $I = 100$ A (with snubber) | 64 |
| Figure 6-15 | Feeder Crossing** | 65 |
| Figure 6-16 | Feeder on contact line* | 65 |
| Figure 6-17 | Cross Feeder ($L=1$ mH=>$1,5$ mH, $C=3$ μF=>5 μF) | 66 |
| Figure 6-18 | Cross Feeder ignorance L,C on overhead line | 66 |
| Figure 6-19 | Crossing Feeder measure* | 67 |
| Figure 6-20 | Cross Feeder (with snubber) | 67 |
| Figure 6-21 | FFT on DC side without Snubber | 68 |
| Figure 6-22 | FFT on DC side with Snubber | 68 |

| | | |
|--------------------|--|----|
| Figure 6-23 | Filter's gain magnitude* | 69 |
| Figure 6-24 | Firing angle control | 69 |
| Figure 6-25 | Asymmetry Operation with Low Aux | 70 |
| Figure 6-26 | Asymmetry Operation Measurement* | 70 |
| Figure 7-1 | Double converter topology** | 72 |
| Figure 7-2 | Direct voltage limits in inverter operation | 73 |
| Figure 7-3 | U-I curve in Braking** | 74 |
| Figure 7-4 | Currents in double converter | 75 |
| Figure 7-5 | Voltage in Overhead line | 76 |
| Figure 7-6 | Square Wave* | 76 |
| Figure 7-7 | The Push-Pull Inversion** | 77 |
| Figure 7-8 | Three Phase DC/AC Invert** | 78 |
| Figure 7-9 | PWM Pulse Made* | 78 |
| Figure 7-10 | New method* | 79 |

Note:

1 All Figures (except in Note 2) are from PSCAD as curve results like Figure 3-15. X-axis is time (second) and Y-axis is voltage (kV)

2

| | X-axis | Y-axis |
|--------------------|------------------------------|------------------------------|
| Figure 3-18 | Current (kilo ampere) | dx (per unit) |
| Figure 3-19 | dx (per unit) | THD (percent) |
| Figure 7-4 | Time (second) | Current (kilo ampere) |

3 Time zone from 0s to 0,05s in PSCAD is system checking in all operation.

List of Tables

| | | |
|-------------------|--|----|
| Table 3-1 | Phase shifting in Transformer** | 19 |
| Table 3-2 | 24-pulse Transformer Power** | 28 |
| Table 3-3 | 24-pulse Voltage Regulation** | 28 |
| Table 3-4 | 24-pulse Transformer Losses** | 29 |
| Table 3-5 | 24-pulse Short Current** | 29 |
| Table 3-6 | THD in no-load** | 29 |
| Table 3-7 | Ripple factor for d.c.** | 29 |
| Table 3-8 | Commutation ratio** | 29 |
| Table 3-9 | Superposed AC voltage on DC side** | 30 |
| Table 3-10 | Harmonic current on AC side** | 30 |
| Table 3-11 | General Evaluation* | 34 |
| Table 4-1 | Odd-numbered Harmonics (non-multiple to 3)* | 44 |
| Table 4-2 | Full load with harmonics from net** | 44 |
| Table 5-1 | Harmonic Analysis by FFT** | 49 |
| Table 6-1 | Harmonics on DC side** | 68 |

*) The sources of Figures, Tables are from SIEMENS TS web site or other open-share documents in SIEMENS AG or other references.

***) All source of Figures, Tables are from the author's own work

APPENDIX A Rectifier Diode

| | |
|--|---|
| Key Parameters $V_{RRM} = 1700 \text{ V}$ $I_{FAVM} = 1310 \text{ A}$ $I_{FSM} = 15.0 \text{ kA}$ $V_{F0} = 0.74 \text{ V}$ $r_F = 0.25 \text{ m}\Omega$ | Avalanche Rectifier Diode 5SDA 11D1702 |
|--|---|

Doc. No. 58YA 1119 - 01 Apr-98

Features

- Optimized for line frequency rectifiers
- Low on-state voltage, narrow V_F -bands for parallel operation
- Self protected against transient overvoltages
- Guaranteed maximum avalanche power dissipation
- Industry standard housing

Blocking

| Part number | 5SDA 11D1702 | 5SDA 11D1402 | 5SDA 11D1102 | Condition |
|-------------|----------------------|--------------|--------------|--|
| V_{RRM} | 1700 | 1400 | 1100 | $f = 50 \text{ Hz}$ $t_F = 10 \text{ ms}$ |
| V_{RSM} | 1870 | 1540 | 1200 | $t_F = 10 \text{ ms}$ $T_J = 160^\circ\text{C}$ |
| I_{RRM} | $\leq 50 \text{ mA}$ | | | V_{RRM} $T_J = 160^\circ\text{C}$ |
| P_{RSM} | $\leq 70 \text{ kW}$ | | | $t_F = 20 \mu\text{s}$ $T_J = 45^\circ\text{C}$ |
| | $\leq 50 \text{ kW}$ | | | $t_F = 20 \mu\text{s}$ $T_J = 160^\circ\text{C}$ |

Mechanical data

| | | | |
|-------|---------------------------|------------------|--------------------|
| F_M | Mounting force | min. | 10 kN |
| | | max. | 12 kN |
| a | Acceleration | Device unclamped | 50 m/s^2 |
| | | Device clamped | 200 m/s^2 |
| m | Weight | 0.25 kg | |
| D_s | Surface creepage distance | 30 mm | |
| D_a | Air strike distance | 20.5 mm | |

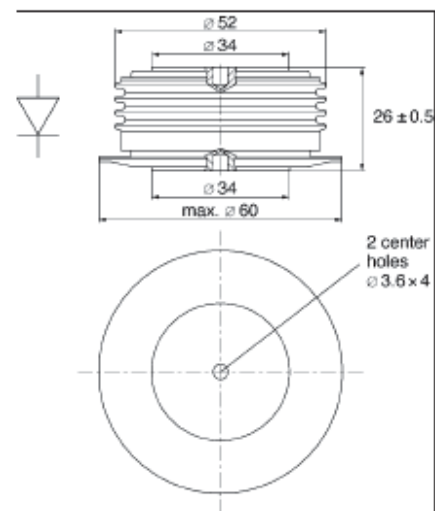


ABB Semiconductors AG

ABB

ABB Semiconductors AG

5SDA 11D1702

On-state

| | | | | |
|------------|--|---------------------------------------|--|---|
| I_{FAVM} | Max. average on-state current | 1310 A | Half sine wave, $T_C = 85^\circ\text{C}$ | |
| I_{FRMS} | Max. RMS on-state current | 2060 A | | |
| I_{FSM} | Max. peak non-repetitive surge current | 15 kA | $t_p =$ | 10 ms |
| | | 16 kA | $t_p =$ | 8.3 ms |
| I^2t | Limiting load integral | $1130 \cdot 10^3 \text{ A}^2\text{s}$ | $t_p =$ | 10 ms |
| | | $1070 \cdot 10^3 \text{ A}^2\text{s}$ | $t_p =$ | 8.3 ms |
| V_{FO} | Threshold voltage | 0.74 V | $I_F =$ | 1000 - 3000 A |
| r_F | Slope resistance | 0.25 m Ω | | |
| V_{Fmin} | On-state voltage | 1.05 V | $I_F =$ | 1800 A |
| V_{Fmax} | On-state voltage | 1.20 V | | |
| | | | | $T_J = 160^\circ\text{C}$ |
| | | | | After surge: $V_R \approx 0\text{V}$ |
| | | | | $T_J = 160^\circ\text{C}$ |
| | | | | $T_J = 25^\circ\text{C}$ |

Thermal

| | | | |
|------------|--|-------------|---------------------|
| T_J | Storage and operating junction temperature range | -40...160°C | |
| R_{thJC} | Thermal resistance junction to case | 80 K/kW | Anode side cooled |
| | | 80 K/kW | Cathode side cooled |
| | | 40 K/kW | Double side cooled |
| R_{thCH} | Thermal resistance case to heat sink | 16 K/kW | Single side cooled |
| | | 8 K/kW | Double side cooled |

Analytical function for transient thermal impedance:

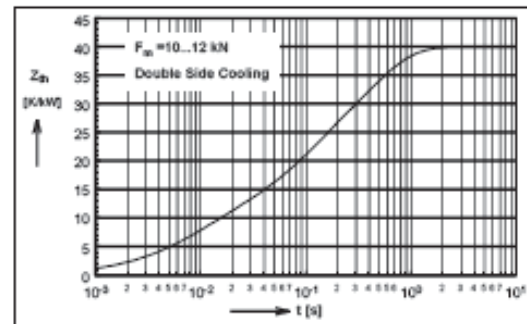
$$Z_{thJC}(t) = \sum_{i=1}^4 R_i(1 - e^{-t/\tau_i})$$

| i | 1 | 2 | 3 | 4 |
|--------------|-------|-------|-------|--------|
| $R_{(K/kW)}$ | 20.95 | 10.57 | 7.15 | 1.33 |
| τ_i (s) | 0.396 | 0.072 | 0.009 | 0.0044 |

For a given case temperature T_C at ambient temperature T_A the maximum on-state current can be calculated as follows:

$$I_{FAVM} = \frac{-V_{FO} + \sqrt{(V_{FO})^2 + 4 \cdot f^2 \cdot r_F \cdot P}}{2 \cdot f^2 \cdot r_F}$$

$$\text{where } P = \frac{T_{Jmax} - T_C}{R_{thJC}} \text{ or } P = \frac{T_{Jmax} - T_A}{R_{thJA}}$$



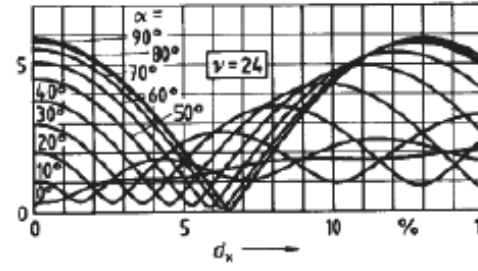
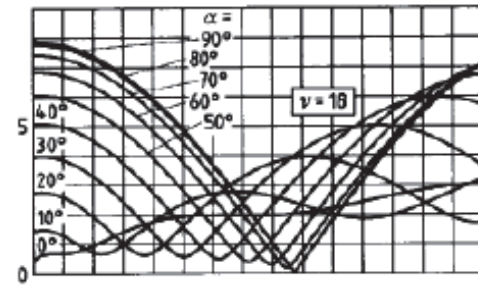
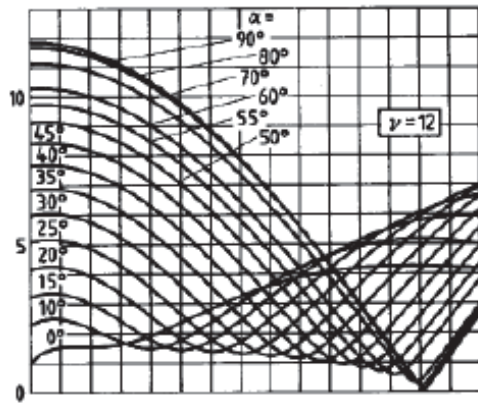
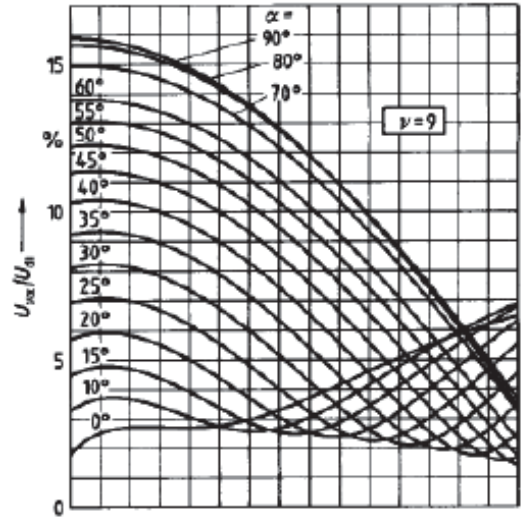
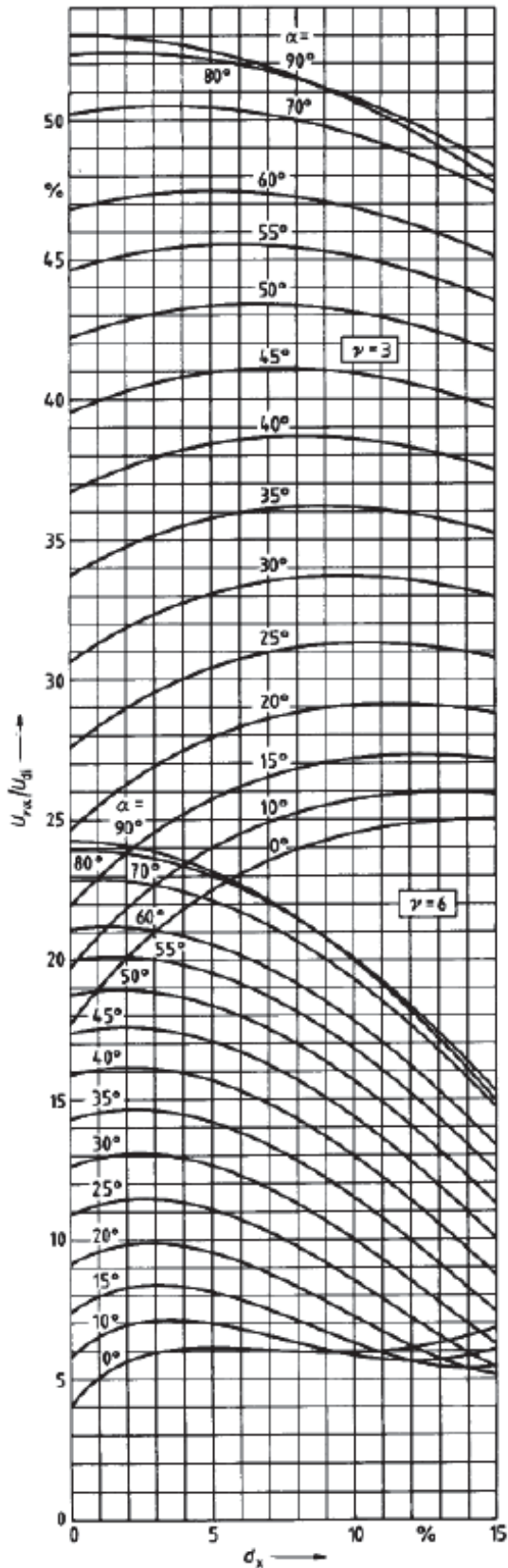
| | | | |
|--------------------------------|----------------------------|----------------------------|--------------------|
| I_{FAVM} (A) | P (W) | V_{FO} (V) | r_F (Ω) |
| T_{max} ($^\circ\text{C}$) | T_C ($^\circ\text{C}$) | T_A ($^\circ\text{C}$) | |
| R_{thJA} (K/kW) | R_{thJC} (K/kW) | | |
| $f^2 =$ | 1 for DC current | | |
| | 2.5 for half-sine wave | | |
| | 3.1 for 120° el. sine | | |
| | 6 for 60° el. sine | | |

APPENDIX B IEC 60146-1

Direct voltage Harmonic content

Overlaid voltage on DC side and Harmonic current on AC side

| p | 2 | | 3 | | 6 | | 12 | | 18 | | 24 | |
|-----|------------------------------|------------------------------|------------------------------|------------------------------|------------------------------|------------------------------|------------------------------|------------------------------|------------------------------|------------------------------|------------------------------|------------------------------|
| v | $\frac{U_{vi}}{U_{di}}$ % | $\frac{I_{vi}}{I_{ii}}$ % | $\frac{U_{vi}}{U_{di}}$ % | $\frac{I_{vi}}{I_{ii}}$ % | $\frac{U_{vi}}{U_{di}}$ % | $\frac{I_{vi}}{I_{ii}}$ % | $\frac{U_{vi}}{U_{di}}$ % | $\frac{I_{vi}}{I_{ii}}$ % | $\frac{U_{vi}}{U_{di}}$ % | $\frac{I_{vi}}{I_{ii}}$ % | $\frac{U_{vi}}{U_{di}}$ % | $\frac{I_{vi}}{I_{ii}}$ % |
| 2 | 47,14 | — | — | 50,00 | — | — | — | — | — | — | — | — |
| 3 | — | 33,33 | 17,68 | — | — | — | — | — | — | — | — | — |
| 4 | 9,43 | — | — | 25,00 | — | — | — | — | — | — | — | — |
| 5 | — | 20,00 | — | 20,00 | — | 20,00 | — | — | — | — | — | — |
| 6 | 4,04 | — | 4,04 | — | 4,04 | — | — | — | — | — | — | — |
| 7 | — | 14,29 | — | 14,29 | — | 14,29 | — | — | — | — | — | — |
| 8 | 2,24 | — | — | 12,50 | — | — | — | — | — | — | — | — |
| 9 | — | 11,11 | 1,77 | — | — | — | — | — | — | — | — | — |
| 10 | 1,43 | — | — | 10,00 | — | — | — | — | — | — | — | — |
| 11 | — | 9,09 | — | 9,09 | — | 9,09 | — | 9,09 | — | — | — | — |
| 12 | 0,99 | — | 0,99 | — | 0,99 | — | 0,99 | — | — | — | — | — |
| 13 | — | 7,69 | — | 7,69 | — | 7,69 | — | 7,69 | — | — | — | — |
| 14 | 0,73 | — | — | 7,14 | — | — | — | — | — | — | — | — |
| 15 | — | 6,67 | 0,63 | — | — | — | — | — | — | — | — | — |
| 16 | 0,55 | — | — | 6,25 | — | — | — | — | — | — | — | — |
| 17 | — | 5,88 | — | 5,88 | — | 5,88 | — | — | — | 5,88 | — | — |
| 18 | 0,44 | — | 0,44 | — | 0,44 | — | — | — | 0,44 | — | — | — |
| 19 | — | 5,26 | — | 5,26 | — | 5,26 | — | — | — | 5,26 | — | — |
| 20 | 0,35 | — | — | 5,00 | — | — | — | — | — | — | — | — |
| 21 | — | 4,76 | 0,32 | — | — | — | — | — | — | — | — | — |
| 22 | 0,29 | — | — | 4,55 | — | — | — | — | — | — | — | — |
| 23 | — | 4,35 | — | 4,35 | — | 4,35 | — | 4,35 | — | — | — | 4,35 |
| 24 | 0,25 | — | 0,25 | — | 0,25 | — | 0,25 | — | — | — | 0,25 | — |
| 25 | — | 4,00 | — | 4,00 | — | 4,00 | — | 4,00 | — | — | — | 4,00 |



d_x relative induktive Gleichspannungsänderung
 α Steuerwinkel (bei Wechselrichterbetrieb ist anstelle von α der Löschwinkel γ einzusetzen).

- α Delay angle (in the case of inverter operation, use extinction angle γ)
- d_x Inductive direct voltage regulation. (IEC 60146-1; DIN 41750)

APPENDIX C Harmonic Disturbances

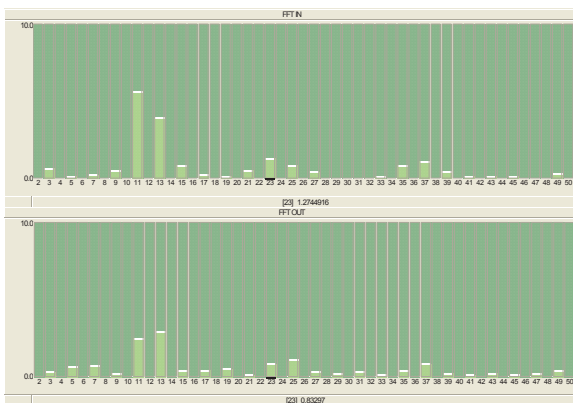
Fast Fourier Transform Results with different connection



FFT analyze results with 4S



FFT analyze results with 2P2S

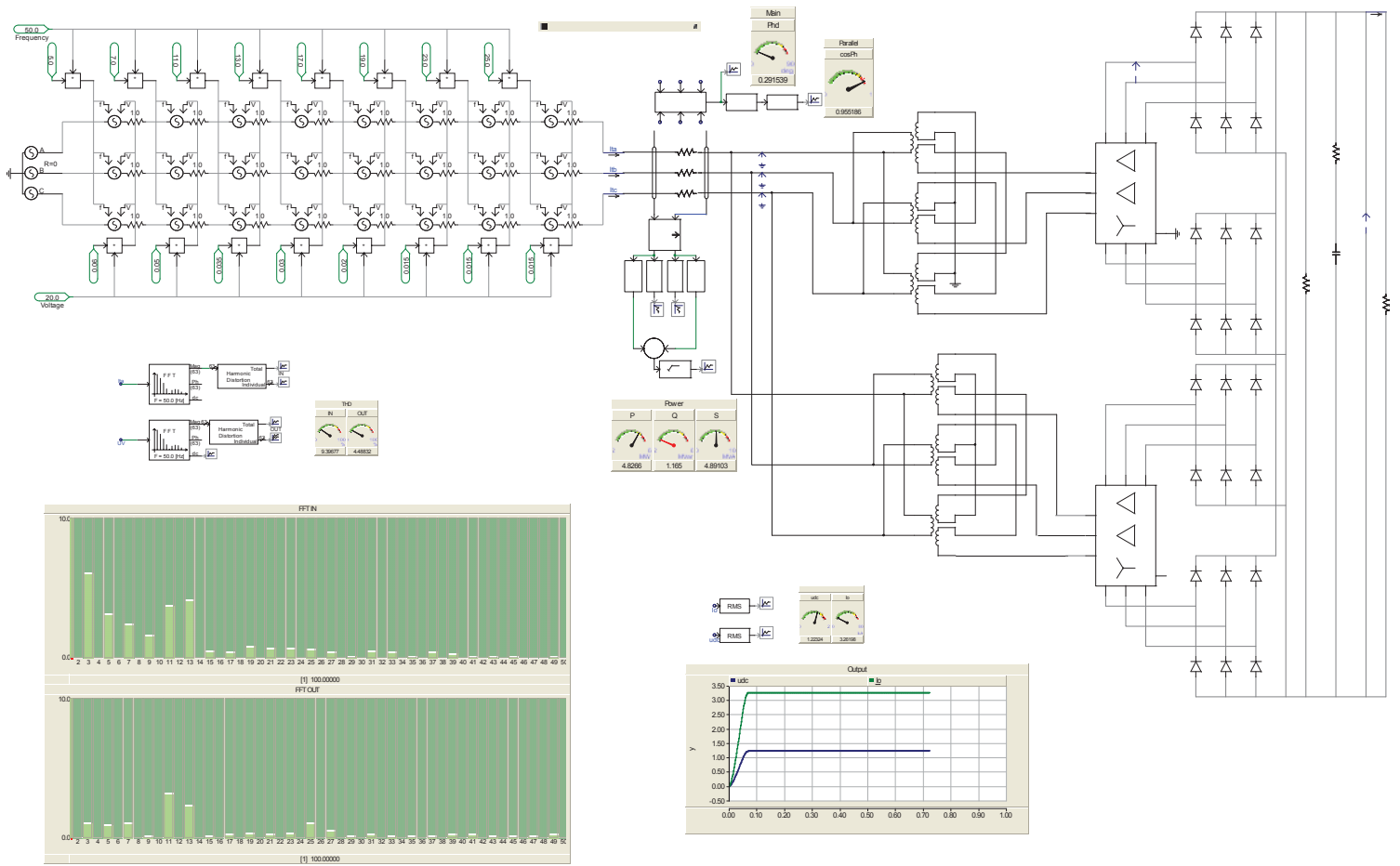


FFT analyze results with 2S2P



FFT analyze results with 4P

PSCAD simulator's topology
as followed



APPENDIX D SNCF Data

AC side Harmonic Analyze

| 4P | Standard ¹⁾ | - 5 % | - 2,5 % | 2,5 % | 5 % |
|------|------------------------|--------|---------|--------|--------|
| 3rd | 0,0000 | 0,0155 | 0,0395 | 0,0408 | 0,0144 |
| 5th | 0,0000 | 0,0113 | 0,0196 | 0,0195 | 0,0062 |
| 7th | 0,0564 | 0,0206 | 0,0115 | 0,0161 | 0,0137 |
| 9th | 0,0572 | 0,0157 | 0,0026 | 0,0101 | 0,0107 |
| 11th | 0,0004 | 0,7871 | 0,3955 | 0,3790 | 0,7165 |
| 13th | 0,0004 | 0,3099 | 0,1568 | 0,1492 | 0,2891 |
| 15th | 0,0264 | 0,0021 | 0,0105 | 0,0147 | 0,0156 |
| 17th | 0,0262 | 0,0059 | 0,0052 | 0,0082 | 0,0134 |
| 19th | 0,0000 | 0,0133 | 0,0230 | 0,0149 | 0,0172 |
| 21st | 0,0000 | 0,0167 | 0,0210 | 0,0185 | 0,0000 |
| 23rd | 1,2211 | 1,0083 | 1,0387 | 1,0260 | 1,0225 |
| 25th | 1,0350 | 0,6613 | 0,6907 | 0,6891 | 0,6962 |
| 31st | 0,0585 | 0,0218 | 0,0124 | 0,0203 | 0,0179 |
| 33rd | 0,0596 | 0,0252 | 0,0164 | 0,0239 | 0,0177 |
| 35th | 0,0001 | 0,1793 | 0,0904 | 0,0871 | 0,1714 |
| 37th | 0,0001 | 0,1330 | 0,0690 | 0,0669 | 0,1244 |
| 39th | 0,0142 | 0,0059 | 0,0088 | 0,0083 | 0,0090 |
| 41st | 0,0198 | 0,0041 | 0,0064 | 0,0059 | 0,0066 |
| 43rd | 0,0001 | 0,0313 | 0,0202 | 0,0204 | 0,0353 |
| 45th | 0,0001 | 0,0365 | 0,0274 | 0,0270 | 0,0420 |
| 47th | 0,2690 | 0,1633 | 0,1915 | 0,1946 | 0,1657 |
| 49th | 0,2159 | 0,1227 | 0,1434 | 0,1493 | 0,1302 |

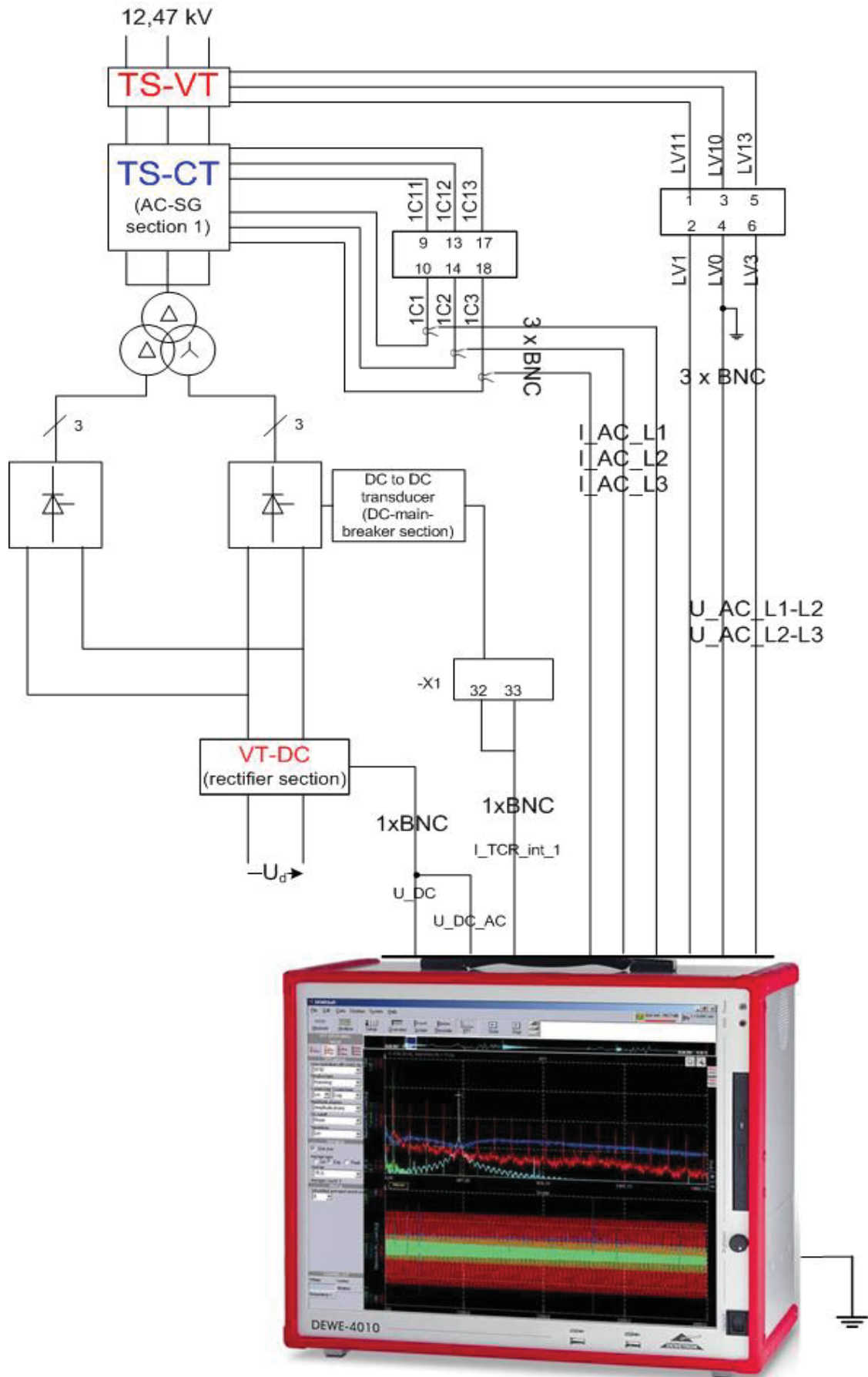
1) 4 kA / 1,5 kV / 6,6 MVA in output (also in the three follow table)

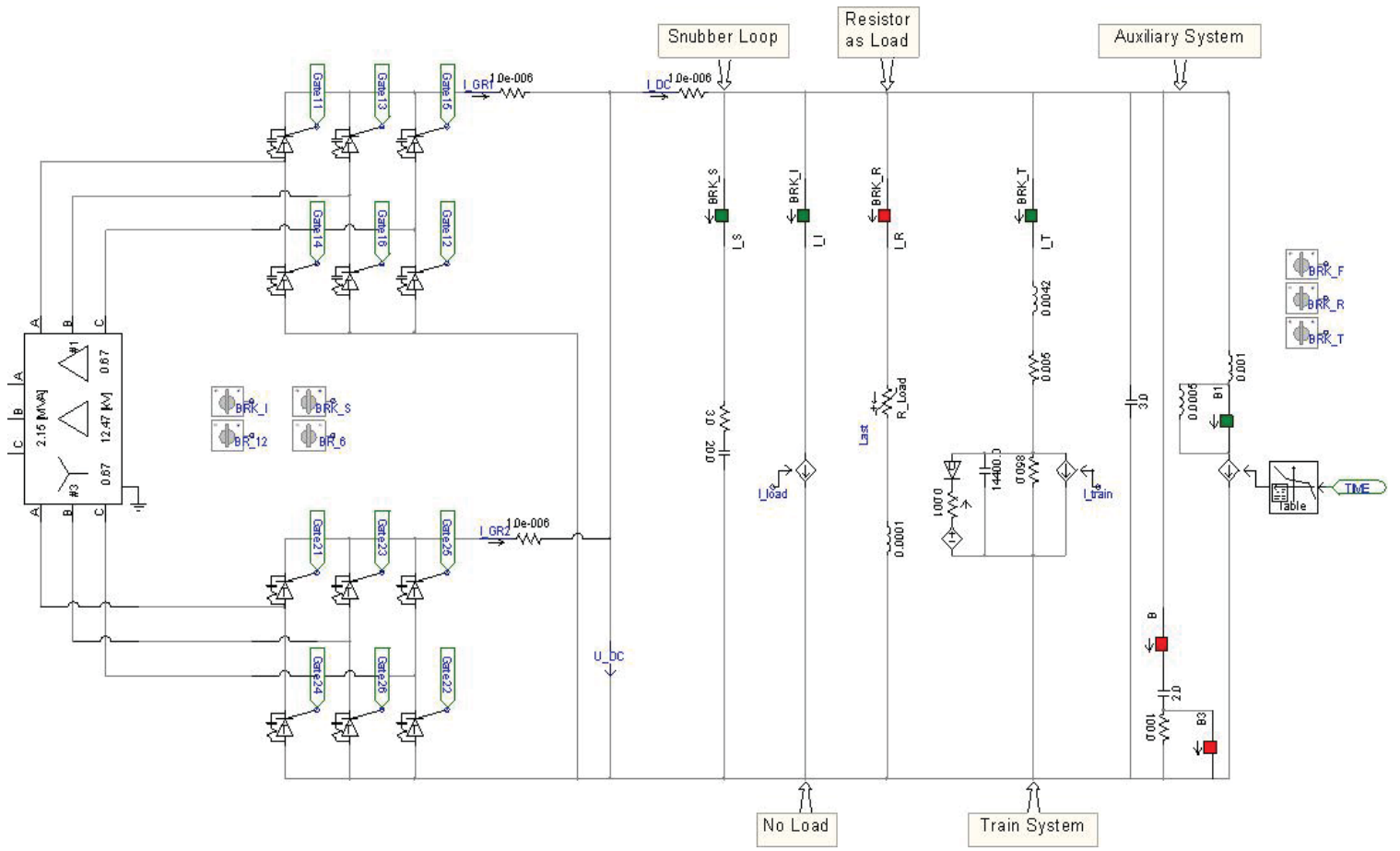
| 2P2S | Standard | - 5 % | - 2,5 % | 2,5 % | 5 % |
|------|----------|--------|---------|--------|--------|
| 3rd | 0,0000 | 0,0194 | 0,0154 | 0,0192 | 0,0188 |
| 5th | 0,0000 | 0,0142 | 0,0131 | 0,0111 | 0,0089 |
| 7th | 0,0479 | 0,0160 | 0,0041 | 0,0047 | 0,0140 |
| 9th | 0,0509 | 0,0141 | 0,0009 | 0,0030 | 0,0143 |
| 11th | 0,0004 | 0,7398 | 0,3582 | 0,3423 | 0,6618 |
| 13th | 0,0003 | 0,3497 | 0,1678 | 0,1621 | 0,3111 |
| 15th | 0,0095 | 0,0122 | 0,0083 | 0,0048 | 0,0047 |
| 17th | 0,0084 | 0,0091 | 0,0070 | 0,0028 | 0,0053 |
| 19th | 0,0000 | 0,0117 | 0,0182 | 0,0181 | 0,0215 |
| 21st | 0,0153 | 0,0112 | 0,0159 | 0,0161 | 0,0212 |
| 23rd | 0,0000 | 0,8258 | 0,8542 | 0,8439 | 0,8042 |
| 25th | 0,0001 | 0,5822 | 0,6053 | 0,6017 | 0,5757 |
| 31st | 0,0000 | 0,0140 | 0,0159 | 0,0144 | 0,0151 |
| 33rd | 1,1474 | 0,0174 | 0,0162 | 0,0158 | 0,0176 |
| 35th | 0,9158 | 0,1670 | 0,0864 | 0,0856 | 0,1599 |
| 37th | 0,0000 | 0,1092 | 0,0564 | 0,0566 | 0,1050 |
| 39th | 0,0000 | 0,0031 | 0,0014 | 0,0048 | 0,0086 |
| 41st | 0,0450 | 0,0028 | 0,0012 | 0,0040 | 0,0074 |
| 43rd | 0,0518 | 0,0216 | 0,0166 | 0,0191 | 0,0295 |
| 45th | 0,0001 | 0,0257 | 0,0192 | 0,0219 | 0,0350 |
| 47th | 0,0001 | 0,1234 | 0,1497 | 0,1512 | 0,1296 |
| 49th | 0,0127 | 0,1027 | 0,1255 | 0,1292 | 0,1130 |

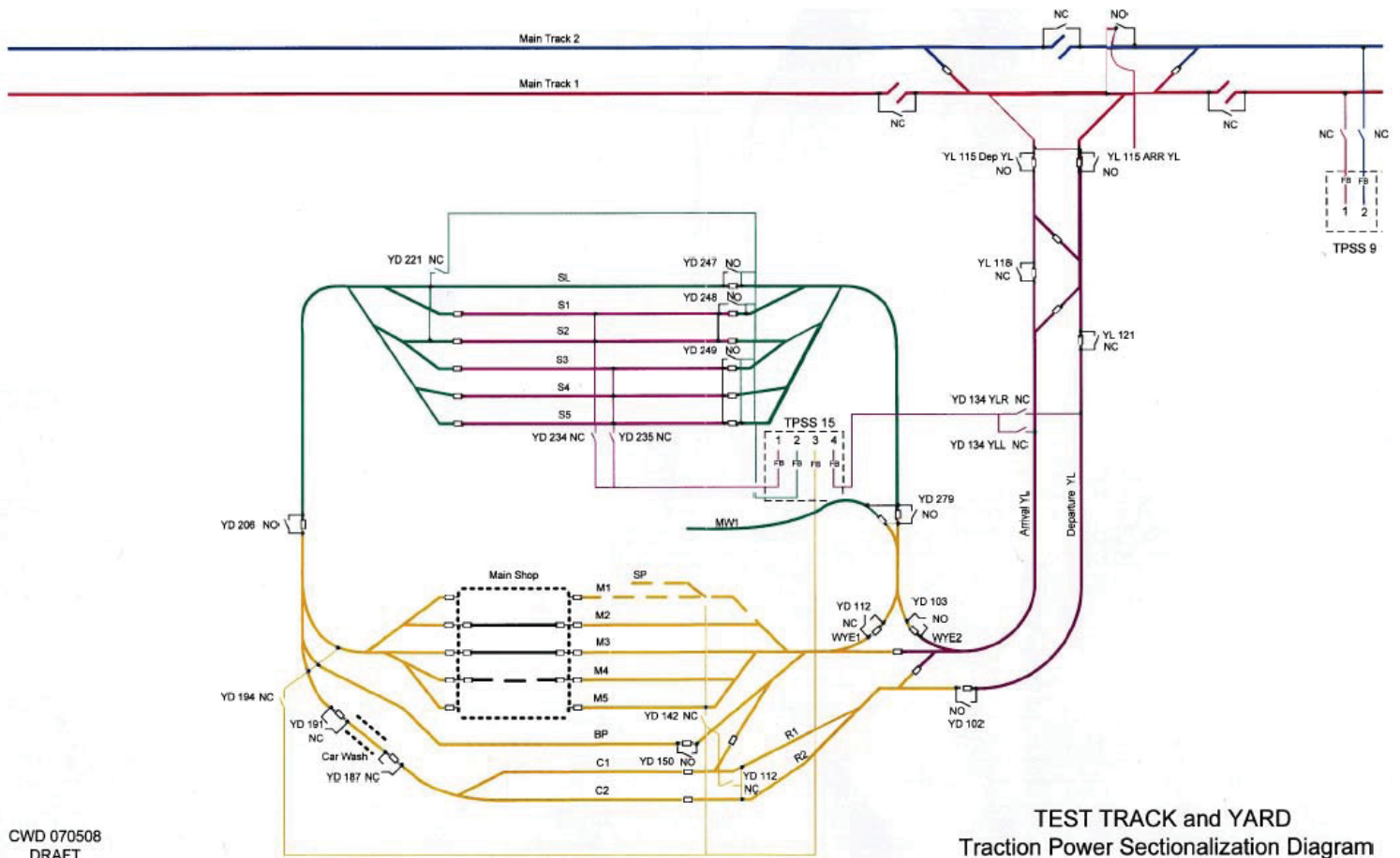
| 2S2P | Standard | - 5 % | - 2,5 % | 2,5 % | 5 % |
|------|----------|--------|---------|--------|--------|
| 3rd | 0,0000 | 0,0212 | 0,0301 | 0,0214 | 0,0294 |
| 5th | 0,0000 | 0,0145 | 0,0281 | 0,0225 | 0,0237 |
| 7th | 0,0324 | 0,0219 | 0,0141 | 0,0188 | 0,0288 |
| 9th | 0,0295 | 0,0214 | 0,0166 | 0,0123 | 0,0293 |
| 11th | 0,0007 | 1,0511 | 0,5180 | 0,4870 | 0,9574 |
| 13th | 0,0005 | 0,5958 | 0,2940 | 0,2794 | 0,5446 |
| 15th | 0,0049 | 0,0071 | 0,0058 | 0,0058 | 0,0086 |
| 17th | 0,0051 | 0,0058 | 0,0011 | 0,0029 | 0,0037 |
| 19th | 0,0000 | 0,0206 | 0,0224 | 0,0281 | 0,0166 |
| 21st | 0,0000 | 0,0242 | 0,0238 | 0,0241 | 0,0179 |
| 23rd | 1,0365 | 1,0020 | 1,0407 | 1,0272 | 0,9842 |
| 25th | 0,8022 | 0,6111 | 0,6393 | 0,6340 | 0,6077 |
| 31st | 0,0101 | 0,0116 | 0,0203 | 0,0180 | 0,0132 |
| 33rd | 0,0082 | 0,0181 | 0,0264 | 0,0210 | 0,0216 |
| 35th | 0,0001 | 0,2009 | 0,1051 | 0,0957 | 0,1778 |
| 37th | 0,0001 | 0,1597 | 0,0847 | 0,0764 | 0,1424 |
| 39th | 0,0056 | 0,0079 | 0,0080 | 0,0019 | 0,0089 |
| 41st | 0,0044 | 0,0075 | 0,0055 | 0,0017 | 0,0053 |
| 43rd | 0,0000 | 0,0449 | 0,0285 | 0,0313 | 0,0347 |
| 45th | 0,0000 | 0,0520 | 0,0337 | 0,0339 | 0,0388 |
| 47th | 0,2014 | 0,1720 | 0,2080 | 0,2002 | 0,1614 |
| 49th | 0,1671 | 0,1431 | 0,1716 | 0,1650 | 0,1328 |

| 4S | Standard | - 5 % | - 2,5 % | 2,5 % | 5 % |
|------|----------|--------|---------|--------|--------|
| 3rd | 0,0000 | 0,0168 | 0,0217 | 0,0249 | 0,0179 |
| 5th | 0,0000 | 0,0152 | 0,0120 | 0,0186 | 0,0142 |
| 7th | 0,0185 | 0,0219 | 0,0051 | 0,0101 | 0,0153 |
| 9th | 0,0179 | 0,0167 | 0,0007 | 0,0063 | 0,0096 |
| 11th | 0,0005 | 0,7114 | 0,3459 | 0,3344 | 0,6437 |
| 13th | 0,0003 | 0,4274 | 0,2101 | 0,2022 | 0,3870 |
| 15th | 0,0092 | 0,0133 | 0,0082 | 0,0100 | 0,0122 |
| 17th | 0,0094 | 0,0107 | 0,0058 | 0,0067 | 0,0047 |
| 19th | 0,0000 | 0,0118 | 0,0146 | 0,0099 | 0,0070 |
| 21st | 0,0000 | 0,0100 | 0,0112 | 0,0056 | 0,0055 |
| 23rd | 0,6150 | 0,7767 | 0,8006 | 0,7870 | 0,7573 |
| 25th | 0,6115 | 0,5405 | 0,5575 | 0,5545 | 0,5399 |
| 31st | 0,0036 | 0,0122 | 0,0091 | 0,0053 | 0,0086 |
| 33rd | 0,0009 | 0,0150 | 0,0062 | 0,0052 | 0,0091 |
| 35th | 0,0001 | 0,1417 | 0,0681 | 0,0640 | 0,1264 |
| 37th | 0,0000 | 0,1067 | 0,0496 | 0,0476 | 0,0960 |
| 39th | 0,0044 | 0,0024 | 0,0061 | 0,0007 | 0,0092 |
| 41st | 0,0017 | 0,0020 | 0,0043 | 0,0015 | 0,0070 |
| 43rd | 0,0000 | 0,0166 | 0,0075 | 0,0047 | 0,0094 |
| 45th | 0,0000 | 0,0181 | 0,0084 | 0,0038 | 0,0092 |
| 47th | 0,1331 | 0,1064 | 0,1209 | 0,1177 | 0,1078 |
| 49th | 0,1012 | 0,0906 | 0,0998 | 0,0951 | 0,0875 |

APPENDIX E TPSS in Phoenix







CWD 070508
DRAFT

TEST TRACK and YARD
Traction Power Sectionalization Diagram



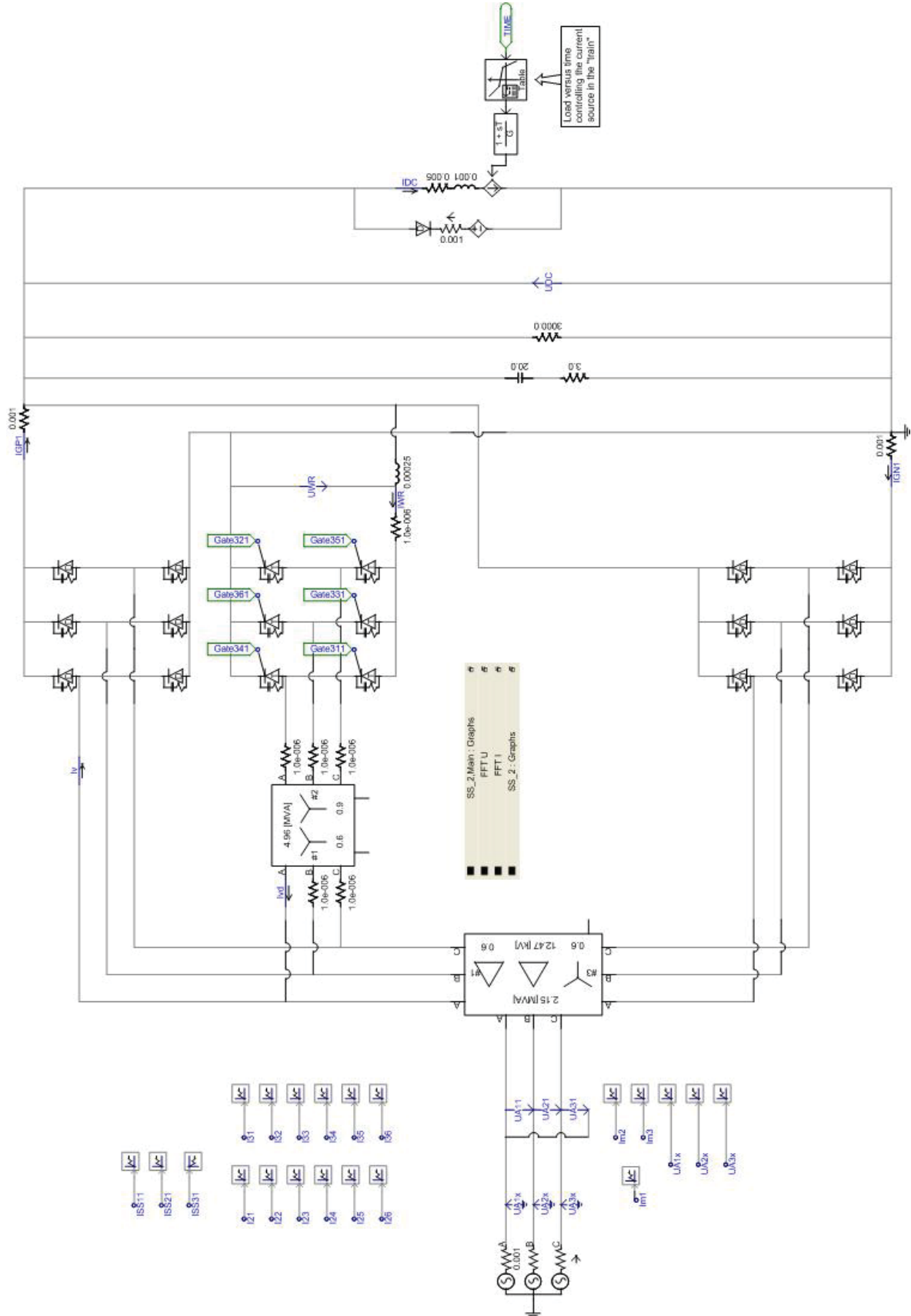
The Substation Control System in Phoenix (U.S.A.)



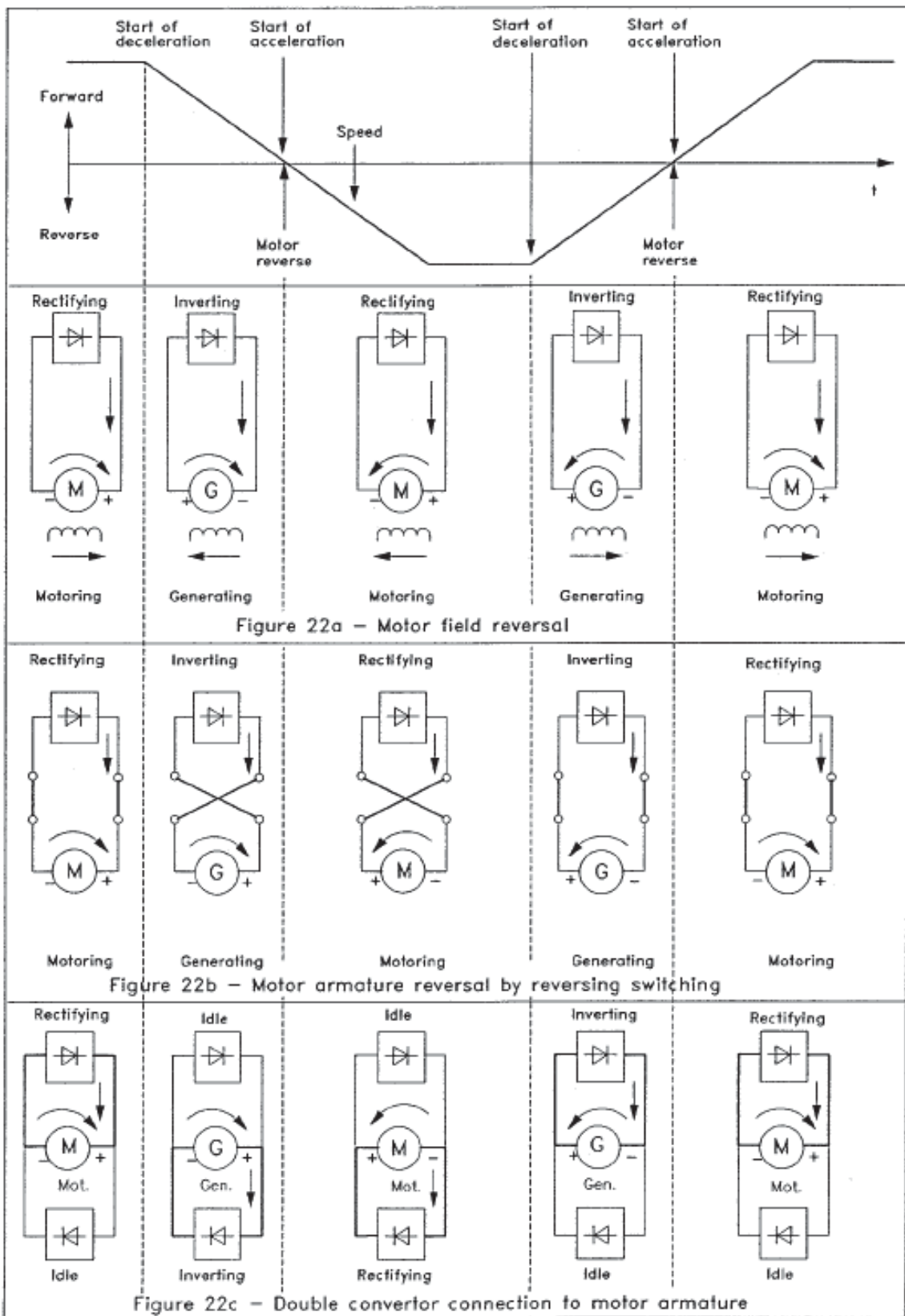
Control System Inside (Phoenix, U.S.A.)

APPENDIX F 12pDGR6pWR

Topology for (B6)2P rectification + 6-pulse line-commutated inverter



Operating sequences of converters serving a reversible d.c. motor



Curriculum Vitae

The author was born in Shanghai, China. He received his B.S. degree with major in electrical technology in the Department of Electrical Engineering, from Shanghai University of Engineering Science, China, in 1999.

From 1999 to 2004 he worked as an electrical engineer at Huayi Group, a chemical industry company. His work dealt with distribution electric system installing as Project Manager.

Since February 2004, he has been studying in Montanuniversität Leoben (Austria) to pursue the Diplom Ingenieur degree in Environmental Electrical Energy Engineering